Desmosomal armadillo proteins in zebrafish cardiac development

A thesis submitted to the National University of Ireland for the degree of

Doctor of Philosophy

by

Rebecca Ryan B.Sc. (Hons.)

Discipline of Biochemistry
School of Natural Sciences
College of Science
National University of Ireland Galway

December 2012

Research Supervisors:

Dr. Maura Grealy,
Discipline of Pharmacology
&Therapeutics,
School of Medicine

Dr. Lucy Byrnes,
Discipline of Biochemistry,
School of Natural Sciences,
College of Science

Head of Discipline:
Dr. Michael Carty,
Discipline of Biochemistry
School of Natural Sciences
College of Science

Acknowledgements

My supervisors, Drs. Lucy Byrnes and Maura Grealy, for providing me with the opportunity, and for their support, guidance and understanding throughout.

My parents, Eleanor and Bill, for everything. Their love, support and encouragement has been invaluable and limitless, and they have made all my accomplishments possible.

Evan and Karen, for indulging my role as the little sister at college for such a long time and for helping me all the way for eight years. Keith Emmett, for support and understanding beyond all expectations, for managing to make me laugh (often in spite of myself) in my moments of extreme lunacy, and for always being there to help me keep things in perspective or allow me blow things out of proportion.

All members of the Byrnes-Grealy lab, past and present. Particularly Catherine, Shaun, Denise and Miriam for getting me started, and Elke and Elaine for helping me finish.

Professor Didier Stainier and his lab at UCSF, especially Dr. Xiaoyan Ge, for allowing me to visit, and for teaching me the TALEN method.

Certainly the vast majority of the Biochemistry Department have been instrumental at one time or another, with advice, equipment and experimental empathy. Particular thanks to Aisling, Donna, Karen, Kasia and Shane for being right there with me, and to Laura and Trish for joining in along the way. I'm indebted to Christine for her help with the final countdown, especially my arch nemesis of formatting.

The quality and necessity of friends outside the lab becomes rapidly apparent when you delve into post-graduate education. For providing balance, distractions and maintaining the links between art and science, Caroline, Joss, Ken, Liam, Maria, Rob, Ronan, Rosemary, Siobhán and Tracy...you've just been epic.

Abbreviations

AC – arrhythmogenic cardiomyopathy
ALPM – anterior lateral plate mesoderm
ANOVA – analysis of variance
APC – adenomatous polyposis coli
ARM – armadillo
ARVC – arrhythmogenic right ventricular cardiomyopathy
AV – atrioventricular
AVC – atrioventricular canal
BMP – bone-morphogenetic protein
bp – base pair
BSA – bovine serum albumin
CFC – cysteine-flanked core
CK1 – casein kinase 1
cmlc2 – cardiomyosin light-chain 2
Cx43 – connexin 43
DEPC – diethyl pyrocarbonate
DKK-1 – Dickkopf-1
DNA – deoxyribonucleic acid
Dvl – Dishevelled
EDTA – ethylene diamine tetra acetic acid
EF1-α – elongation factor 1α
EGF – epidermal growth factor
FGF – fibroblast growth factor
GFP – green fluorescent protein
GSK-2 – glycogen sythase kinase 3
HRMA – high resolution melt analysis
IDP – inner dense plaque
LEF – lymphoid enhancer factor-1
LPM – lateral plate mesoderm
LRP – low-density lipoprotein
MAP – mitogen activated protein
MBT – mid-blastula transition
mRNA – messenger RNA
Ndr1 – nodal-related-1
NFAT – nuclear factor of activated T-cells
ODP – outer dense plaque
Oep – one-eyed pinhead
PBS – phosphate buffered saline

PCP – planar cell polarity
PG – plakoglobin
PKC – protein kinase C
PKP2 – plakophilin-2
PP1 – protein phosphatase 1
PPAR – peroxisome proliferator-activated receptor
qPCR – quantitative PCR
RNA – ribonucleic acid
ROCK – rho-associated protein kinase
RT-PCR – reverse transcription polymerase chain reaction
RVD – repeat-variable di-residue
SDS-PAGE – sodium dodecyl sulphate-polyacrylamide gel electrophoresis
SNP – single nucleotide polymorphism
TALENS – transcription activator-like effector nucleases
TBL1 – transducin β-like protein 1
TBS – tris buffered saline
TCF – T-cell factor
TEM – transmission electron microscopy
TILLING – targeting induced local lesions in genomes
UTR – untranslated region
vmhc – ventricular myosin heavy chain
YSL – yolk syncytial layer
ZFNs – zinc finger nucleases

Abstract

Plakoglobin and plakophilin-2 are desmosomal armadillo proteins, required for correct cardiac development in zebrafish. Mutations in the human genes can cause the congenital heart defect arrhythmogenic right ventricular cardiomyopathy (ARVC). Both proteins have structural and signalling roles in development, with plakoglobin implicated as a negative regulator of Wnt signalling. Our lab has previously established zebrafish loss of function models for both proteins using morpholino antisense oligonucleotides. Loss of plakoglobin has previously been shown to up-regulate expression of Wnt target genes at early stages of development. This study shows the up-regulation to be transient and stage-dependent. Wnt target genes *bmp4*, *ndr1* and *dharma* show a tendency towards increased expression in the early blastula stage, with *ndr1* and *dharma* mRNA expression levels normalised by late blastula, and *bmp4* by 48 hpf. Cardiac and developmental defects caused by loss of plakoglobin can be rescued by co-injection of Wnt inhibitor Dickkopf-1 (Dkk1). This study shows that though Dkk1 can restore cardiac patterning it is not sufficient to compensate for loss of plakoglobin in cell-cell junctions (desmosomes).

Whole-mount *in-situ* hybridisation experiments and qPCR were used to investigate the expression of Wnt target genes in plakophilin-2 knockdown embryos. Wnt target gene expression was unaffected at the developmental stages examined. Left-right patterning defects previously observed in plakophilin-2 morphant embryos suggested the Nodal signalling pathway as a target for further investigation. Using the same methods, cardiogenic genes were examined in plakophilin-2 morphant embryos at the 18 somite stage. Expression of Nodal target genes *lefty1, bmp4, southpaw, one-eyed pinhead* and *ndr1* was significantly increased, with concomitant down-regulation of *lefty2*. These results are the first reported incidence of an interaction between plakophilin-2 and the Nodal signalling pathway.

Our group aims to establish a zebrafish model that recapitulates the cardiac and signalling defects of ARVC. To investigate if signalling aspects of the human condition are replicated in the morphant embryos, expression levels of ARVC-related genes *connexin 43*, *desmoplakin-a*, adipogenic transcription factor *Wnt5b* and adipogenic marker *PPAR-γ* were examined by qPCR. All genes were decreased in plakoglobin morphant embryos, and unaffected in plakophilin-2 morphant embryos.

Complete protein loss has failed to accurately mimic molecular features of the disease, hence TALEN targeting was used to induce mutations in exon 4 of the plakoglobin protein *in vivo* and the resulting mutant embryos were characterised and assessed as a model for ARVC. The achieved germline mutations are predicted to encode premature stop codons, truncating the plakoglobin protein. This putative shortened protein resulted in cardiac, signalling and developmental defects reminiscent of the plakoglobin knock-down phenotype, with additional epithelial defects observed in a small subset of mutant embryos. The cardiac defects arising from TALEN-induced mutations in plakoglobin indicate potential for the development of an improved zebrafish model for ARVC using this technique to introduce mutations in different regions of the gene.

1 Introduction

1.1 Zebrafish and research

The zebrafish, *Danio rerio*, is a small tropical freshwater fish that has become increasingly popular as a model system in recent years, particularly in the field of cardiovascular research. As further information is gleaned regarding the complex process of cardiac development the need for a suitable model that permits researchers to delve further into the underlying genetic, cellular and molecular processes becomes more pressing and the zebrafish presents a suitable candidate.

1.1.1 The zebrafish as a model system

The zebrafish has several compensatory features that are extremely beneficial for an *in vivo* model, despite the anatomical differences between mature zebrafish and human hearts. External fertilisation and high fecundity ensure large numbers of easily obtainable embryos, and the natural optical clarity of early-stage embryos allows for the examination of internal structures and monitoring of developmental processes without the need for invasive procedures. Additionally, their rapid rate of development facilitates the study of the complete process of cardiogenesis in just a few days (Figure 1.1).

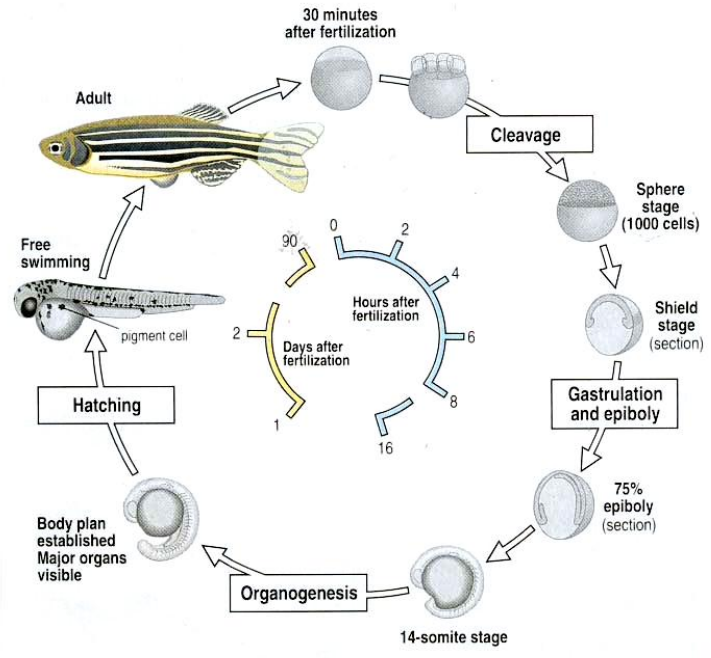

Figure 1.1 Life cycle of the zebrafish.
(Wolpert, 1998)

In addition to their rapid development, the zebrafish has another advantage over mammalian models. Defects in early heart development are embryonic lethal in the majority of vertebrates, yet, due to their small size, zebrafish can survive for several days without a functional cardiovascular system because sufficient perfusion with oxygen can be achieved by passive diffusion (Pelster and Burggren, 1996; Pelster, 1999). This trait, coupled with the wide range of genetic manipulation tools available (such as zinc finger nucleases (ZFNs), Targeting Induced Local Lesions in Genomes (TILLING), Transcription Activator-Like Effector Nucleases (TALENs) and the well-established morpholino anti-sense oligonucleotides) favours the zebrafish as a model for numerous developmental processes and, in particular, cardiogenesis.

1.1.2 Zebrafish heart patterning and development

In vertebrate embryos, the first organ to form and function is the heart. Fate mapping studies provide information on the location of cardiac progenitors as early as the blastula stage, where myocardial progenitors have been identified proximal to the embryonic margin, and on both sides of the embryo. Atrial and ventricular progenitors occupy separate locations, with ventricular progenitors situated closer to the embryonic margin and more dorsally than the atrial progenitors. Endocardial progenitors are also found close to the margin at this early stage, but without the chamber-specification seen in the myocardial progenitors (Stainier et al., 1993; Lee et al., 1994; Keegan et al., 2004).

By early segmentation myocardial progenitors are localised to the posterior half of the anterior lateral plate mesoderm (ALPM), with ventricular progenitors maintaining a more dorsal position (relative to the atrial progenitors) at this stage (Yelon et al., 1999). As these separate populations of myocardial precursors differentiate they also migrate towards the embryonic midline (Figure 1.2). By the 20 somite stage these independent populations have fused to form a shallow cone, with ventricular cells located at the centre and apex, and atrial cells found at the base (Stainier et al., 1993). As the myocardial precursors are migrating towards the midline the endocardial precursors move from the anterior of the ALPM towards the centre and posterior, and combine with the myocardium, spreading across the

interior of the cardiac cone as it forms (Bussmann et al., 2007; Schoenebeck and Yelon, 2007). The endocardial and myocardial precursors, once joined, migrate asymmetrically, using a process of involution to form a linear heart tube by 24 hpf (Stainier et al., 1993; Yelon et al., 1999).

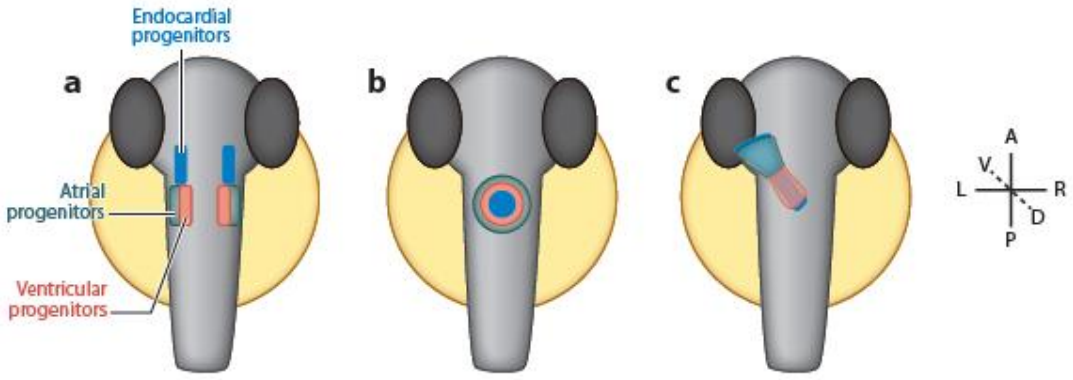

Figure 1.2 Early zebrafish heart development.
(*a-c*) Heart development before looping. Embryos are shown in a dorsal view. (a) At 12 hpf the myocardial progenitors are located in the anterior lateral plate mesoderm (ALPM), ventricular progenitors are more dorsally situated than atrial progenitors. Endocardial progenitors are located in the anterior of the ALPM. (b) The myocardial and endocardial progenitors migrate asymmetrically towards the midline and fuse to form the cardiac cone by 19 hpf (20 somite stage). (c) The myocardium involutes to surround the endocardium and form a linear heart tube by 24 hpf (Staudt and Stainier, 2012).

After formation of the linear heart tube, at approximately 24 hpf, the earliest visible sign of cardiovascular asymmetry occurs with the leftward "jogging" and subsequent rightward "looping" of the heart tube (Chen et al., 1997). The heart loops to the right (at approximately 36 hpf) positioning the ventricle to the right of the atrium (Chin et al., 2000). As looping progresses, distinct chambers form as bulges in the cardiac tube in a process called ballooning. These "bulges" are further defined as separate chambers when cardiac cushions form at the atrio-ventricular boundary at 48 hpf (Hu et al., 2000). By 55 hpf a layer of polarized cuboidal endocardial cells is present at both the superior and inferior portions of the atrio-ventricular canal (AVC). This layer of endocardial cells develops and by invagination forms projections in both the inferior and superior atrio-ventricular canal. These projections form the inferior and superior valve leaflets of the AVC, and are clearly

visible and connected to the myocardial trabeculae by 7 dpf (Scherz et al., 2008). Though the heart is fully functional by 7 dpf, cardiac development is not complete. The valve leaflets have a thickness of two-cell layers at this stage, which does not alter until at least 28 dpf, and by the adult stage there are a total of four leaflets in the AV valve (Beis et al., 2005).

1.2 Wnt signalling

A highly conserved pathway across vertebrate and invertebrate species, Wnt signalling is required for many biological processes including embryogenesis, cell polarity and motility, and cell fate decisions. Genes of the Wnt family are identified by sequence homology to the first described members, murine *Wnt-1* (originally *int-1*) and *wingless* in Drosophila (van Ooyen and Nusse, 1984; Cabrera et al., 1987). Wnt family genes encode cysteine-rich, palmitoylated, secreted glycoproteins that are typically 300-450 amino acids in length with a conserved domain of 23-24 cysteine residues (Cadigan and Nusse, 1997). Wnt proteins act upon various cellular pathways, which can be divided into canonical (β-catenin dependent) and non-canonical Wnt pathways, which will be discussed in Sections 1.2.1 and 1.2.3 respectively.

1.2.1 Canonical Wnt signalling

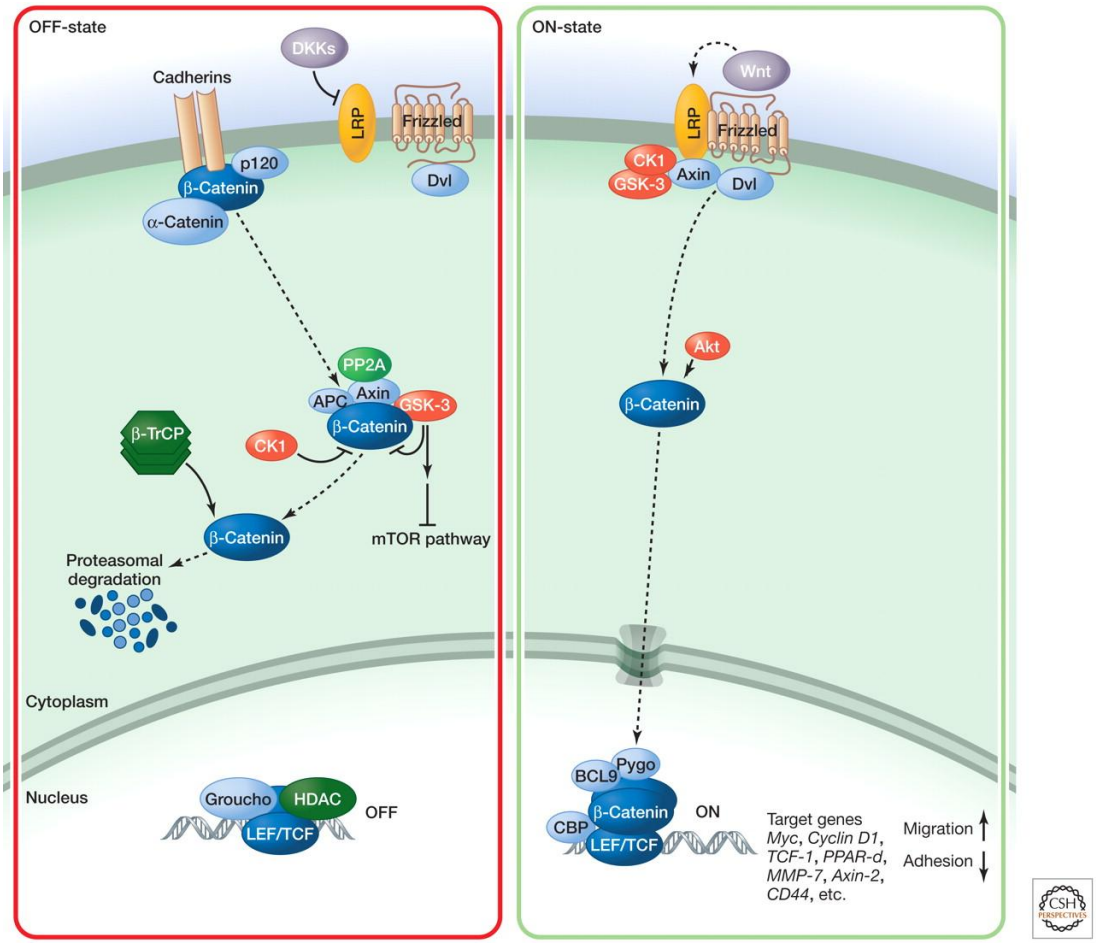

Figure 1.3 The Canonical Wnt signalling pathway.
In the "off" state (*left*) β-catenin is maintained at low levels by axin and APC, and protein kinases GSK-3 and CK1. In the "on" state (*right*) Wnt ligands bind to members of the Frizzled family of receptors, activating a canonical signalling pathway that targets members of the TCF/LEF transcription factor family. Binding of Wnt to Frizzled re-arranges the receptors, activating proteins of the Dishevelled family. Activation of Dishevelled inhibits the axin-GSK-3-APC complex, which normally promotes destruction of intracellular β-catenin. Inhibition of the β-catenin "destruction complex" allows a pool of cytoplasmic β-catenin to stabilize, some of which is able to enter the nucleus and consequently promote gene expression via its interaction with members of the TCF/LEF family of transcription factors (diagram from Nusse, 2012).

The most important regulatory step in the canonical Wnt pathway is the phosphorylation, ubiquitination and resulting degradation of β-catenin (a Wnt down-stream effector protein) by a destruction complex.

In the inactive state a low level of free intracellular β-catenin protein is present in the cytosol. This cytosolic pool is sequestered by the destruction complex which consists of Axin, APC and protein kinases GSK-3 and CK1 (Figure 1.3). β-catenin is primed by CK1 phosphorylation and then further phosphorylated by GSK-3 targeting it for ubiquitination by β-TrCP ubiquitin E3 ligase, after which it is degraded by the proteasome.

Phosphorylation of APC and GSK-3 by the kinases in the destruction complex, and de-phosphorylation of axin by protein phosphatase 1 (PP1) reduces axin-GSK-3 association, hence degradation of β-catenin can also be reduced (Luo et al., 2007). Adhesion complexes containing cadherins and α-catenin can also regulate β-catenin, and negative regulator Dickkopf-1 (DKK1) can inhibit Wnt signalling by binding to the low-density lipoprotein-related 6 (LRP6) receptor (Semenov et al., 2001).

During signalling (i.e. in the active state shown in Figure 1.3) members of the Wnt family bind to members of the Frizzled family of receptors and the co-receptor LRP5/6, targeting LEF/TCF transcription factors (Tamai et al., 2000; Mao et al., 2001). This process ultimately facilitates translocation of β-catenin to the nucleus via interaction with Dishevelled, but many aspects of it are still poorly understood.

Transducin β-like protein 1 (TBL1) and TBL-1 related proteins mediate the targeting of β-catenin to the promoter (Li and Wang, 2008). Nuclear Dvl, c-Jun, β-catenin and TCF can form a complex on Wnt gene promoters which results in the regulation of gene transcription, hence β-catenin binding to TCF/LEF induces transcription of Wnt target genes (Behrens et al., 1996; Molenaar et al., 1996; Gan et al., 2008).

A number of models have been proposed to explain further the β-catenin stabilisation mechanism that occurs in the wake of canonical Wnt pathway activation. Sequestration of Axin1 by binding LRP5/6 is thought to reduce the availability of destruction complexes, hence permitting the accumulation of β-catenin. Wnt-induced de-phosphorylation and de-stabilisation of Axin may also be mediated by its translocation to the membrane (Mao et al., 2001; Zeng et al., 2005). Degradation of Axin by activated Wnt-receptors or Dishevelled has also been

proposed as a mechanism by which β-catenin may be stabilised (Mao et al., 2001; Lee et al., 2003; Tolwinski et al., 2003).

An alternative model whereby Axin and APC dissociate from GSK-3 or β-catenin has also been proposed. Dishevelled binds directly to Axin and may disrupt the destruction complex when the Wnt pathway is activated, hence cytosolic β-catenin is not captured by the destruction complex (Logan and Nusse, 2004; Liu et al., 2005; Malbon and Wang, 2006).

Inhibition of GSK-3 activity, de-phosphorylation of phosphorylated β-catenin, sequestration of GSK-3 from the cytosol and APC-mediated disassembly of the Axin destruction complex have also been proposed as alternative methods by which stabilisation of β-catenin is achieved upon activation of the canonical Wnt signalling pathway (reviewed by MacDonald et al., 2009).

Recently, a mechanism has been proposed where β-catenin phosphorylation, ubiquitination and degradation by the proteasome all occur within an intact Axin complex. Li et al. (2012) propose a model that contradicts existing studies, as neither disassembly of the destruction complex, nor inhibition of phosphorylation of Axin-bound β-catenin were found during active Wnt signalling in their study. Instead, a model whereby inhibition of β-catenin degradation occurs within an intact destruction complex is posited, with activated Wnt signalling suppressing the ubiquitination of β-catenin that occurs within the destruction complex. As a result, the Axin complex is saturated with phosphorylated β-catenin, and so this newly synthesised β-catenin can accumulate in the Axin complex in a free cytosolic form in response to Wnt signalling, and interact with nuclear TCF transcription factors (Li et al., 2012).

1.2.2 Plakoglobin and canonical Wnt signalling

The structural similarities between plakoglobin and β-catenin confer similar binding capabilities on these two armadillo proteins. The central arm repeat domain of both

proteins is capable of interaction with TCF-4, and the amino- and carboxy-terminal tails of both plakoglobin and β-catenin are able to bind to the arm domains, thus determining the specificity and affinity of each protein for its co-factors (Solanas et al., 2004). As catenin proteins, β-catenin and plakoglobin have roles in both adhesion and signalling. Both proteins can be degraded by the "destruction complex" which targets them for phosphorylation by β-TrCp and subsequent degradation by the ubiquitin pathway (Sadot et al., 2000; Lee et al., 2003). However, phosphorylation of plakoglobin is inhibited by O-glycosylation near the GSK-3 phosphorylation site, thus post-translational stability of plakoglobin is increased (Hu et al., 2006).

In vitro plakoglobin mutants lacking amino- and carboxy- terminal tails have induced formation of a transcriptionally active complex of plakoglobin/TCF/LEF in a human embryonic kidney cell line (Zhurinsky et al., 2000). Plakoglobin and β-catenin occupy separate and distinct binding sites on TCF-4 and complexes of plakoglobin/β-catenin/TCF-4 can be detected, indicating that these proteins can bind simultaneously to TCF-4. Transcriptional activity of TCF-4 has been observed to increase in TCF-4 mutants with decreased plakoglobin interaction, which suggests that plakoglobin has an antagonistic role in the regulation of canonical Wnt signalling (Miravet et al., 2002).

A signalling role for plakoglobin has been demonstrated in several *in vitro* systems, where it has shown limited ability to activate TCF/LEF-dependent transcriptional activity, however it may be argued that the endogenous plakoglobin and β-catenin present in the cell lines used for these studies could potentially interfere with the observed results (reviewed by Swope et al., 2012b). Increased transcriptional activity has been observed in one study following co-transfection of plakoglobin with TCF-4 or LEF, and knockdown of endogenous plakoglobin had the opposite effect, coinciding with a slight decrease in TCF/LEF reporter activity (Maeda et al., 2004). Most importantly a mesothelial cancer cell line lacking endogenous β-catenin was used for this study, countering the argument that extant plakoglobin or

β-catenin may have influenced results obtained in previous studies. Published data on the effect of plakoglobin on Wnt signalling is summarised in Table 1.1.

Table 1.1 Effect of plakoglobin on Wnt signalling

	Effect of Plakoglobin on Wnt Signalling
Salic et al. (2000)	↑
Williams et al. (2000)	↑
Zhurinsky et al. (2000)	↑
Miravet et al. (2002)	↓
Maeda et al. (2004)	↑
Martin et al. (2009)	↓

Evidence from our lab implicates plakoglobin as a negative regulator of canonical Wnt signalling. Expression of Wnt target genes such as *ndr1*, *bmp4* and *dharma* was up-regulated in zebrafish embryos following loss of plakoglobin by morpholino knockdown (Martin et al., 2009). A direct role for plakoglobin in regulating gene expression has also been suggested, with plakoglobin shown to suppress c-Myc expression in an Lef-1-dependent manner in keratinocytes (Williamson et al., 2006).

1.2.3 Non-canonical Wnt signalling

Many different pathways have been grouped under the heading of non-canonical Wnt signalling, but perhaps the best understood are the planar cell polarity (PCP) and Wnt/calcium pathways. Differences of note between the two groupings (canonical and non-canonical) are the specific ligands activating each pathway, and the ability of the non-canonical pathways to inhibit the canonical signalling pathway. Activators of the non-canonical pathways include Wnt4a, Wnt5a and Wnt11 (Komiya and Habas, 2008).

In the PCP pathway ligand binding to the Frizzled receptor recruits Dvl, which then forms a complex with Daam1. Daam1 activates Rho via guanine exchange factor, and Rho in turn activates Rho-associated protein kinase (ROCK), the major cytoskeletal organiser (Habas et al., 2001; Liu et al., 2008). Dvl forms an additional complex with Rac1, which mediates binding of profilin to actin (Schlessinger et al., 2009; Tada and Kai, 2009; Wang, 2009; Miller and McCrea, 2010). Rac1 is thought

to activate the c-Jun N-terminal kinase (JNK)-type mitogen activated protein (MAP) kinase cascade, which can lead to polymerisation of actin (Kikuchi et al., 2007; Tada and Kai, 2009; Miller and McCrea, 2010; Miller et al., 2011). Interestingly, deletion of a single copy of Daam1 has recently been reported to cause a congenital heart defect (Bao et al., 2012).

In the Wnt/calcium pathway Wnt5a and Frizzled co-operate to regulate intracellular calcium levels. Purified Wnt5a has been shown to activate calcium signalling in cell culture models. This rapid signalling process is dependent upon heterotrimeric G proteins, and once the Ca^{2+} has been released it activates calcium-dependent enzymes like calcium/calmodullin-dependent kinase (CaMK)II, protein kinase C (PKC) and calcineurin (Kuhl et al., 2000a; Kuhl et al., 2000b; Kremenevskaja et al., 2005; Dejmek et al., 2006; Ma and Wang, 2006). The regulation of PKC by Wnt ligands is required for cardiac differentiation, with isoform PKCδ thought to be of particular importance (Pandur et al., 2002; Belema Bedada et al., 2005; Koyanagi et al., 2009). The Wnt/calcium pathway connects to nuclear factor of activated T cells (NFAT) through calcineurin (Saneyoshi et al., 2002; Dejmek et al., 2006), and both calcineurin and NFAT have been implicated in cardiac hypertrophy (Heineke and Molkentin, 2006).

1.3 Nodal signalling

Body patterning and axis specification are key elements of early vertebrate development, and provide the scaffold for the more complex developmental events, such as organ positioning, that occur later. Numerous signalling pathways act in a co-ordinated way to regulate these processes, and of these the Nodal cascade is thought to control many of the molecular events that specify the final body plan. An overview of the Nodal signalling pathway is shown in Figure 1.4.

1.3.1 Signalling components of the Nodal pathway

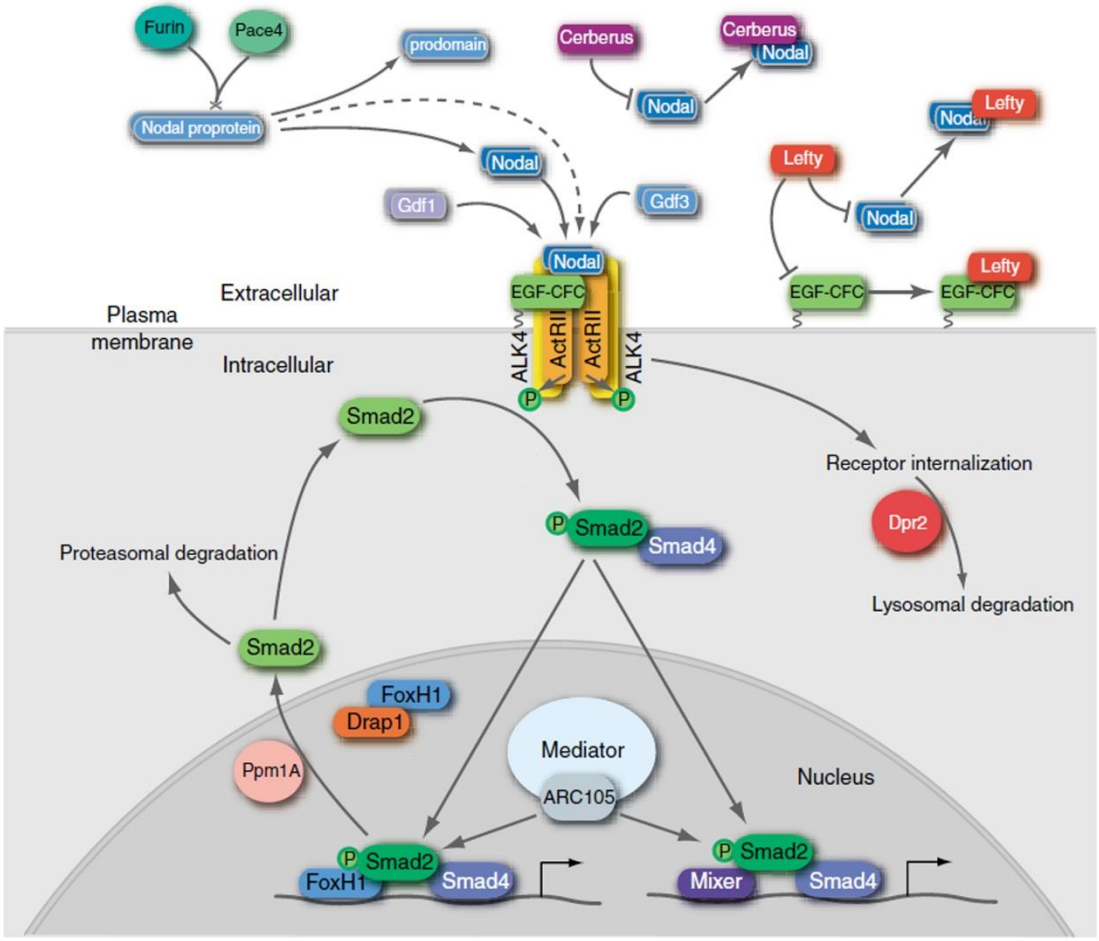

Figure 1.4 The Nodal Signalling Pathway.
Homodimeric proprotein Nodal ligands can be cleaved extracellularly by proprotein convertases Furin and Pace4. Mature Nodal ligands can bind to EGF-CFC co-receptors forming a complex with type I (ALK4) and type II (ActRII/ActRIIB) dimers. Interaction of Nodal ligands with Cerberus or Lefty proteins has an inhibitory effect on Nodal signalling. Activation of the Nodal receptor leads to phosphorylation of type I receptors by type II kinase, and phosphorylation of Smad2/Smad3. These activated Smads associate with Smad 4 and translocate to the nucleus. The receptor complex is internalized by endosomes and can be targeted by Dapper2 (Dpr2) for lysosomal degradation. Once in the nucleus, activated Smad complexes interact with winged-helix transcription factor FoxH1 or Mixer homeoproteins on target promoters. Interactions with Mediator or ARC105 can then result in transcriptional activation. Drap1/FoxH1 or Smad phosphatase Ppm1A interactions can inhibit Nodal pathway activity. Reproduced and adapted with permission of Development. Article available online at http://dev.biologists.org/content/134/6/1023 . (Shen, 2007).

Signalling molecules of the Nodal pathway are members of the transforming growth factor β (TGFβ) superfamily. TGFβ ligands elicit their cellular effects via binding to type I and II serine-threonine kinase transmembrane receptors. Nodal pathway molecules signal specifically through the type I receptor ALK4 and the type II

receptors ActRII and ActRIIB (Reissmann et al., 2001; Yeo and Whitman, 2001; Yan et al., 2002). Downstream of their receptors, Nodal signals are transduced by Smad2 and Smad3 (intercellular signal transducers for the TGFβ family). Formation of transcriptional complexes in the nucleus occurs after activated receptors phosphorylate Smad2 and/or Smad3 causing interaction with Smad4 (Schier and Shen, 2000; Shen, 2007). The Mixer subclass of homeodomain proteins and the transcription factor FoxH1 are required for the interaction of Nodal ligands with Smads 2 and 3, as they contain Smad-interaction motifs that enable the formation of transcriptional complexes (Germain et al., 2000; Randall et al., 2004).

Extracellular growth factor–CFC (EGF-CFC) proteins are membrane-bound extracellular factors with essential roles during vertebrate development, and the CFC in their nomenclature is derived from three members of this family, Cripto, FRL-1, and Cryptic. Despite being a small group of only six members the co-receptors of the EGF-CFC family are essential components unique to the Nodal signalling pathway, conferring specificity for ALK4 (Yeo and Whitman, 2001; Yan et al., 2002). Mammalian genes *Cripto* and *Cryptic*, batrachian genes *XCR1-3*, and the zebrafish gene *one-eyed pinhead* (*oep*) encode all of the known proteins included in the EGF-CFC classification (Schier and Shen, 2000; Dorey and Hill, 2006). These cysteine-rich extra-cellular proteins utilise a glycosyl-phosphatidylinositol linkage to adhere to the plasma membrane, and are identifiable by their amino-terminal signal sequence, a divergent epidermal growth factor (EGF)-like motif, a second conserved cysteine-rich domain (the CFC motif) and a carboxy-terminal hydrophobic region (Shen et al., 1997; Zhang et al., 1998).

Antagonism of the Nodal pathway occurs via a number of extracellular inhibitors. A subclass of the TGFβ factors, the Lefty inhibitors, interacts with EGF-CFC proteins and Nodal ligands and thus prevents receptor complexes from forming. They do not however interact with receptors ALK4 or ActIIB and hence proteins of the Lefty family are not thought to act via competitive inhibition (Chen and Shen, 2004; Cheng et al., 2004). A study in *Xenopus* has shown that the extra-cellular protein Cerberus, required for head induction, is also capable of inhibiting Nodal signalling by directly interacting with Nodal ligands (Piccolo et al., 1999). Other antagonists to

the Nodal pathway have been proposed, including membrane-associated proteins Nicalin, Nomo and Tomoregulin-1, but their mechanism of inhibition is, as yet, unclear (Harms and Chang, 2003; Haffner et al., 2004).

1.3.2 The Nodal Pathway in zebrafish development

At the early stages of zebrafish development Nodal signals are required for establishment of the shield and formation of the organizer and mesendoderm (Erter et al., 1998; Feldman et al., 1998). As shown in Figure 1.5 below, the Yolk-Syncytial Layer (YSL), which develops synchronously with the onset of zygotic genome activation, is the region where mesoderm-inducing factors and Nodal-related signals are expressed (Schier and Shen, 2000). Kupffer's vesicle, the zebrafish "organ of asymmetry" is thought to be the site of initiation for Nodal signalling, where cilia motility and asymmetric fluid flow drive expression of the Nodal ligand to the LPM (Raya and Izpisua Belmonte, 2006) after which Nodal signalling is self-propagating and dependent upon its antagonists to maintain correct localisation of expression.

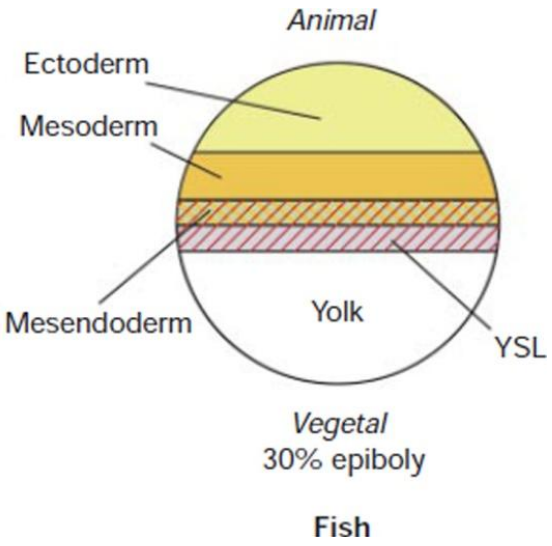

Figure 1.5 Nodal activities in fish.
Expression patterns of Nodal-related genes (shown in red hatching) superimposed on fate map of developing fish embryo (adapted from Schier and Shen, 2000).

Zebrafish loss-of-function studies have yielded much of the extant data on the Nodal pathway, its regulation and its members. Though only one Nodal ligand exists in most vertebrates (humans, mice and chicks) zebrafish have three: *ndr1*, *ndr2*, and *southpaw.* Zebrafish studies on *oep* and Nodal-related genes *ndr1* and *ndr2* have shown the requirement of EGF-CFC proteins for Nodal signalling. *Ndr2* (also known as *cyclops*) is expressed in the left lateral plate and within the diencephalon, an expression pattern that is highly conserved between fish and mammals (Rebagliati et al., 1998; Sampath et al., 1998). Though *ndr2* mutations alone cause only minor disruptions to the asymmetric patterning of the internal organs, double mutants for *ndr1* and *ndr2* bear strikingly similar developmental defects to embryos lacking *oep*, where head and trunk mesendoderm and endoderm do not form, and the anterior-posterior axis is mis-aligned with disrupted asymmetry of the viscera and diencephalon (Chen et al., 1997; Feldman et al., 1998; Gritsman et al., 1999; Yan et al., 1999; Bisgrove et al., 2000; Chin et al., 2000; Liang et al., 2000). Zebrafish *flh* (*floating head*) mutants display bilateral expression of *Pitx2* but lack expression of *antivin* (which recognises lefty 1 and lefty 2) in the LPM (Chin et al., 2000). Antivin has a high level of structural similarity to murine Lefty and ectopic expression of *antivin* can completely abolish induction of the mesoderm in early zebrafish development (as can Lefty) via competitive inhibition of Activin (Thisse and Thisse, 1999).

A loss-of-function study has shown that Nodal ligand *southpaw* is required to establish correct asymmetrical patterning of the heart (including cardiac jogging and looping), pancreas and diencephalon (Long et al., 2003). Mis-expression of Nodal has also been linked to altered heart patterning in frog and chick models, including looping defects (Levin et al., 1997; Sampath et al., 1997). As Nodal signalling operates on a long-range basis the importance of the Lefty feedback inhibitors cannot be underestimated, particularly in their role maintaining the asymmetry of expression of the Nodal ligands in the left LPM (Lenhart et al., 2011).

As the Nodal signalling molecules, and in particular *southpaw,* are capable of controlling the asymmetric positioning of the organs they may be considered the left determinants in zebrafish development.

1.4 Signalling and heart development

Three main pathways regulate the early stages of heart development; bone morphogenetic protein (BMP) signalling, fibroblast growth factor (FGF) signalling and Wnt signalling, with later stages of cardiac development controlled by the Notch and Nodal pathways. Loss-of-function studies, cell fate-mapping and molecular analyses have provided much of the extant information on the importance of these signalling cascades in development, however current information is still far from providing a comprehensive understanding of the entire mechanism and interactions of the different pathways.

1.4.1 BMP signalling and heart development

BMPs are a subgroup of the TGF-β protein superfamily, named for their ability to induce bone differentiation. Since their initial discovery, numerous other roles have been identified for BMP proteins, including a very important role in heart development. In zebrafish, left-dominant expression of bmp4 occurs prior to any morphological evidence of asymmetry in the developing embryo, and analysis of mutants with abnormal cardiac asymmetry revealed disrupted patterning of bmp4 in all mutants (Chen et al., 1997). These data strongly suggest that cardiac expression of bmp4 is responsible for the correct establishment of heart asymmetry.

More recently, a role for bmp4 in left-right asymmetry has been mapped to two distinct time points in development. Chocron et al. have shown a requirement for *bmp4* during early segmentation to antagonise expression of *southpaw* in the right LPM and regulate laterality of the gut and heart. A second wave of *bmp4* is then required during segmentation to regulate the expression of Nodal pathway genes *cyclops*, *lefty1* and *lefty2,* yet this second time-point is concerned only with regulation of cardiac laterality (Chocron et al., 2007). This both supports previously published data describing the necessity of bmp4 for correct cardiac development, and demonstrates a role for bmp4 in regulation of Nodal signalling, where it may act up- or down-stream of the Nodal pathway.

1.4.2 FGF signalling and heart development

FGF signalling regulates multiple aspects of embryogenesis, including cell proliferation, differentiation and migration. *In vitro* synergistic interaction between FGF and BMP signalling in the endoderm induces formation of cardiac tissue from the adjoining mesoderm (Barron et al., 2000). *In vivo* the importance of FGF signalling in early cardiac development has been described in several species, including *Drosophila*, zebrafish and mouse. In *Drosophila* a null mutant for *Heartless (Htl)* lacks induction of several cell fate lineages and results in defective heart development (Beiman et al., 1996). Mouse embryos hypomorphic for Fgf8 have numerous cardiovascular defects and also show craniofacial and pharyngeal arch abnormalities, suggesting a role for FGF signalling in neural crest cell development (Abu-Issa et al., 2002). Fgf10-expressing cells contribute to the arterial pole of the murine heart (Kelly et al., 2001) and loss of the Fgf10 ligand or its major receptor Fgfr2-IIIb also induces overt cardiac phenotypes in mice (Marguerie et al., 2006). Embryos lacking Fgf10 show abnormal positioning of the heart in the thorax, while late developmental impairment of the cardiac outflow tract and right ventricular wall were observed in mice lacking Fgfr2-IIIb (Marguerie et al., 2006). A zebrafish mutation of *fgf8* is associated with down-regulation of nkx2.5 and Gata4, disrupting induction and differentiation of the heart and causing abnormal formation of the ventricle (Reifers et al., 2000).

1.4.3 Wnt signalling and heart development

The majority of evidence suggests a positive role for canonical Wnt/β-catenin signalling in cardiac development. Inhibition of endogenous Wnt signalling prevents formation of heart valves (Hurlstone et al., 2003). In pluripotent embryonal carcinoma cells Wnt signalling is activated prior to cardiogenic differentiation, and is capable of promoting cardiomyogenesis (Nakamura et al., 2003). Naito et al., (2006) have demonstrated the potential for Wnt signalling to act in a stage-specific manner, with early activation of Wnt during embryoid body formation leading to increased differentiation of murine embryonic stem cells into cardiomyocytes and suppressed expression of haematopoietic and vascular markers. Late stage

activation had the opposite effect on both differentiation and expression of markers, indicating a bi-phasic role for Wnt signalling in heart development (Naito et al., 2006). A bi-phasic role for Wnt/β-catenin signalling in development has also been shown in zebrafish indicating that Wnt/β-catenin signalling promotes cardiogenesis prior to gastrulation and later defines the size of the heart-forming field (Ueno et al., 2007). Loss and gain of function studies of β-catenin within the secondary heart field found Wnt signalling to be important in regulating growth of cardiac progenitor cells such as the cells of the right ventricle and interventricular myocardium (Ai et al., 2007).

Most recently, however, a model proposing four distinct roles for Wnt signalling during the first three days of zebrafish development has been proposed. Dohn and Waxman (2012) have further clarified the role of Wnt signalling in the regulation of cardiomyocyte formation in the zebrafish. Zebrafish paralogs of Wnt8a are required and sufficient to promote specification of both atrial and ventricular cardiomyocytes in the pre-gastrula embryo, which occurs indirectly through the promotion of the ventro-lateral mesoderm. During gastrulation and early somitogenesis the pre-cardiac mesoderm is sensitive to Wnt signalling, which has a second function at this stage inhibiting cardiomyocyte differentiation and may subsequently lead to their death through a p53/Caspase-3 independent mechanism. The length of this second “phase”, where cardiomyocyte progenitor specification is inhibited by Wnt signalling was previously unknown (Ueno et al., 2007), but it now seems that the pre-cardiac mesoderm is sensitive to increased Wnt signalling for a long time period extending from early gastrulation to the onset of somitogenesis (Dohn and Waxman, 2012). During cardiomyocyte differentiation a third “phase” is active, where Wnt signalling promotes additional specification and differentiation of atrial progenitors (Dohn and Waxman, 2012). These data, combined with the knowledge that Wnt signalling prevents proliferation of differentiated ventricular cells (Rottbauer et al., 2002), have led Dohn and Waxman to propose a model whereby cardiomyocytes respond to four distinct phases of Wnt signalling during the initial three days of zebrafish development: (1) promotion of cardiomyocyte development in pre-gastrula embryos, (2) restriction of

cardiomyocyte development in the pre-cardiac mesoderm, (3) promotion of specification and differentiation of atrial progenitor cells, and (4) repression of proliferation of differentiated ventricular cells (Dohn and Waxman, 2012).

1.4.4 Nodal and Notch signalling in heart development

The zebrafish mutant *one-eyed pinhead (oep)*, in which a Nodal signalling co-factor is lost, has consequential cardiac defects indicating a role for Nodal signalling in heart development. *Oep* mutants have a greater loss of ventricular cardiomyocytes than atrial cardiomyocytes, indicating that Nodal signalling may be responsible for assigning a ventricular fate to cardiac progenitors (Reiter et al., 2001; Keegan et al., 2004). Nodal signalling is required for correct cardiac formation, and loss and gain of function experiments in both mice and zebrafish have shown the requirement for Notch activity to induce Nodal expression and determine the left/right axis (Raya et al., 2003).

1.5 Cell-cell adhesion

Junctional complexes are required to maintain the structural integrity and functionality of cells, tissues, and organs. Individual cells have several junctional complexes to mediate the requirements for communication and adhesion, i.e. adherens junctions, desmosomes, gap junctions and tight junctions. Gap junctions are essential for communication, whereas adhesion between individual cells is mediated by desmosomes, adherens and tight junctions. The components of these junctional complexes have a wide variety of functions and hence disruption to formation of cell-cell junctions can have far-reaching consequences and roles in numerous diseases.

1.5.1 Desmosomes

Desmosomes are intercellular junctions that provide strong adhesion between cells in tissues that undergo a high level of mechanical stress (for example cardiac muscle tissue), and hence require a high level of adhesion to maintain their integrity. Desmosomes link intracellularly to the intermediate filaments, and this complex (the desmosome-intermediate filament complex) provides the network

responsible for maintaining the strength and integrity of tissues. Structurally, desmosomes can be divided into three sections: the desmoglea (extracellular core region), the outer dense plaque (ODP) and inner dense plaque (IDP). The desmosome is composed of several different proteins, with the major components being the desmosomal cadherins (desmogleins 1-4 and desmocollins 1-3), members of the armadillo protein family (plakoglobin and plakophilins 1-3) and the plakin linker protein desmoplakin, which anchors the intermediate filaments. Desmogleins and desmocollins mediate adhesion via their extracellular domains, and their cytoplasmic tails interact with the desmosomal plaque proteins. The outer dense plaque is composed of the cytoplasmic tails of the desmosomal cadherins which bind to members of the armadillo and plakin families (Figure 1.6).

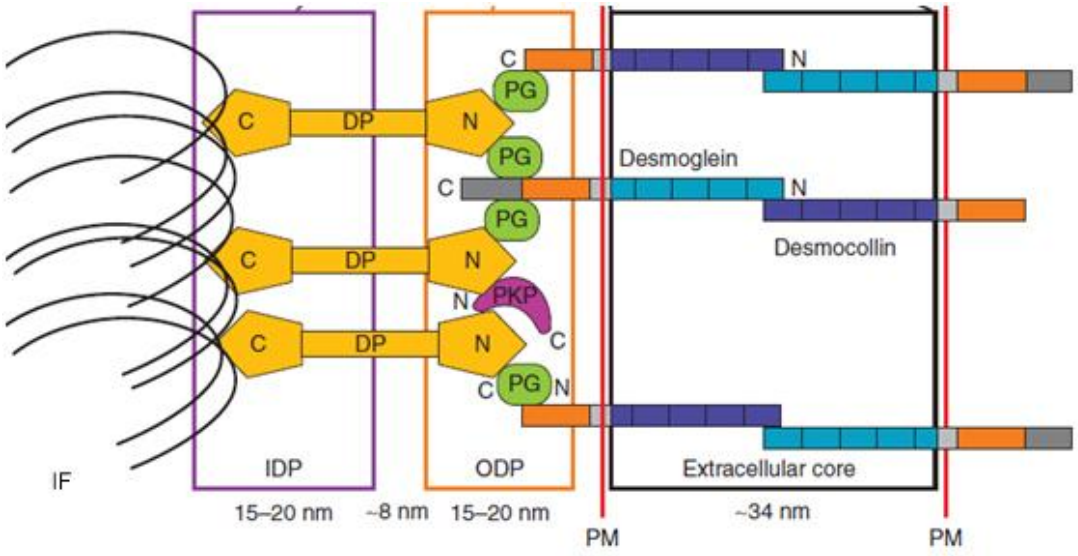

Figure 1.6 Structure of desmosomes.
Schematic of desmosomal proteins and relative distance from the plasma membrane (PM). The desmosomal cadherins (desmogleins and desmocollins) extend into the extracellular core and outer dense plaque (ODP) to establish contact and adhere to neighbouring cells in a Ca^{2+}-dependent manner. The cadherin cytoplasmic tails associate linker proteins, plakoglobin (PG), the plakophilins (PKP), and desmoplakin (DP). DP binds to the intermediate filaments (IF) within the inner dense plaque (IDP), serving to tether the intermediate filaments to the plasma membrane (adapted from Kottke et al., 2006; Delva et al., 2009).

1.5.2 Plakoglobin

Plakoglobin (also known as junctional plakoglobin (JUP) or γ-catenin) is an 83 kDa member of the armadillo (ARM) protein family and a major component of both adherens junctions and the outer dense plaque of desmosomes. Armadillo proteins have a central "armadillo" domain consisting of a series of imperfect repeats of about 40 amino acids, flanked by distinct amino- and carboxy- terminal domains. Plakoglobin shares a high level of structural and functional similarity with another of the armadillo proteins, β-catenin. The central arm domains of human plakoglobin and β-catenin have 83% amino acid similarity while the N- and C-terminal tails share 57% and 15% similarity respectively, with this disparity between tail domains thought to be responsible for their ligand specificity (Williams et al., 2000; Solanas et al., 2004). Zebrafish plakoglobin has over 79% similarity to the central arm domain of human plakoglobin, with considerably lower similarity at the tail domains (42% at the N-terminal and a mere 9% at the C-terminal) (Cerda et al., 1999). Both β-catenin and plakoglobin are responsible for binding the cytoplasmic tail of adherens junction cadherins and linking them to the actin cytoskeleton, with α-catenin mediating this linkage (Nelson, 2008). In adherens junctions E-cadherin binds to plakoglobin in the region containing ARM repeats 4 and 5 (McCrea et al., 1991), whereas N-cadherin binds to the region where repeats 7 and 8 are found (Knudsen and Wheelock, 1992). In desmosomes, plakoglobin has a fundamental role in promoting the clustering of desmosomal cadherins and linking them to the cytoskeleton via desmoplakin, and is required for effective anchorage of the intermediate filaments (Acehan et al., 2008; Swope et al., 2012b). Desmocollin and desmoglein (the desmosomal cadherins) bind to the central arm domain of plakoglobin in a similar manner to the cadherin components of adherens junctions. Despite the high level of functional overlap between plakoglobin and β-catenin, the latter has been more extensively studied.

In zebrafish plakoglobin protein has been detected at all developmental stages with increased expression between 12 and 24 hpf. Interestingly, plakoglobin and β-catenin are co-localized in the developing embryo until 12 hpf, and at 24 hpf distinct cardiac domains of expression for each protein become visible, likely due to

the requirement for plakoglobin in the desmosomes. Structurally, β-catenin is an essential component of adherens junctions, whereas plakoglobin is found in both adherens junctions and desmosomes (Martin and Grealy, 2004). Loss of plakoglobin causes problems with cardiac development, with plakoglobin knockdown embryos showing smaller hearts, reduced heart rate, cardiac oedema and blood pooling (Martin et al., 2009).

1.5.3 Plakophilin-2

Plakophilins are a subgroup of armadillo proteins that are members of the $p120^{ctn}$ family (reviewed by Hatzfeld, 2005; reviewed by Hatzfeld, 2007). The plakophilin subgroup comprises of three members: plakophilins 1, 2 and 3. In addition to their role as components of the submembrane plaque of intercellular junctions (including desmosomes and the cardiac area composita) plakophilins can also be found in the cytoplasm and the nucleus (Mertens et al., 1996; Schmidt et al., 1997; Schmidt et al., 1999; Godsel et al., 2004; Franke et al., 2006).

Plakophilin-2 is similar in sequence to its sibling proteins 1 and 3, with each composed of a basic N-terminal head domain followed by a series of imperfect arm repeats and a short C-terminal tail (Bonne et al., 1999). Plakophilins 1-3 are constituents of the desmosomal plaques where they associate tightly with other armadillo proteins, cadherins and desmoplakin, linking the C-termini of the desmosomal cadherins to the N-terminus of desmoplakin which then binds the intermediate filaments of the cytoskeleton (McGrath et al., 1997). Plakophilin-2 is specifically required for efficient assembly of desmoplakin into desmosomes, by facilitating the association of desmoplakin with PKC-α (required for assembly), and regulating the availability of PKC-α for phosphorylation of other cellular substrates (Bass-Zubek et al., 2008). Plakophilin-2 is the most widely distributed of all the plakophilins, occurring in the desmosomes of all proliferative tissues, in meningiothelia and meningiomas, and in the cardiomyocytes and Purkinje fibres of the heart (Mertens et al., 1996; Mertens et al., 1999; Borrmann et al., 2000; Akat et al., 2003; Borrmann et al., 2006; Franke et al., 2006; Akat et al., 2008). It is also the

only member of the plakophilin family found in the heart, thus demonstrating its importance in the maintenance of cardiac structural integrity.

At a molecular level various roles for plakophilin-2 (PKP2) have been demonstrated. Loss of PKP2 has been linked to sodium current deficit both *in vivo* and *in vitro*. PKP2 haploinsufficiency leads to sodium current deficit and arrhythmogenesis in murine hearts (Cerrone et al., 2012), and loss of PKP2 expression results in decreased sodium current, sodium channel remodelling and increased re-entrant activity in cultured cardiomyocytes (Sato et al., 2009; Deo et al., 2011; Sato et al., 2011). In a colon carcinoma cell line PKP2 has demonstrated an ability to associate with β-catenin and increase Wnt signalling (Chen et al., 2002). Despite these varied reported roles, little is really known about the role of PKP2 in signalling. We have recently shown an association between zebrafish PKP2 and the Nodal signalling pathway, where loss of PKP2 results in complete ablation of *lefty2* in early cardiogenesis, and an increase in expression of several other Nodal pathway genes (Moriarty et al., 2012).

Zebrafish PKP2 is predicted to encode an 815 amino acid protein with nine of the characteristic arm repeats, sharing conserved sites for *N*-glycosylation, myristoylation and GSK-3, CK2 and PKC phosphorylation with mammalian armadillo proteins. It is expressed both maternally and zygotically, with ubiquitous expression during early blastula stages restricting to epidermal and cardiac tissue during gastrulation (Moriarty et al., 2008).

1.6 Arrhythmogenic Right Ventricular Cardiomyopathy

Arrhythmogenic Right Ventricular Cardiomyopathy (ARVC) is a progressive disease, characterised by arrhythmias, fibro-fatty replacement of the myocardium (primarily of the right ventricle) and sudden death (Basso et al., 2009). Arrhythmia in ARVC is proposed to result from conduction block, and the formation of macro re-entry circuits caused by the fibrotic myocardial tissue that results from desmosome dehiscence (Wolf and Berul, 2008). Though it was first described anatomically in 1977 (Fontaine et al., 1977), molecular genetics have since identified the disorder

as primarily autosomal dominant in nature, and a variety of causative mutations within the genes encoding desmosomal components have been reported (Table 1.2), hence ARVC is essentially a disease of the desmosomes. The prevalence of ARVC is estimated to be between 1:2000 and 1:5000, with males more likely to be affected than females (Basso et al., 2009; Herren et al., 2009) yet determination of distribution is hampered by the lack of diagnostic features evident prior to the sudden cardiac death with which ARVC is commonly associated. Interestingly a study recently published on the geographical distribution of ARVC has indicated that prevalence of some mutated genes is dependent on location, which will be discussed further in Sections 1.6.1 and 1.6.2 (Jacob et al., 2012).

Table 1.2 ARVC-related genes

Gene	No. of reported pathogenic mutations	Associated disease phenotypes
Plakophilin-2	131	ARVC
Plakoglobin	13	ARVC; AC; Naxos Disease; cutaneous defects with no associated cardiomyopathy
Desmin	6	ARVC; cardiomyopathy with limb weakness; bi-ventricular cardiomyopathy
Desmocollin-2	32	ARVC
Desmoglein-2	48	ARVC
Desmoplakin	67	ARVC; bi-ventricular arrhythmogenic cardiomyopathy with epidermolytic palmoplantar keratoderma and woolly hair
TGF-beta 3	2	ARVC
TMEM43	2	ARVC
Titin	8	ARVC

Data collated from ARVC gene variants database (www.arvcdatabase.info; van der Zwaag et al., 2009).

1.6.1 Plakophilin-2 and ARVC

Plakophilin-2 is estimated to be the most commonly mutated gene in cases of ARVC, with 131 pathogenic variants of the 224 reported to date and a high

prevalence of mutations in this gene in populations in the USA and the Netherlands (www.arvcdatabase.info; van der Zwaag et al., 2009; Jacob et al., 2012).

Though mutations in some of the other genes discussed here result in cardiac disease with attendant phenotypic defects, plakophilin-2 mutations seem to result in what we may call "pure" cardiomyopathies, where only heart defects occur. Mutations in the plakophilin-2 gene that may result in ARVC include frame-shift, mis-sense and splice-site, yet despite the wide range of reported mutations there are few differences in the clinical symptoms or cardiac phenotypes reported (Syrris et al., 2006). There are however some detectable molecular differences between mutations. Using neonatal rat myocytes one study has compared two N-terminal mutations in plakophilin-2 and identified mutation-dependent differences in the association of PKP2 with connexin 43 and desmoplakin proteins, identifying the N-terminal region between amino acids 79 and 178 of the PKP2 sequence as essential for maintaining these proteins within the same junctional complex (Joshi-Mukherjee et al., 2008). Another plakophilin-2 mutation (a splice-product mutation) located within the ninth arm repeat has been reported to cause ARVC with attendant gap junction remodelling (Tandri et al., 2008). Though there are no observed external phenotypic differences it seems that, on a molecular level, plakophilin-2 mutations encompass a number of structural and localisation defects.

1.6.2 Plakoglobin and ARVC

Unlike plakophilin-2, there are few documented mutations in plakoglobin that result in cardiac defects, with the two best-characterised occurring at opposite ends of the sequence and with disparate effects. An N-terminal serine insertion is associated with ventricular tachycardia and characteristic fibro-fatty replacement of the right ventricle, and examination of protein localisation at the intercalated discs of cardiac myocytes revealed decreased localisation of plakoglobin, desmoplakin and connexin 43 (Asimaki et al., 2007).

A deletion of 2 base-pairs at the C-terminal of plakoglobin results in a frame-shift and premature termination of the protein, which causes a different cardiomyopathy, the autosomal recessive Naxos Disease (named for the island

where it was first identified in 1986). In addition to the characteristic cardiac defects of ARVC, individuals affected by Naxos Disease also display distinctive palmoplantar keratosis and rough bristly hair (Protonotarios et al., 1986; McKoy et al., 2000). Gap junction remodelling is also seen to occur in patients with Naxos Disease, and localisation of both the mutant plakoglobin protein and connexin 43 is altered (Kaplan et al., 2004b). Interestingly, two mutations (splice site and nonsense) in the 5' region have been reported to cause the skin fragility, palmoplantar keratoderma and woolly hair phenotype associated with Naxos Disease, but without the attendant cardiomyopathy that results from the Naxos mutation (Cabral et al., 2010).

The ARVC genetic variants database (www.arvcdatabase.info; van der Zwaag et al., 2009) has catalogued a total of thirteen pathogenic mutations in the plakoglobin gene, four of which have been discussed above. Of the nine additional pathogenic plakoglobin mutations reported, eight are missense mutations occurring at regions throughout the gene from exon 2 to exon 11. The majority of these mutations have been reported in isolation, yet there are two exceptions (van der Zwaag et al., 2009). One of these, T19I, occurs when a threonine residue at position 19 is replaced with isoleucine, manifesting in ARVC (den Haan et al., 2009; Tan et al., 2010; Garcia-Pavia et al., 2011). There have also been multiple reports of missense mutation V159L, a leucine replacement of the valine residue located at position 159 resulting in an arrhythmogenic cardiomyopathy involving both ventricles (Ly et al., 2008; Xu et al., 2010). The final reported mutation is a deletion of three base-pairs towards the N-terminal, detected in an individual with confirmed ARVC in accordance with standard Task Force diagnostic criteria (McKenna et al., 1994; Xu et al., 2010).

Though several plakoglobin-related cardiomyopathies have been well characterised their prevalence world-wide is generally quite rare (with the exception of Denmark, Greece and Cyprus) with incidences of plakoglobin mutations almost negligible in comparison to those of other desmosomal mutations (Jacob et al., 2012). Though plakoglobin mutations are not the most common cause of ARVC the protein does play a central role, as plakoglobin localisation is so universally and specifically

diminished across all forms of ARVC that its distribution has been proposed as a diagnostic test (Asimaki et al., 2009).

1.6.3 Other desmosomal protein mutations

Cutaneous defects like those observed in Naxos Disease are not seen with any of the plakophilin-2 mutations identified to date, yet they are not unique to plakoglobin. A similar condition, also characterised by striated palmoplantar keratoderma, woolly hair and cardiomyopathy, has been identified and linked to a mutation in desmoplakin. Carvajal Syndrome is caused by deletion of a single nucleotide in the tail domain which introduces a premature stop codon and hence truncation of the desmoplakin protein (Norgett et al., 2000). Though Carvajal Syndrome and Naxos Disease are caused by similar mutations of different proteins and have broadly similar phenotypic and clinical presentations there is one key element of the cardiac component that differs - Naxos Disease primarily affects the right ventricle, whereas diagnosis of Carvajal Syndrome involves dilation of the left ventricle (Carvajal-Huerta, 1998). Carvajal Syndrome appears to affect distribution of desmoplakin and other desmosomal proteins, with localisation of desmoplakin, connexin 43 and plakoglobin all diminished in the myocardium of affected patients (Kaplan et al., 2004a).

As in plakoglobin, there are also mutations in desmoplakin that cause cardiomyopathy with no associated cutaneous defects (Navarro-Manchon et al., 2011; Gomes et al., 2012). Though the disease classification of ARVC was primarily based on those cardiomyopathies affecting the right ventricle the increasing number of left-associated cases presenting with otherwise identical disease manifestations and causative genes has led to the expanded classification of Arrhythmogenic Cardiomyopathy (AC) that encompasses both left and right ventricular forms.

Mutations in desmosomal cadherins desmocollin-2 and desmoglein-2 are also associated with ARVC. Desmoglein-2 mutations have a high level of penetrance in reported cases of arrhythmogenic cardiomyopathy with a majority of right ventricle-associated cases (Syrris et al., 2007; Gehmlich et al., 2010; Gehmlich et al.,

2012) and the study of a desmocollin-2 mutation has provided increased understanding of the molecular consequences of ARVC, with patient samples showing changes in the phosphorylation status and localisation of gap-junction protein connexin 43, altered localisation of plakoglobin and desmoplakin, and decreased total protein content for desmoglein-2, desmocollin-2 and plakoglobin (Gehmlich et al., 2011).

1.6.4 Connexin 43

Changes in expression, phosphorylation and localisation of gap junction protein connexin 43 have been reported in many studies on ARVC (Kaplan et al., 2004a; Kaplan et al., 2004b; Asimaki et al., 2007; Joshi-Mukherjee et al., 2008; Tandri et al., 2008; Gehmlich et al., 2011; Gomes et al., 2012). As the major gap junction protein in the heart, connexin 43 is required for cardiac conduction and correct formation of gap junctions (Verheule et al., 1997). In zebrafish embryos connexin 43 mRNA is expressed from 2 hpf onwards, and is detectable in the outflow tract of the developing cardiovascular system from 48 hpf. From 60 hpf to 72 hpf transcripts are localised to the dorso-lateral margins of the heart tube at the ventricle, AV junction and atrium, but not the *sinus venosus*, and cardiac expression appears to cease after this stage (Chatterjee et al., 2005).

1.6.5 Animal Models of ARVC

A good animal model should resemble the required aspects of human physiology, be easily manipulable to recapitulate the main features of the disease phenotype, and have highly conserved molecular pathways to facilitate imitation of molecular aspects of the disease in question. Short generation or maturation time is also extremely advantageous from a research point of view, as is a model that can be maintained at low cost and used for high-throughput studies.

A number of animal models for ARVC have been developed using various techniques. Loss-of-function studies are typically more limited than those of mutations as the importance of the target organ often means that embryonic lethality prevents long-term studies of the developmental defects.

A feline cardiomyopathy that bears close resemblance to human ARVC has been identified, with common domestic cats of various breeds showing enlargement of the right atrium and ventricle, ventricular lesions, apoptosis of the right ventricle wall and repair via fibrous and/or fatty tissue replacement (Fox et al., 2000). Though it is interesting to note the existence of a feline condition, it is of limited use as a model until further study can be done to elucidate the genetic basis. A cardiomyopathy with striking similarities to human ARVC has also been identified in Boxer dogs, with arrhythmias and right ventricular cardiac myocyte replacement by adipose or fibrous tissue. Most strikingly this canine model showed familial inheritance of the disease and sudden cardiac death, which were not seen in the feline model (Basso et al., 2004). A more recent study has identified a deletion in the 3' UTR of the striatin gene as causative for ARVC in Boxer dogs, and has co-localised striatin protein with plakophilin-2, plakoglobin and desmoplakin at the intercalated disk (Meurs et al., 2010). These data suggest that striatin may represent a potentially unidentified causative gene for human ARVC.

Recapitulation of many important features of the human disease phenotype has been shown in several other models. Murine studies on heterozygous plakoglobin-deficient mice have shown that endurance training can accelerate development of right ventricular dysfunction, yet this can be alleviated by pharmacological therapy to reduce the ventricular load (Kirchhof et al., 2006; Fabritz et al., 2011). Though these heterozygous plakoglobin-deficient models mimicked some aspects of the disease, histology and electron microscopy images did not present any evidence for aberrant myocardium or desmosome structure. A plakoglobin-null mouse model has previously been shown to be embryonic-lethal, with mutant embryos showing pericardial oedema, developmental delay and ruptured ventricles. Examination of the junctional ultrastructure of the intercalated disks revealed a loss of desmosomes and changes to the morphology of adherens junctions, which were present with particularly dense, extended plaques (Ruiz et al., 1996). Another study on plakoglobin null mice also demonstrated cardiac defects in developing embryos, including thin, weak myocardium, blood leakage, and reduced numbers of desmosomes. More detailed ultra-structural examination also revealed alterations

of the desmosomes, with less dense plaques and atypical desmoglea observed. Additionally, these plakoglobin-null mice had skin defects including blistering and notably thin epidermis with poor resistance to mechanical stress due to subcorneal acantholysis (Bierkamp et al., 1996).

Two recent publications from the Radice laboratory have reported particularly noteworthy murine models for ARVC using modified knockouts. A tissue-specific knock-out was used to completely ablate cardiac plakoglobin, with the resulting embryos having loss of myocytes, fibrotic replacement of the cardiac tissue and a decrease in the expression of desmosomal proteins plakophilin-2, desmoglein and desmoplakin (Li et al., 2011a). A cardiac-restricted double knock-out (DKO) of catenin proteins β-catenin and plakoglobin also successfully recapitulates several of the hallmark features of the human condition, with DKO mice developing abnormal hearts with enlarged ventricles, cardiomyopathy, myocardial fibrosis, and conduction abnormalities that resulted in cardiac death in all animals (Swope et al., 2012a).

Despite the similarities between these modified knockout models and ARVC (in particular the fibrotic replacement of myocardial tissue) no cardiac adipocytes were detected in either study. Modelling of this final aspect remains elusive, yet it is possible that complete ablation of plakoglobin is not sufficient, and induced mutations in the genes encoding desmosomal proteins may be the only way to achieve a model that emulates this final facet of the disease. It must also be considered that ARVC is a progressive disease, and it may be impossible to model such a late-onset symptom of the cardiomyopathy at relatively early stages of development in experimental animal models. Mouse modelling of plakophilin-2 defects has demonstrated abnormal heart development with blood leakage and cardiac rupture, however embryonic lethality in early development was a limiting factor in this study (Grossmann et al., 2004). Embryonic lethality has also been a limiting factor in a cardiac-specific homozygous desmoplakin knockout, yet heterozygous desmoplakin-deficient mice can survive and emulate key aspects of the human condition including arrhythmias, increased adipose tissue and fibrosis (Garcia-Gras et al., 2006).

Morpholino knockdown has also been used to generate loss-of-function models in zebrafish embryos. Embryos lacking desmosomal proteins plakoglobin or plakophilin-2 had similar cardiac phenotypes, with cardiac oedema, reduced heart rates, blood pooling and kinked tails, and altered desmosome composition and numbers at the intercalated disks (Martin et al., 2009; Moriarty et al., 2012). Plakoglobin knockdown embryos also had small hearts in comparison to controls, and reflux of blood between the heart chambers (probably due to the observed defects in valvulogenesis). Morpholino knockdown of desmocollin-2 resulted in cardiac oedema, brachycardia and altered desmosome structure in morphant hearts (Heuser et al., 2006). Though morpholino-based assays provide valuable data on cardiac development they are limited by the transient nature of the knockdown and so can only provide insights into the early effects, making it impossible to recapitulate the later stage features of a progressive disease such as ARVC.

1.7 Targeted gene knockdown using morpholino antisense oligomers

First described in 1997, morpholino antisense oligomers were championed as a powerful genetic tool capable of blocking protein translation, with such desirable properties as complete resistance to nucleases, good targeting predictability, high *in vivo* efficiency and high sequence specificity (Summerton and Weller, 1997; Summerton, 1999). Morpholinos can be easily delivered to 1-2 cell zebrafish embryos by micro-injection providing a simple and effective knockdown strategy. Since the initial paper describing the efficacy of morpholino knockdown in zebrafish (Nasevicius and Ekker, 2000), the sequencing of the zebrafish genome and an exponential increase in popularity of the technique have greatly aided the study of zebrafish genetics, enabling transient knock-down of numerous zebrafish proteins.

There are two extant strategies for morpholino-based gene knockdown. Morpholinos may be targeted to the AUG or 5’ UTR (untranslated region) to block translation of the mRNA, resulting in maternal and zygotic knockdown of the gene of interest. Though this complete knockdown is perhaps more desirable than the splice method, knockdown can only be confirmed by examining protein expression

and the lack of availability of custom antibodies for zebrafish can in some cases be a limiting factor. The alternative method, splice morpholinos, target splice junctions causing alternative splicing and hence results can be monitored by reverse transcriptase-polymerase chain reaction, but maternal gene expression is unaffected by this approach (Draper et al., 2001).

Morpholino anti-sense oligonucleotides have now facilitated loss-of-function studies for over a decade, and have become one of the most commonly used techniques in zebrafish developmental studies (Draper et al., 2001). The ease of delivery, reliability, and relatively low cost of morpholino oligonucleotides has contributed to their popularity, in addition to the fact that inhibition of protein translation provides a consistent phenotype once a suitable dose has been established.

Though an important and commonly-used tool, there are associated limitations of morpholinos. The transient nature of the knockdown prevents long-term loss-of-function studies. Off-target effects and toxicity are constantly a source of concern with morpholinos, though these can be combated to a large extent by the use of "control" morpholinos. An additional consideration for large-scale studies is the requirement for individual injections to each embryo, which is time-consuming and labour-intensive, particularly when genetic material is required for protein or cDNA-based techniques.

Several techniques have emerged in the last decade that may eventually supersede the use of morpholinos, not least due to their heritable characteristics. TILLING (Targeting Induced Local Lesions in Genomes), is a reverse genetics approach first described in *Arabidopsis* (McCallum et al., 2000) used to identify mutations in specific genes of interest. TILLING in zebrafish has been documented using two different screening methods, Cel1-based detection (Wienholds et al., 2003b; Draper et al., 2004) and the re-sequencing of target genes from single mutagenised fish (Wienholds et al., 2003a; Wienholds and Plasterk, 2004). Cel1-based detection utilises the ability of this extracellular glycoprotein to cleave heteroduplex DNA at all possible single nucleotide mismatches to detect mutations (Oleykowski et al.,

1998). Zinc-finger nucleases (ZFNs), a chimera of zinc-finger protein and the nuclease domain of FokI, have been used to generate heritable targeted gene disruption via the introduction and subsequent imperfect repair of a double-strand break. ZFNs have been used successfully in many model systems including zebrafish (Doyon et al., 2008; Meng et al., 2008). Despite their heritable nature, TILLING and ZFNs have yet to achieve the popularity of morpholinos, due in part to their relatively high cost, and also due to difficulties with specificity and customization. The now-emerging use of transcription-like effector endonucleases (discussed further in Section 1.8) has several promising features as a technique that may yet eclipse the more established TILLING and ZFN methods.

1.8 Targeted genome editing using Transcription Activator-Like Effector Endonucleases

Recent advances have demonstrated the use of transcription activator-like effector endonucleases (TALENs) as a novel technique for targeted, heritable genome editing in zebrafish. Dependent upon the imperfect nature of endogenous DNA repair mechanisms, the TALEN procedure seems to alleviate the problems associated with existing methods. Their heritable nature excludes problems of toxicity, off-target effects and transience associated with the popular method of gene knock-down via morpholinos. In addition, the simplicity of the assembly process permits the synthesis of a virtually limitless number of TALEN constructs with inexpensive materials in-house. The flexibility of design and relatively low-cost of required materials favour TALEN over existing methods such as zinc finger nucleases (ZFNs) and TILLING.

1.8.1 The TALEN mechanism

Nucleases for targeted genome editing have been engineered using a customizable DNA-biding domain, consisting of an array of transcription activator-like (TAL) effector repeats, fused to the nonspecific FokI cleavage domain, and these constructs then bind and cleave DNA in pairs (Figure 1.7).

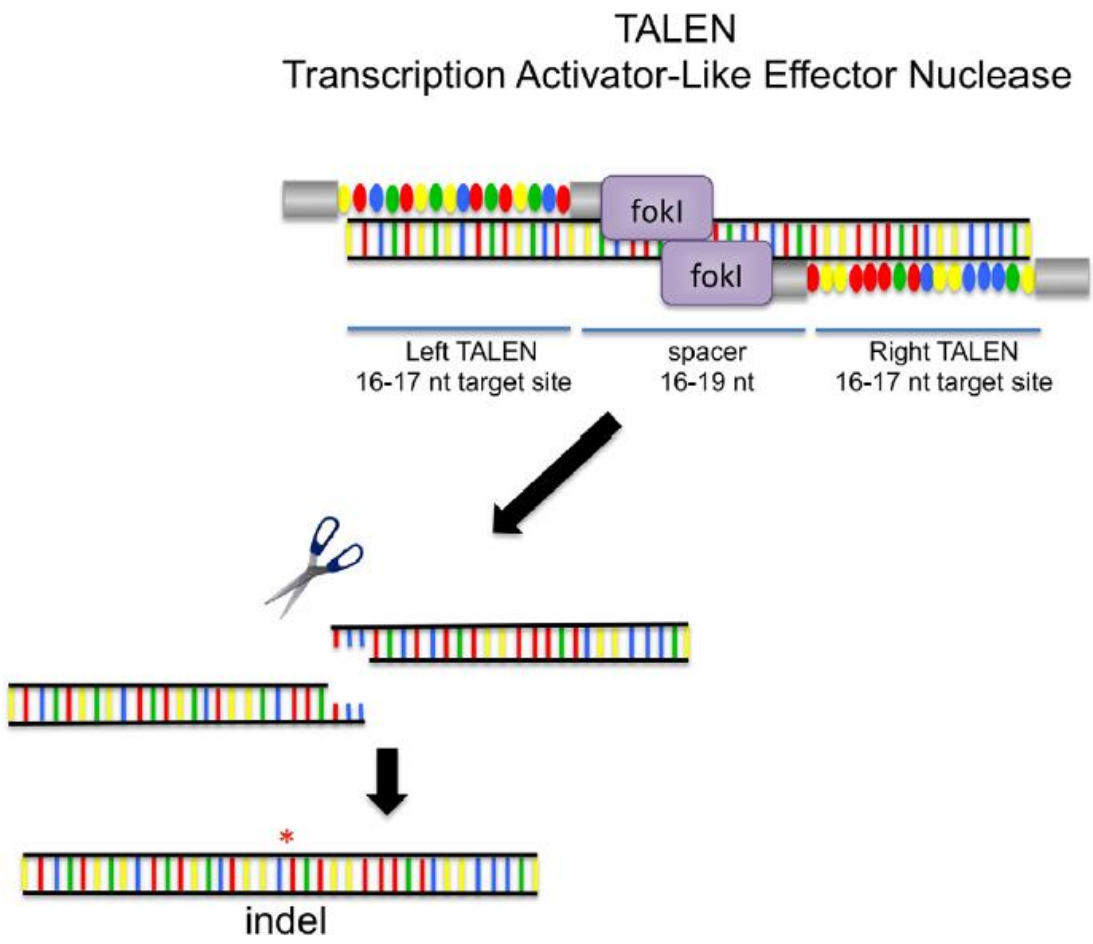

Figure 1.7 Targeted genome editing using TALENs
TALENs bind DNA using TAL effector repeat domains that recognise individual nucleotides. TALE repeats are ligated together, creating binding arrays capable of recognising extended DNA sequences. Coloured ovals represent the DNA-binding domain of the TALEN, with each colour representing a sequence that binds to one of the four nucleotides, enabling the targeting of specific DNA sequences. Each TALEN binds to a half-site with FokI cleaving the DNA within the central spacer region. DNA mutations are introduced by the natural process of DNA repair, and dependent upon its imperfect nature. Nuclease-induced double-strand breaks are repaired by error-prone non-homologous end joining, resulting in the creation of insertion or deletion mutations (*indels). (Adapted from Moore et al., 2012)

TAL effectors are produced by plant pathogens, from the genus *Xanthomonas*, with their native function being to directly modulate gene expression in the host organism (Bogdanove et al., 2010). They are delivered to the nucleus via the bacterial type III secretion system (sometimes referred to as “the injectosome”, a protein appendage found in gram-negative bacteria), after which the TAL-effectors enter the nucleus, bind to effector-specific sequences in host gene promoters and activate transcription.

The specificity of the DNA binding is determined by the central domain consisting of tandem 33-35 amino acid repeats, followed by a single truncated repeat of 20 amino acids, with naturally occurring TAL effectors tending to have 12-27 full repeats (Boch and Bonas, 2010). A polymorphic pair of residues at positions 12 and 13 in each repeat, the 'repeat-variable di-residue' (RVD) has been identified as the region that confers specificity for the target sequence. Each repeat specifies for one targeted nucleotide, with each of the four most common RVDs associating preferentially with one of the four bases. Naturally occurring recognition sites are uniformly preceded by a T which is required for TAL effector activity (Boch et al., 2009; Moscou and Bogdanove, 2009). The simple nature of this sequence relationship has enabled the construction of customised TAL effector repeat domains to bind to DNA sequences of interest (Christian et al., 2010; Morbitzer et al., 2010; Miller et al., 2011; Zhang et al., 2011).

The fusion of TAL effectors with the catalytic domain of the FokI nuclease has been used for *in vivo* genome editing to create DNA double- strand breaks at targeted regions (Christian et al., 2010; Li et al., 2011b; Mahfouz et al., 2011; Miller et al., 2011). FokI cleaves as a dimer, hence these fused constructs of TAL-effectors and FokI act in pairs. The constructs bind to target regions on opposing strands across a spacer region over which the FokI domains come together and induce the break. Repair then occurs in the region of the break; however the imperfect nature of the repair mechanism can result in insertions, deletions or the replacement of bases, i.e. a mutation. Repair of the double-strand break can occur by either one of two processes which are highly conserved, (1)- non-homologous end joining, which is the predominant repair mechanism, but as it can be imprecise, small insertions or deletions can occur in the repaired sequence, and (2)- homologous recombination, which is commonly used for gene targeting to insert or replace the gene of interest (though this does not occur regularly in practice).

1.8.2 Use of TALENs for genome editing

Recently Cermak et al., have adapted the Golden Gate method of cloning to engineer a complete set of plasmids for assembling novel repeat arrays of TALENs

(Cermak et al., 2011). The Golden Gate method utilises the cleavage properties of Type II restriction enzymes to enable digestion and ligation in the same reaction mixture. Type II restriction endonucleases cleave outside their recognition sites, creating unique 3' or 5' overhangs ("sticky ends") that can consist of any nucleotide. Thus, multiple sticky ends can be produced at different DNA fragments in a single reaction (e.g. 256 different overhangs can be created with a Type II restriction endonuclease that cleaves to produce a four nucleotide overhang) (Engler et al., 2008; Engler et al., 2009). It is important to note that the binding sites of Type II restriction endonucleases are directional (i.e. non-palindromic), thus if a fragment is flanked by four nucleotide overhangs and two Type II restriction endonuclease binding sites digestion will produce pre-defined sticky ends on either side. Careful design and selection results in alignment of the digested fragments in a pre-defined order upon ligation (Figure 1.8).

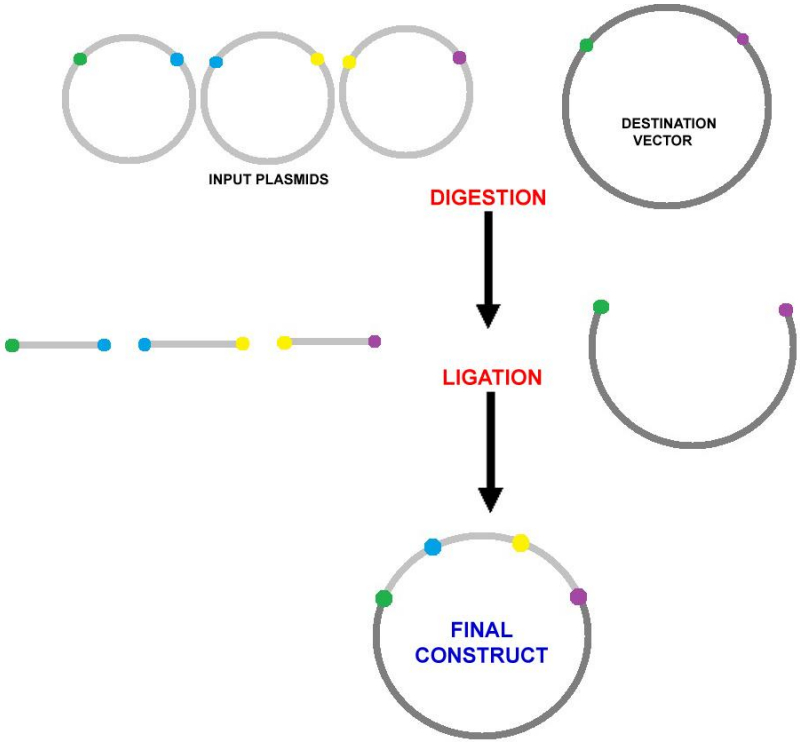

Figure 1.8 Golden Gate cloning mechanism
Schematic demonstrating the basic mechanism of Golden Gate cloning. Input plasmids, destination vector and a Type II restriction endonuclease are mixed together in a single reaction with DNA ligase. Digestion results in unique sticky ends (coloured dots represent these complementary sites), hence careful experimental design permits ordered assembly of the ligated fragments into the destination vector.

Golden Gate cloning is a “one pot” reaction, with fragments, enzymes and ligase all reacting together in a thermocycler. Repeated cycles cause repetitious digestion and ligation of the DNA fragments. In ligation reactions, the digested DNA fragment either re-ligates into the original plasmid, or assembles with the other fragment (the desired result). In Golden Gate cloning, the assembled parts lack the restriction site for type II endonucleases; hence they are trapped within the destination vector. The use of this one step process for multiple ligation reactions has greatly reduced the time required to synthesise customised TALEN constructs, and contributed to the overall efficiency of the TALEN method of targeted genome editing.

The relative simplicity of design, the flexibility of the assay and the cost-effective nature of the TALEN procedure are all important factors that will undoubtedly lead to an increase in the popularity of this technique for genome editing. In addition to this, the heritable nature of the mutations provides a rapid method for the generation of mutant lines, presenting a significant advantage over the more established technique of morpholino micro-injection. An efficiency of up to 25% has been reported for TALEN-based genome editing, placing the technique on a par with more established techniques such as zinc-finger nucleases (Miller et al., 2011). The use of TALENS has already been successfully reported in a number of *in vivo* systems including yeast, human cell lines and zebrafish (Cermak et al., 2011; Huang et al., 2011; Miller et al., 2011; Sander et al., 2011; Bedell et al., 2012).

There are some disadvantages to TALEN targeting in its current form. Current design guidelines specify base composition of target sites and the length of the spacer region, and as naturally occurring target sites are always preceded by a T this is also a requirement. Though adherence to these guidelines for successful targeting may prove unnecessary in time, they are recommended at present and may inhibit the induction of mutations at specific sites where the target sequence does not meet requirements. The other main consideration is the occurrence of germline mosaicism, as the F_1 progeny resulting from TALEN founder fish outcrossed with wild-types carry a variety of mutations within the targeted region (Cade et al., 2012; Dahlem et al., 2012; Moore et al., 2012). This mosaicism, combined with the unpredictable nature of the repair process on which TALEN

targeting depends, does not favour studies in which an exact mutation is required (e.g. induction of a point mutation). Overall however TALEN targeting represents a significant development in forward genome editing and overcomes many of the problems associated with existing methods for *in vivo* genome manipulation.

1.9 Aims of this study

Previous work in our lab has established zebrafish knockdown models for both plakoglobin and plakophilin-2 using morpholino anti-sense oligonucleotides. Loss of plakoglobin revealed both structural and signalling roles for this armadillo protein, with embryos lacking plakoglobin having both developmental defects and up-regulation of Wnt target genes. Knockdown of plakoglobin resulted in embryos with reduced heart size, cardiac oedema, blood reflux between the atrium and ventricle, a decreased heart rate and a twisted tail. Cell junction formation was also affected, with plakoglobin morphant embryos having decreased numbers of desmosomes and adherens junctions. Examination of Wnt target gene expression identified an antagonistic role for plakoglobin in the Wnt signalling pathway (Martin et al., 2009). Knockdown of plakophilin-2 resulted in a similar phenotype of disrupted cardiac development. Embryos lacking plakophilin-2 had decreased heart rates, cardiac oedema, blood pooling, incorrect cardiac patterning and twisted tails, and a decreased number of desmosomes in morphant hearts (Moriarty et al., 2012).

This study aims to elucidate further the signalling roles of plakoglobin and plakophilin-2 in zebrafish development, and develop an improved zebrafish model for ARVC by generating a plakoglobin mutant line using TALENs. The specific aims were:

1. To further examine the interactions between plakoglobin and Wnt signalling
2. To identify a signalling role for plakophilin-2 during cardiac development
3. To evaluate plakoglobin and plakophilin-2 morphant embryos as molecular models for the congenital heart condition arrhythmogenic right ventricular cardiomyopathy
4. To develop a zebrafish plakoglobin mutant using TALEN targeting and assess the resulting phenotype.

2 Materials and Methods

2.1 Materials

2.1.1 Zebrafish

Zebrafish is the common name of the *Danio rerio; Eukaryota; Metazoa; Chordata; Craniata; Vertebrata; Euteleostomi; Acrinoptrygii; Neopterygii; Teleosteri; Euteleosteri; Ostariophysi; Cypriniformes; Cyprinoidea; Cyprinidae; Rasborinae; Danio*. Zebrafish AB adult fish were obtained from the Zebrafish International Resource Centre at Eugene, Oregon. Transgenic zebrafish (*cmlc2*:eGFP-*ras and* apc^{mcr} lines) were obtained as a gift from the Stainier lab at University of California, San Francisco (UCSF).

2.1.2 Chemicals and laboratory plastics

All chemicals were of standard analytical grade. Distilled water was used in preparation of solutions.

The following chemicals were purchased from Sigma Aldrich (www.sigmaaldrich.com); acrylamide/bisacrylamide, ammonium acetate, ammonium persulphate, ampicillin, benzyl alcohol, benzyl benzoate, bovine serum albumin (BSA), bromophenol blue, calcium chloride, chloroform, chloroform/isoamylalcohol 24:1, Coomassie blue R-250, developer, diethyl pyrocarbonate (DEPC), dithiothreitol (DTT), 1,1,2-trichloro-trifluorethane (Freon), ethanol, ethidium bromide, ethylene diamine tetra acetic acid (EDTA), ethylene glycol tetra acetic acid (EGTA), fixer, formaldehyde, formamide, glucose, glycerol, glycine, 5-bromo-4-chloro-3-indolyl β-D-galactose (X-gal), hydrochloric acid, isopropanol, isopropyl-β-D-thio-galactopyranoside (IPTG), Luria Bertani (LB) agar, LB broth, magnesium chloride, magnesium sulfate, methyl cellulose, 3-[N-Morpholino]propanesulfonic acid (MOPS), paraformaldehyde, phenol, phenylthiourea (PTU), phosphate buffered saline tablets (PBS), phenylmethylsulphonyl fluoride (PMSF), polyoxyethylenesorbitan monolaurate (Tween 20), Ponceau S solution, potassium chloride, potassium sulphate, protease inhibitor cocktail, sheep serum, sodium bicarbonate, sodium chloride, sodium dodecyl sulphate (SDS), sodium hydroxide, N,N,N',N'-Tetramethylethylenediamine (TEMED), tricaine, tris(hydroxymethyl)aminomethane (Tris) , triton X-100.

Multi-purpose agarose, BM purple AP substrate, Anti-digoxigenin-AP Fab fragments and SP6/T7 digoxigenin-labelling kit were purchased from Roche (www.roche.com). New England Biolabs supplied the 1 kb and 500 bp ladders (www.neb.com). Protein marker was purchased from Biorad (www.bio-rad.com). Promega (www.promega.com) supplied the RNA marker, 10x *Taq.* buffer, magnesium chloride, and nuclease-free water. Pipette tips, microcentrifuge tubes, centrifuge tubes and Petri dishes were supplied by Sarstedt (www.sarstedt.com). Capillary Eppendorf tips were supplied by Eppendorf (www.eppendorf.com) and glass capillaries from Narishige (www.narishige.co.jp). Glass Pasteur pipettes were purchased from Labkem (www.labkem.ie). Kodak Film was purchased from Sigma Aldrich. Supersignal west pico chemiluminescent substrate was purchased from Pierce (www.pierce.com). Trizol reagent was manufactured by Invitrogen. Low fat powdered milk was commercially available. ZM-000 to ZM-500, sea salts and *Artemia* were supplied by ZM Ltd (www.zmsystems.co.uk). SYBR-green Fast qPCR mix, 96-well optical plates and film lids were purchased from Applied Biosystems. Random hexamers were supplied by Invitrogen. Takara LA Taq polymerase was obtained from Clontech.

2.1.3 Oligonucleotides and markers

Oligonucleotides were supplied by Eurofins MWG Operon (www.eurofinsdna.com).

Table 2.1 Oligonucleotides

Gene	Oligo name	Sequence (5' – 3')
β-actin	β-actin forward	ACG CTT CTG GTC GTA CTA
	β -actin reverse	GAT CTT GAT CTT CAT GGT
β -catenin	β -cat F1 forward	CGC TGC GGG TTG TTC TCT CAC A
	β -cat R1 reverse	TCA CAG CCG GGC ACA GCT ACT A
Bone morphogenic protein 4 (bmp4)	Bmp4f1 forward	GCG AGC GAA ACG CAG CCC TA
	Bmp4r2 reverse	ATC CAG GCG GCG CCA CAA TC
Connexin 43	Cxn43F3 forward	TCC ACG CCG ACG CTC CTG TA
	Cxn43R3 reverse	ATG GAG CTC AAC GTC GCC GC
Desmoplakin-a	Dsp-aF1 forward	TGG CGG TTC AGA AGC GAG CT
	Dsp-aR1 reverse	TTT CCG CAG CTG ATC CAT GGC G
Dharma	dhaF4 forward	GCT CGA GCG ACT CTT CGC GG
	dhaR4 reverse	TCC TCG CTG AGG CCC GTG TT
Elongation factor 1-α (EF1-α)	EF1 forward	GTG GTA TCA CCA TTG ACA TTG C
	EF1 reverse	TCA GCC TGA GAA GTA CCA GTG A
Lefty 1	Lefty1F forward	TGG ATC ATC GAG CCG TCC GGT
	Lefty1R reverse	CGG CAG CCG CCT TTA CAC CT
Lefty 2	Lefty2F forward	CGG AGG CAC CAC AGG CCG AT
	Lefty2R reverse	GGC CTG GGT CAC GTC GAA GC
Nodal-related 1 (ndr1)	Ndr1-F2 forward	AGT TTT GGC CCT CGC GGT CG
	Ndr1-R1 reverse	GAT GTC GGC CGT GAC CTG CC
One-eyed pinhead (oep)	oepF forward	TCG AGT CAG GAT GTG AGG GGT CA
	oepR reverse	TTG ACG TTG CGG CGT TTG CG
Pitx2c	Pitx2cF forward	CGC CGC TTT CGA TGG CCT CT
	Pitx2cR reverse	TCT TTC TCT ACG GAC TCT GGA CTG G
Plakoglobin	PG-F1 forward	AAC GTC AAG CGT GTG GCA GCT
	PG-R1 reverse	AGC AGC ATA GGT GGC GAT CCC T
PPAR-γ	PPAR-gF forward	AGA CGT TTG GCT GGC CCG TG
	PPAR-gR reverse	GCG AGT GCG TGT CGT CCT CC
Southpaw (spaw)	spawF forward	AGA CCG GGT CAC GGC ACC A
	spawR reverse	CGC TTC CAC TTC CAC TGC CCT G
Wnt1	Wnt1F forward	AGG ACC GTT TTG ACG GCG CA
	Wnt1R reverse	TGC GCT GGG TTT TCT GGT TCC A
Wnt5b	Wnt5bF forward	AAG CAC AGG TTT TTG CTC GGG A
	Wnt5bR reverse	TGC AAA GCG CCT CCT CAG ATG G

Table 2.2 Oligonucleotides for TALEN experiments

Primer	Sequence (5'-3')
PGexon4F	CGT GTG AGG GCG GCC ATG TT
PGexon4R	AGA TGG TTC GGC CAG CTT CTG T
PGexon15F	TGC AGG ATA CGG TGG ATA TGC TG
PGexon15R	TCT GGC CAT GGA GTT GTA GGG CA
pCr8F1	ttg atg cct ggc agt tcc ct
pCR8_R1	cga acc gaa cag gct tat gt
TAL_F1	ttg gcg tcg gca aac agt gg
TAL_R2	ggc gac gag gtg gtc gtt gg
HRM_PGexon4F	CGG CCA TGT TTC CTG AGA CT
HRM_PGexon4R	CTG TAC ATT GGT CTG CTG GGA
HRM_PGexon15F	CCT GCA GGA TAC GGT GGA TA
HRM_PGexon15R	ATG CCG CCC CTA TAA TCG TC

Oligonucleotides designed specifically for this study are capitalised, those used as standard for TALEN construction are shown in lower-case lettering.

Table 2.3 Molecular Markers

	Fragment size	Supplier
1 kb	10, 8, 6, 5, 4, 3, 2, 1.5, 1, 0.5 kb	New England Biolabs
100 bp	1517, 1200, 1000, 900, 800, 700, 600, 500, 400, 300, 200, 100 bp	New England Biolabs
Prestained protein marker	250, 150, 100, 75, 50, 37, 25, 20, 15, 10 kDa	Biorad

2.1.4 Enzymes and kits

Restriction enzymes (with buffers) were purchased from New England Biolabs. Proteinase K was purchased from Invitrogen. Plasmid preparation kits (maxi and mini), PCR purification kit and gel extraction kit were obtained from Qiagen. SP6/T7 mMESSAGE mMACHINE kit, MEGAclear kit and the DNaseI enzyme and buffer were purchased from Ambion. pGEM-T Easy kit was purchased from Promega.

2.1.5 Morpholinos and antibodies

Morpholinos were purchased from GeneTools, Oregon (www.gene-tools.com).

Table 2.4 Morpholino oligonucleotides

Morpholino name	Sequence
Plakoglobin anti-sense	GAGCCTCTCCCATGTGCATTTCCAT
Plakoglobin 5 bp mismatch control	GA**C**CCTCT**G**CCAT**C**TG**G**ATTT**G**CAT
Plakophilin-2 anti-sense (5'UTR)	GTCACCTCTCCAAAGATCGTGTTTC
Plakophilin-2 5 bp mismatch control	GT**G**AC**C**TCT**C**CAAA**C**ATCGT**C**TTTC

Table 2.5 Antibodies

Primary Antibodies			
Antigen	**Host Species**	**Isotype**	**Supplier**
Anti-Plakoglobin	Mouse	IgG_{2a}	BD Bioscience
Anti-α-tubulin	Mouse	IgG_1	Sigma
Anti-Connexin43	Rabbit	IgG_1	ProteinTech
Secondary Antibodies			
Antigen	**Host Species**	**Conjugate**	**Supplier**
Anti-rabbit IgG	Goat	Peroxidase	Sigma
Anti-mouse IgG	Goat	Peroxidase	Sigma

Table 2.6 Whole Mount In-Situ Probes

In situ probe	Sense or antisense	Restriction enzyme	Transcription Polymerase	Reference
Bmp4	Antisense	Xba I	T7	Yost lab
Boz	Antisense	BG1 III	Sp6	Hirano lab
Squint	Antisense	BamHI	T7	Dawid lab
Lefty1	Antisense	EcoR I	T7	Thisse lab
Lefty2	Antisense	Mlv I	T7	Thisse lab

2.1.6 Equipment

Zebrafish tanks and filters were supplied by Western Aquatics. LSM incubator and MSE Sonicator were supplied by Mason Technologies. Cell-vu slides were supplied by Fisher. Narishige supplied an IM 300 microinjector and needles. Model P-97 Flaming Brown pipette puller was purchased from the Sutter instrument company. Electrophoresis gel apparatus AE-6450 was from Atto Instruments. Western semi-dry transfer system was supplied by CBS Scientific Co. and powered by a Powerpac 200 power supply. The platform shaker was manufactured by Grant Boekel. The bag sealer was manufactured by Russell Hobbs. The waterbath was manufactured by Grant. Reagents were weighed using a Mettler Toledo balance. Pipetteman pipettes were supplied by Gilson. The pH of solutions was determined using a Mettler Toledo pH meter. The Eppendorf microcentrifuges used were the 5415R and 5415D bench centrifuges. QBT1 Grant & Stewart heating blocks were used. The PCR machine, PTC-200 Peltier Thermal Cycler, was manufactured by MJ Research. The UV transilluminator was manufactured by UVP. Gel images were captured using an Ingenius gel documentation system from Syngene in conjunction with GeneSnap software. Nucleic acid quantification was performed using a Nanodrop spectrophotometer ND-1000. Embryos were examined using Nikon SMZ645 microscopes. Quantitative PCR was performed using an ABI 7500 Fast qPCR machine from Applied Biosystems. An Eco Illumina PCR machine was used for high resolution melt analysis experiments.

2.2 Methods

2.2.1 Zebrafish maintenance

Unless stated all solutions and protocols used in the care and maintenance of the zebrafish were taken from The Zebrafish Book (Westerfield, 1995). Adult zebrafish were housed at a stocking density of approximately 20 fish per 20 litre tank and fed thrice daily. Morning and evening feeds consisted of ZM500 ground food, and in the afternoon a feed of live *Artemia*. *Artemia* cysts (3 g) were incubated with 70 g of Instant Ocean salt in a 1 litre hatchery for a minimum of 24 hours with strong aeration at a constant temperature of 28°C. Fish were maintained at 28°C on a 14:10 light : dark cycle. Fish were spawned once a week in spawning trays (20 cm X 9 cm) by placing male fish in the tray with a female placed in a mesh insert above on the evening prior to spawning. Male and female fish were mixed together in the upper insert after lights turned on the following morning. Embryos were collected from the bottom of the spawning trays and cultured in 90 cm Petri dishes (approximately 50 embryos per dish). Embryos were incubated at 28°C in E3 medium (5 mM NaCl, 0.17 mM KCl, 0.33 mM $CaCl_2$, 0.33 mM $MgSO_4$, and 10 ppm Methylene Blue) if being cultured to adulthood for breeding or in filter-sterilised egg water (60 µg/ml stock salts in distilled water) if used for experiments. Fish housing tanks were washed weekly while the fish were on to spawn, with all tanks being washed once monthly with a solution of Milton sterilising fluid and water. Filters were thoroughly rinsed with water and tanks were re-filled using dechlorinated tap water.

2.2.2 General experimental preparation

All pipette tips and microcentrifuge tubes were autoclaved and bench surfaces were wiped with 70% ethanol. Gloves were worn and changed regularly to prevent RNase contamination in molecular experiments. Nuclease-free water was used in all molecular experiments for re-suspension of nucleic acids, dilutions and PCR mixes.

2.2.3 Gene knockdown

Morpholinos to block translation of the plakoglobin and plakophilin-2 proteins had previously been designed and optimised by Drs. E.D. Martin and M.A. Moriarty respectively. A 5-base pair mismatch control morpholino for each gene of interest was used for controls in all experiments unless otherwise stated. Wild-type un-injected embryos from injection days were also monitored alongside morpholino-injected embryos as an additional control.

Microinjection protocol

Glass capillaries were used to make microinjection needles using a Flaming-Brown pipette puller programmed as follows: 300 units heat, 8 units of pull force and a velocity of 50 m/s.

Morpholinos were diluted to a final concentration of 5 ng/nl in nuclease-free water and a 0.05% solution of phenol red stock solution (0.0014M phenol red and 0.2M KCl). Solutions were backloaded in microinjection needles using an Eppendorf microloader pipette tip. The microinjection needle was then fitted in the microinjection apparatus (Narishige IM-300 microinjector) set at a pressure of 40 psi. Injection volume was calibrated to 1 nl by adjusting the injection time to release a drop of 1 nl as measured on a gridded Cell-vu slide.

Injection trays were prepared by pouring a 1.2% agarose solution into 90 cm Petri dishes with microinjection needles used to mould rows to hold embryos in a fixed position for injecting. Freshly fertilised embryos were lined up in these rows. All embryos were injected at the 1-cell stage with a constant injection volume of 1 nl. Phenol red was used in the vehicle as a means of visualising the injection bolus. Control embryos were those injected with control morpholino only and wild-type sibling embryos were also monitored as additional controls. Embryos were allowed develop until the appropriate developmental stage.

2.2.4 RNA extraction and cDNA synthesis

Isolation of total RNA

Embryos were harvested at the desired developmental stage in batches of 50-150. Trizol reagent was used to extract RNA from the whole tissue, with 100 µl of Trizol being added per 20 embryos in a 1.5 ml microcentrifuge tube. A sterile 1 ml syringe and needle (21G) were used to shear the tissue which was then incubated for five minutes at room temperature. Chloroform (200 µl per 1 ml Trizol) was then added and samples were vortexed immediately and incubated at room temperature for three minutes. Samples were then centrifuged at 4 °C for 15 minutes at a force of 12,000 g.

The resulting upper aqueous phase was transferred to a fresh pre-cooled 1.5 ml microcentrifuge tube. Isopropanol was added (500 µl per 1 ml Trizol) and the samples were incubated at room temperature for 10 minutes. Tubes were then centrifuged for a further 10 minutes at 12,000 g and 4°C. The supernatant was removed and the pellet was washed with 100 µl of 75% ethanol (pre-chilled on ice). Tubes were vortexed and centrifuged at 12,000 g for 10 minutes at 4 °C. The ethanol supernatant was then removed and the pellet was left to air-dry for 5-10 minutes. The RNA pellet was re-suspended in 88 µl of DEPC water and incubated at 55°C for 10 minutes.

The RNA solution was DNase treated by adding 10 µl DNase buffer and 2 µl DNase enzyme, and samples were incubated at 37 °C for ten minutes. All samples were then diluted to a total volume of 400 µl by addition of 200 µl phenol, 80 µl of nuclease-free water and 20 µl of 3 M sodium acetate. Samples were thoroughly mixed and centrifuged at 13200 g at a temperature of 4 °C for five minutes. The supernatant was then transferred to a new microcentrifuge tube to which 200 µl of chloroform : isoamyl alcohol (24:1) was added and tubes were vortexed. This chloroform : isoamyl alcohol step was repeated, and the resulting supernatant was once again transferred to a fresh tube. Isopropanol (200 µl) was added to the supernatant, and the samples were then incubated at -70°C for twenty minutes. Tubes were then centrifuged for a further 30 minutes at 13,200 g and 4°C. The

supernatant was then removed and the RNA pellet was washed with 200 µl of a pre-chilled 70% ethanol solution. Tubes were centrifuged for 5 minutes at 13,200 g and 4°C. The ethanol supernatant was then removed and the pellet was left to air-dry for 5-10 minutes before re-suspension in 8 µl of nuclease-free water and stored at -70°C. The total RNA concentration and quality was determined by spectrophotometry.

cDNA synthesis

Total RNA was reverse transcribed using random hexamers. The reaction mixture contained 1 µg of total RNA, 0.5 µM random hexamers, 4 µl of Superscript II first strand buffer (50 mM Tris-HCl, 75 mM KCl, 3 mM $MgCl_2$), 2 µl of 0.1 M DTT, 10 µl nuclease-free water, 1 µl of 10 mM dNTP mix and 1 µl of the reverse transcription polymerase. The reaction was incubated for 1 hour at 42°C and then 15 minutes at 70°C to heat inactivate the enzyme. cDNA was stored at -20 °C.

2.2.5 Polymerase Chain Reaction

RT-PCR protocol

Polymerase chain reactions consisted of a 50 µl reaction mixture containing 1X reaction buffer (50 mM KCl, 10 mM Tris-HCl, 0.1% Triton X-100), 200 µM of dATP, dCTP, dGTP, dTTP, 1.5-4 mM $MgCl_2$, 10 pmoles of forward primer, 10 pmoles of reverse primer, 1.25 Units of *Taq* DNA polymerase and 0.6 µg of template cDNA. Annealing temperatures varied depending on primers used. The elongation time chosen was based on the length of DNA to be amplified. Negative controls were included for all reactions, with the template cDNA replaced by nuclease-free water.

The programme for a typical polymerase chain reaction featured a 30 second denaturation step at 95°C, a 30 second primer annealing step and an elongation step at 70 °C (1 minute per 1 kb of DNA to be amplified). This programme was repeated for 29-34 cycles and followed by a final 10 minute extension step at 70 °C.

The NCBI Primer-BLAST programme (http://www.ncbi.nlm.nih.gov/tools/primer-blast) was used to design primers for DNA amplification. Primers were designed at a

length of 20-25 base-pairs, with a GC content of 40 -60% and without inverted repeats or complementary sequences.

Quantitative RT-PCR

Quantitative reverse transcription PCR was performed using a protocol adapted from "High Throughput Real-Time Quantitative Reverse Transcription PCR" from Current Protocols in Molecular Biology (Bookout et al., 2006). SYBR Green chemistry and the $\Delta\Delta C_T$ method were used for all assays.

Primer design and validation

Primers were designed to meet the specific requirements for quantitative RT-PCR, with a 40-60% GC content and melting temperatures of approximately 60 °C. Oligonucleotides containing runs of the same nucleotide, repetitive sequences or more than two G or C bases at the 3' end were deemed unsuitable. Primers were also designed to produce an amplicon of 50 – 150 bases in length. Primer validity was assessed using a standard cDNA dilution series from which linear regression curves were plotted. A primer set with a slope of -3.3 $\pm$ 0.1 was deemed valid for use in further experiments.

Template cDNA (synthesis as described in Section 2.2.5) was serially diluted to give a range of concentrations from 50 – 0.08 ng/µl. A 5 µl aliquot of each cDNA concentration was then added to a microcentrifuge tube on ice. A 35 µl aliquot of reaction mixture with final concentrations of 1X SYBR Green mix and 150 nM of both forward and reverse primers for the gene of interest (GOI) was then added to each cDNA concentration and this mixture was vortexed and pipetted in triplicate into the 96-well optical plate. No-template controls (NTC) were also prepared in which nuclease-free water was substituted for the cDNA solution. As an additional control a sample set was prepared using a previously validated primer set (for reference gene EF1-α), which was then assayed on the same plate as the primer set(s) to be validated. A sample plate layout is shown in Figure 2.1. Once successfully validated to meet the specified parameters a primer set was deemed suitable for use in quantitative PCR assays.

50ng /µl **EF1-α**	50ng /µl **EF1-α**	50ng /µl **EF1-α**	10ng/ µl **EF1-α**	10ng/ µl **EF1-α**	10ng/ µl **EF1-α**	2.0ng /µl **EF1-α**	2.0ng /µl **EF1-α**	2.0ng /µl **EF1-α**	0.4 ng/µl **EF1-α**	0.4 ng/µl **EF1-α**	0.4 ng/µl **EF1-α**
0.08 ng/µl **EF1-α**	0.08 ng/µl **EF1-α**	0.08 ng/µl **EF1-α**	NTC **EF1-α**	NTC **EF1-α**	NTC **EF1-α**	50ng/ µl **GOI**	50ng/ µl **GOI**	50ng/ µl **GOI**	10ng/ µl **GOI**	10ng/ µl **GOI**	10ng /µl **GOI**
2.0ng /µl **GOI**	2.0ng /µl **GOI**	2.0ng /µl **GOI**	0.4ng /µl **GOI**	0.4ng /µl **GOI**	0.4ng /µl **GOI**	0.08 ng/µl **GOI**	0.08 ng/µl **GOI**	0.08 ng/µl **GOI**	NTC **GOI**	NTC **GOI**	NTC **GOI**

Figure 2.1 Sample plate layout for validation of qPCR primers
Template cDNA concentrations or no-template control (NTC) wells are shown with primers for reference gene EF1-α or gene of interest (GOI).

Relative gene expression assays

Successfully validated primer sets were used in the subsequent gene expression assays to measure fold-changes in expression of particular RNA transcripts between samples. A 1:1 mixture of forward and reverse primer was diluted to a final concentration of 150 nM. As before, template cDNA was synthesized by reverse-transcribing 1 µg of total RNA isolated from control and target morpholino-injected embryos. Template cDNA was then diluted to give a final concentration of 10-50 ng/µl.

The reaction mixture per sample (to be aliquoted in triplicate) consisted of: 20 µl of 2X SYBR Green mix, 4.8 µl of a 1.25 mM mixture of both the forward and reverse primers, 5 µl of template cDNA (at a concentration of 10-25 ng) and 10.2 µl of nuclease-free water. A sample plate layout is shown below (Figure 2.2).

Control **10 ng/µl EF1-α** →			Morphant **10 ng/µl EF1-α** →			NTC **0 ng/µl EF1-α** →			Control **10 ng/µl GOI** →		
Morphant **10 ng/µl GOI** →			NTC **0 ng/µl GOI** →								

Figure 2.2 Sample plate layout for ΔΔCT qPCR experiments.
Triplicate wells shown for a sample plate examining gene expression in control (blue) and morphant (red) embryos, with no-template control (NTC) wells shown in black.

The average cycle time for each of the three replicates of a sample was calculated and the GOI cycle time values were normalised to those of the reference gene for the same sample (ΔCt=average cycle time$_{GOI}$ – average cycle time$_{REFERENCE\ GENE}$). House-keeping gene EF1-α was chosen as the reference gene for all experiments as it has been shown to be stably, precisely and reproducibly expressed at consistent levels in all tissues, and validated as a suitable reference gene for use in qPCR by several studies (Nicot et al., 2005; Ingerslev et al., 2006; Tang et al., 2007)

A calibrator sample was then chosen for each sample, i.e. the control morpholino sample to which the morphant sample data would be compared. The calibrated value, or $\Delta\Delta Ct$, for each sample was then calculated ($\Delta\Delta Ct=\Delta Ct_{sample} - \Delta Ct_{calibrator}$). The fold-change for each sample relative to the calibrator was then calculated (fold-change=$2^{(-\Delta\Delta Ct)}$). Fold-change was then efficiency corrected using the Pfaffel method, i.e. by adjusting the efficiency value (E) of the reaction from the standard value of 2 (assuming perfect doubling of the PCR template) to a value obtained from the standard curve validation assay e.g if a primer validation assay yielded an efficiency value of 97% the E value would be adjusted to 1.97.

2.2.6 Gel electrophoresis

DNA electrophoresis

DNA fragment size was estimated by comparison to standard base-pair markers. Samples were electrophoresed in tandem with DNA base-pair ladders. Agarose gels of varying concentrations (from 1-1.5%) were used, depending on the size of the DNA fragment of interest. A 2 µl aliquot of a 10 mg/ml stock solution of ethidium bromide was added to 60 ml of agarose and the 1X TAE running buffer consisted of 1 X Tris, acetic acid and EDTA at pH 8. Samples were electrophoresed in accordance with Sambrook et al., (1989). Gels were visualised using an InGenius gel documentation system from Syngene.

RNA electrophoresis

RNA quality was analysed by agarose gel electrophoresis on a 1.2% non-degrading formaldehyde gel. Ethidium bromide was added to the sample to enable visualisation of the RNA. A 2:1 ratio of the 28S to 18S ribosomal RNA indicated adequate RNA quality. RNA samples were heated for ten minutes at 65°C to remove secondary structures prior to running on the formaldehyde gel, in accordance with protocols from Sambrook et al., (1989).

Protein electrophoresis

Zebrafish lysate preparation

Embryos at the desired stage were harvested in batches of 50-150 and transferred to microcentrifuge tubes containing 1 ml of deyolking buffer (55 mM NaCl, 1.8 mM KCl, 1.25 mM $NaHCO_3$, 10% protease inhibitor cocktail [0.2 mM 4-(2-aminoethyl) benzenesulfonyl fluoride (AEBSF), 1 mM EDTA, 130 µM bestatin, 14 µM E-64, 1 µM leupeptin and 0.3 µM aprotinin]). Gentle pipetting with a 200 µl pipette tip was used to disrupt the yolk sac. Embryos were then shaken at 1000 g for five minutes and pelleted by centrifugation at 300 g for 30 seconds at room temperature. After removal of the supernatant, the pellet was washed in 1 ml of wash buffer (110 mM NaCl, 3.5 mM KCl, 2.7 mM $CaCl_2$, 10 mM Tris pH 8.5), shaken for one minute and centrifuged at 300 g for 30 seconds at room temperature. The supernatant was discarded and the wash step repeated. Samples were then frozen at -70°C or directly processed.

Embryo samples were thawed on ice and 50 µl of lysis buffer (1% Triton X-100, 10 mM Tris-HCl, pH 7.5, 140 mMNaCl, 5 mM EDTA, 2 mM EGTA, 1 mM PMSF) was added. Samples were sonicated three times for 5 seconds with 30 seconds of cooling time on ice allowed between each sonication. Freon (100 µl) was added to lysates, and tubes were then vortexed for 30 seconds and centrifuged at 13,200 g for thirty minutes. The isolated protein supernatant was then carefully removed to

a new 1.5 ml microcentrifuge tube. Protein concentration was estimated using a BCA assay.

Sodium Dodecyl Sulphate-Polyacrylamide Gel Electrophoresis (SDS-PAGE)

Proteins were separated by SDS-PAGE according to the Laemmli method using an Atto mini-gel system. Stock solutions for SDS-PAGE were prepared, including: Tris 1.5 M pH 8.8, Tris 1 M pH 6.8, 10% SDS, 10% ammonium persulphate, 5X sample buffer (250 mM Tris pH 6.8, 10% SDS, 0.5% bromophenol blue, 50% glycerol, 500 mM DTT) and 10X running buffer (2.5 M Glycine, 0.035 M SDS, 0.25 M Tris, pH 8.3). Samples were resolved on a 7.5% acrylamide gel at 0.04 A for 90 minutes.

Western blotting

Protein transfer was achieved by the semi-dry method. Following SDS-PAGE, nitrocellulose membrane was soaked in distilled water for ten minutes. The SDS-PAGE gel, nitrocellulose membrane and blotting paper were then soaked in transfer buffer (24 mM Tris, 192 mM glycine, 20% methanol, 1.3 mM SDS, pH 8.3) for ten minutes. Proteins were transferred from the SDS-PAGE gel to the membrane using a semi-dry transfer apparatus at 0.15 Amp constant for 90 minutes. Ponceau S solution (Sigma) was then used to stain the blot to show proteins had been transferred. Following a five minute incubation step in Ponceau solution the membrane was thoroughly rinsed with distilled water to visualise the protein bands. The membrane was then de-stained with 0.1 M NaOH and again rinsed thoroughly with distilled water.

Membranes were blocked for one hour at room temperature with gentle agitation in solution of 5% milk in Tris-buffered saline (TBS) (50 mM Tris, 150 mM NaCl, 1 M HCl to pH 7.5). Primary antibodies were diluted to the appropriate concentration with blocking solution and incubated with the membrane overnight at 4°C with gentle agitation. Primary antibody dilutions used were: anti-plakoglobin 1:1000, anti-α-tubulin 1:2000 and anti-connexin 43 1:1000. Membranes were then washed three times in TBS and incubated in secondary antibody, goat anti-rabbit peroxidase

conjugate (1:140,000) or goat anti-mouse peroxidase conjugate (1:8000), at room temperature for 2-3 hours. Membranes were washed three times in TBS and developed using Pierce Super Signal West pico chemiluminescent substrate. Kodak film was used to detect the signal. To remove signal prior to additional antibody incubation, membranes were washed three times in TBS and incubated in stripping buffer (25 mM glycine, 1% SDS, pH 2) for 20 minutes at room temperature with shaking. Membranes were then washed three times in TBS and re-blocked in 5% milk solution before incubation with antibodies as before.

2.2.7 Whole-Mount *In-Situ* Hybridisation

Purification of plasmids

LB broth with 0.25 mg of ampicillin was inoculated with a glycerol stock of the plasmid of interest and cultured overnight at 37°C. These cultures were then centrifuged at 5,000 g for five minutes and plasmid DNA was isolated and purified using a Qiagen mini-prep kit in accordance with the manufacturer's instructions. The concentration and quality of the isolated plasmid DNA was then assessed using a Nanodrop spectrophotometer, with an $A_{260/280}$ ratio of approximately 1.8 indicating good quality pure DNA.

Restriction digestions

Purified plasmid DNA was digested using restriction enzymes in accordance with the manufacturer's instructions. Restriction digestion was monitored by gel electrophoresis, with a single band indicating complete digestion. DNA was then purified by phenol-chloroform extraction as performed for RNA isolation (Section 2.2.4).

Digoxigenin-labelling of probes

A digoxigenin-labelling kit from Roche was used in accordance with manufacturer's instructions to label RNA probes. The reaction mixture of purified and linearised plasmid, DIG RNA labelling mix, transcription buffer, nuclease-free water, RNA

polymerase (SP6/T7/T3), and RNase inhibitor was incubated at 37°C for two hours. A further 15 minute incubation at 37°C was then required for DNase treatment of the samples. Following purification via lithium chloride precipitation probes were re-suspended in 20 µl of nuclease-free water.

To examine the integrity of the probe a 1 µl sample was electrophoresed on a formaldehyde RNA gel with a single band indicating a non-degraded DIG-labelled *in situ* probe.

Whole-mount *In-situ* Hybridisation

Embryos at the desired stage were fixed in 4% paraformaldehyde. Embryos to be harvested post-24 hpf were incubated in phenyl-thiourea to prevent pigmentation. Embryos were rinsed with PBST, dehydrated through a methanol series (25%, 50%, 75%, 100%) and stored at -20°C. Embryos were then re-hydrated through the methanol series, rinsed with PBST and, if older than 24 hpf, treated with proteinase K to facilitate penetration of the probes. Batches of 30 embryos were used for *in situ* hybridisations according to Hauptmann & Gerster (1994). Embryos were pre-hybridized in HY4 solution (50% formamide, 5X Sodium Chloride Sodium Citrate (SSC) [0.15 M NaCl, 0.015M sodium citrate, pH 7], 50 µg/ml Heparin, 0.1% Tween 20, 0.5% Torula RNA) for 2-4 hours at 70°C. DIG-labelled RNA probe was thawed on ice and 2 µl of probe was added to 100 µl of pre-hybridisation buffer. The probe and pre-hybridisation buffer were heated at 100°C for five minutes and cooled on ice before hybridising with embryos overnight at 70°C. Following incubation, embryos were washed twice for 30 minutes with 50% formamide/50% 2 X SSC/0.1% Tween 20, once for 15 minutes with 2 X SSC/0.1% Tween 20 and twice for 30 minutes with 0.2X SSC/0.1% Tween 20. Embryos were blocked for three hours at room temperature with blocking solution (5% heat-inactivated sheep serum in PBS, 0.1% Tween [PBST]). Anti-digoxigenin-AP Fab fragments were diluted in blocking solution (1:5000) and incubated with embryos overnight at 4°C. Embryos were washed three times in PBST for five minutes each and then three times in PBST for 20 minutes each. Embryos were washed twice in staining buffer (100 mM NaCl, 50 mM $MgCl_2$, 100 mM Tris HCl, 0.1 % Tween 20 pH 7.2) and transferred to four-well

plates. BM-Purple AP-Substrate (1 ml) was added to each well and embryos were incubated in the dark until colour developed. Staining was stopped by washing three times in PBST. Embryos were fixed in 4 % paraformaldehyde overnight at 4°C, and dehydrated through a methanol series. Embryos were photographed using a DMX1200C camera mounted on a SMZ800 Nikon microscope with a Fibreoptic-Heim LQ1100 transilluminator or cleared with benzyl benzoate/benzyl alcohol (2:1) (BBA) and photographed using a Nikon DM1200F camera with an Eclipse E600 microscope.

2.2.8 Microscopy

Embryo imaging

Live embryos were photographed using a Nikon SMZ800 microscope and a DMX1200C camera. Whole mount in-situ hybridisations were imaged using a Nikon Camera DXM1200F mounted on an Eclipse E600 microscope.

Transmission Electron Microscopy (TEM)

Dechorionated embryos at the desired stage were fixed in 2.5% glutaraldehyde / 2.5% PFA and post fixed in osmium tetraoxide. The embryos were dehydrated in an ethanol series and embedded in a low viscosity resin (Agar Scientific Ltd.). Embryos were sectioned transversely using a Reichert Jung Ultracut instrument and semi-thin sections (1 μm) of interest stained with toluidine blue and selected using light microscopy. A diamond knife was used to cut ultrathin sections which were stained with uranyl acetate and lead citrate and examined under a Hitachi H7000 electron microscope.

2.2.9 TAL-Effector Nuclease design and synthesis

TAL-effector nucleases were designed and assembled using a protocol for the "Golden Gate" method, adapted from Cermak et al,. (2011). Sequences for all oligonucleotides used in these experiments are shown in Table 2.2. The basic workflow for TALEN experiments in shown in Figure 2.3.

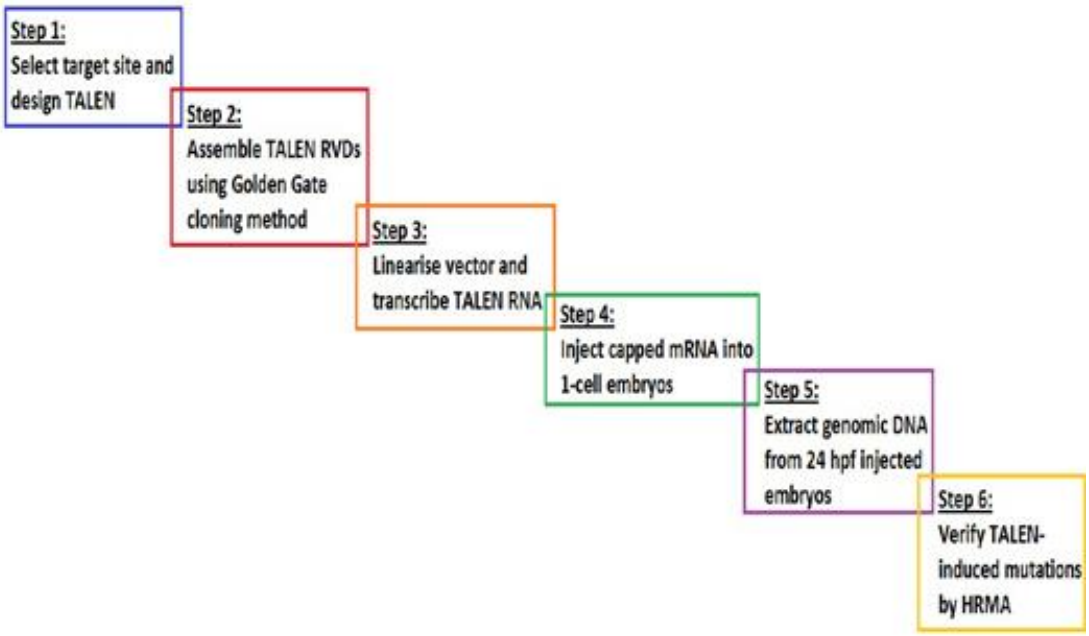

Figure 2.3 Workflow for TALEN targeting
Basic outline of TALEN targeting process, showing major steps required to achieve targeted mutations in zebrafish.

Design preparation

Target sequences were initially screened to ensure TAL-effector nucleases were not designed to target regions that contained SNPs. Twelve healthy wild-type AB fish (6 males and 6 females) were then isolated and tail-clippings were taken for genotyping. Genomic DNA was isolated from the harvested tail material, and used to sequence the region of interest to ensure good fidelity between the proposed target region and the sequence available in the Ensembl zebrafish database (www.ensembl.org/Danio_rerio/index.html). These sequenced fish were then used as parent fish for all subsequent experiments.

Design Guidelines

The TALENs were designed using the TALEN targeter available online (https://boglab.plp.iastate.edu/node/add/talen). In addition to the original targeter guidelines a spacer length of 14-17 was used with a repeat array length of 16-21. BLAST analysis was used to determine that chosen target sites were unique (http://www.blast.ncbi.nlm.nih.gov/).

Construct synthesis using the Golden Gate cloning method

Custom TALEN assembly involves a two-step process, (1) assembly of a series of repeat modules (RVDs) into intermediary arrays of 1-10 repeats, and (2) the joining of these repeats into a "backbone" destination vector to complete the final construct.

RVD plasmids from the TALEN plasmid library (Addgene) for the selected TALEN sequence were chosen and assembled using the Golden Gate cloning method as follows:

- For TALENs 12-21 RVDs in length
    - Plasmids for RVDs 1-10 (e.g. pHD1, pNG2, pNN3, etc.) and destination vector pFUS_A were selected (set A)
    - Plasmids for RVDs 11-(N-1) and destination vector pFUS_B#(N-1) were selected (set B)
- For TALENs 22-31 RVDs in length
    - Plasmids for RVDs 1-10 and destination vector pFUS_A30A (set A1), and plasmids for RVDs 11-20 and destination vector pFUS_A30B (set A2) were selected
    - Plasmids for RVDs 22-(N-1) and destination vector pFUS_B#(N-1) were selected (set B)

Golden Gate Reaction #1 (comprising of 150 ng of each module vector, 1 µl of restriction enzyme BsaI, 1 µl of T4 DNA ligase, 2 µl of 10X T4 DNA ligase buffer and nuclease-free water to a final volume of 20 µl) was mixed separately for each set of vectors. These reactions were then run in a PCR machine for 10x (37°C/5min +16°C/10min) + 50°C/5min+ 80°C/5min. 1 µl of 10 mM ATP and 1 µl of Plasmid-Safe Nuclease was then added to each Golden Gate Reaction #1 and tubes were incubated at 37 °C for 1 hour. A 5 µl aliquot of each reaction was transformed into 45 µl of chemically competent DH5-α cells. Cells were incubated at 37 °C for 1-2 hours following transformation to allow recovery after heat-shock. The recovered cells were spread on spectinomyosin-resistant plates with IPTG and X-gal, and plates were incubated overnight at 37 °C.

Following overnight incubation 1-3 white colonies were selected from each plate and checked by colony PCR using primers pCR8_F1 and pCR8_R1. Correct clones were then cultured overnight at 37 °C in spectinomyocin-resistant LB broth. Plasmid DNA was then extracted and purified, and sequenced using colony PCR primers as above.

Clones confirmed by sequence analysis were then used for Golden Gate Reaction #2 (150 ng of vector set A + B / vector set A1 + A2 + B, 150 ng of the respective pLR vector containing the last RVD, 75 ng of destination vector pCSTAL3DD or pCSTAL3RR, 1 µl of restriction enzyme Esp3I, 1 µl T4 DNA ligase, 2 µl 10X T4 DNA ligase buffer and nuclease-free water to a final concentration of 20 µl). A PCR cycle of 37°C/10min + 16°C/15min +37°C/15min+ 80°C/5min was used to provide suitable reaction conditions. A 5 µl aliquot of this reaction was then transformed; recovered cells were spread on ampicillin-resistant agar plates treated with X-Gal and IPTG, and cultured overnight at 37 °C as before.

Following overnight incubation 1-3 white colonies were selected from each plate and correct clones were identified by colony PCR using primers TAL_F1 and TAL_R2. Correct clones were identified by a “smear-and-ladder” effect visible after gel electrophoresis, and these clones were cultured overnight in ampicillin-resistant LB broth. Overnight cultures were plasmid-extracted and purified, and these final constructs were sent for sequencing.

Completed TALEN constructs were sequenced and analysed using the TAL plasmids sequence assembly tool, available online courtesy of the Bao lab at http://baolab.bme.gatech.edu/Research/BioinformaticTools/assembleTALSequences.html. TALEN constructs confirmed by sequence analysis were then linearized with restriction enzyme Not I and these linearized plasmids were used as template for in vitro mRNA transcription using the SP6 mMessage Machine Kit. Following mRNA transcription sample concentration was determined using a spectrophotometer and samples were normalised to a standard concentration of

100 ng /µl. Injection aliquots were prepared by mixing equal amounts of left and right TALEN mRNA, and all mRNA was then stored at -80 °C.

Microinjection of TALEN constructs

An injection volume of 1 nl was used to deliver a 100 pg dose of the prepared mixture of left and right TALEN constructs to the cytoplasm of zebrafish embryos at the 1-cell stage. Un-injected WT sibling embryos from the same clutch were used as controls.

Genomic DNA extraction protocol for genotyping

Embryos at 24 hpf were inserted into individual 500 µl tubes and incubated for six hours at 55 °C in 50 µl of genomic DNA extraction buffer (500 ml 1M Tris pH 8, 2 ml 5M NaCl, 500 µl 1% Triton X-100, 47 ml distilled H_2O) with 1/10 volume fresh proteinase K. Following incubation samples were heat-shocked at 98 °C for 10 minutes to deactivate the enzyme. The resulting genomic DNA solution was stored at -20 °C.

High Resolution Melt Analysis (HRMA) to verify TALEN-induced mutations

High-resolution melt analysis (HRMA) was used to verify TALEN-induced mutations in a subset of injected embryos harvested for genomic DNA extraction. PCR reactions with high-resolution melt-curves were performed using an Illumina Eco PCR machine. PCR primers were designed to flank the region of interest and amplify a product of less than 100 base-pairs. Primers were diluted to a concentration of 100 pmol and then forward and reverse primers were mixed in a 1:1 ratio. The final reaction volume for each well was 15 µl, consisting of 0.75 µl of the genomic DNA previously extracted from individual embryos, 7.5 µl of 2X SYBR Green Fast PCR Mix, and 6.75 µl of a 1:140 dilution of the 1:1 primer mix. The PCR reaction utilised the following conditions: 2 minute incubation at 50 °C, 10 minute polymerase activation step at 95 °C, and 40 cycles of 95 °C for 10 seconds and 60 °C for 30 seconds. This PCR reaction preceded the high resolution melt curve which used the following parameters: 95 °C for 15 seconds, 55 °C for 15 seconds and 95 °C for 15 seconds. A random selection of wild-type and TALEN-injected samples from each

set of injections were assayed in parallel, and TALEN-injected samples showing a diverging melt-curve in comparison to wild-type controls demonstrated successful TALEN-induced mutations.

Identification of germline mutations

Injected fish from the same batch of somatically screened embryos were raised to adulthood. These "donor" or F_0 fish were outcrossed to wild-type AB fish and embryos were screened for germline mutations. Embryos were assessed both phenotypically and genotypically. For genotypic analysis ten randomly selected embryos per clutch were harvested from individual F_0 crosses and genomic DNA was isolated from these individual embryos at 24 hpf as previously described. The targeted exon was then amplified by PCR using Takara LA Taq and specific oligonucleotides for the exon of interest. The resulting PCR products were purified using a Qiagen PCR Purification Kit and sequenced. The CLUSTALW alignment programme (http://www.ebi.ac.uk/Tools/msa/clustalw2/) was used to identify mutations in F_1 progeny samples by comparing sequence from the targeted region of *plakoglobin* to the sequence available in the Ensembl zebrafish database.

2.2.10 Statistical analysis

All results are shown as mean ± SD, n=3 biological replicates unless otherwise stated. SPSS statistical software was used to perform statistical analyses. Differences between groups were evaluated by *t*-test (if 2 groups) or one way ANOVA and *post-hoc* test after testing for normality with Shapiro Wilkes test (if > 2 groups). $P<0.05$ was considered statistically significant.

3 Effects of Plakoglobin and Plakophilin-2 Knockdown on Signalling in Early-Stage Zebrafish Embryos

3.1 Plakoglobin knockdown and Wnt signalling in zebrafish embryos

It has previously been established that plakoglobin knockdown induces an up-regulation of Wnt target genes both pre-and post-mid-blastula transition (Table 3.1), and that co-injection of the Wnt inhibitor Dickkopf-1 (Dkk1) can rescue the gross cardiac defects seen in plakoglobin morphant embryos; i.e. cardiac oedema, decreased heart size, blood pooling and a twisted tail (Martin et al., 2009).

Table 3.1 Signalling effects on Wnt target genes in plakoglobin knockdown embryos.

Gene	Previous names	Stage	Up-regulated in plakoglobin knockdown
nodal-related-1 (*ndr1*)	*squint*	sphere	✓
Dharma	*bozozok, nieuwkoid*	sphere	✓
bone morphogenetic protein 4 (bmp4)	*z-bmp4*	shield	✓

Data collated from whole-mount in-situ hybridisation and semi-quantitative RT-PCR experiments (Martin et al., 2009).

These data strongly support the theory that plakoglobin itself acts as an antagonist to the Wnt signalling pathway; hence the signalling role of plakoglobin was further investigated.

Though loss of plakoglobin has been previously shown to increase Wnt target gene expression at early stages of development (during blastula), the duration of this up-regulated Wnt signalling is unknown, hence expression of Wnt target genes was examined in plakoglobin morphant embryos at developmental stages pre- and post mid-blastula transition to supplement existing data that proposes a role for plakoglobin as an antagonistic regulator of Wnt signalling in early zebrafish development.

The ability of Dkk1 to rescue the gross phenotype of plakoglobin morphant embryos is also suggestive of an antagonistic role for plakoglobin in the Wnt pathway, however the ultra-structural effects of this “rescue”, and the ability of Dkk1 to compensate for plakoglobin in the desmosomes, had not yet been resolved. To examine the extent to which Dkk1 can compensate for loss of

plakoglobin, the ultra-structure of Dkk1 “rescue” embryos (plakoglobin morpholino plus Dkk1 RNA) was examined.

3.1.1 Wnt signalling in early stage plakoglobin morphant embryos

Loss of plakoglobin has been previously shown to increase Wnt target gene expression at selected early developmental stages (Martin et al., 2009), but it is unknown if this increased activity is maintained pre- and post- mid-blastula transition (MBT). Hence, the expression of a selection of representative Wnt target genes was examined using qPCR at stages both pre- and post- mid-blastula transition to supplement previously published data on increased Wnt signalling in the absence of plakoglobin which has been summarised in Table 3.1 (Martin et al., 2009).

Expression of *bmp4* was significantly up-regulated in sphere stage plakoglobin knockdown embryos, with a tendency towards increase at the post-MBT shield stage. Expression levels of *ndr1* and *dharma* show a strong tendency towards increase at the sphere stage of development, though this tendency is no longer apparent post-MBT (Figure 3.1 Expression of Wnt target genes in plakoglobin knockdown embryos at early stages of development.).

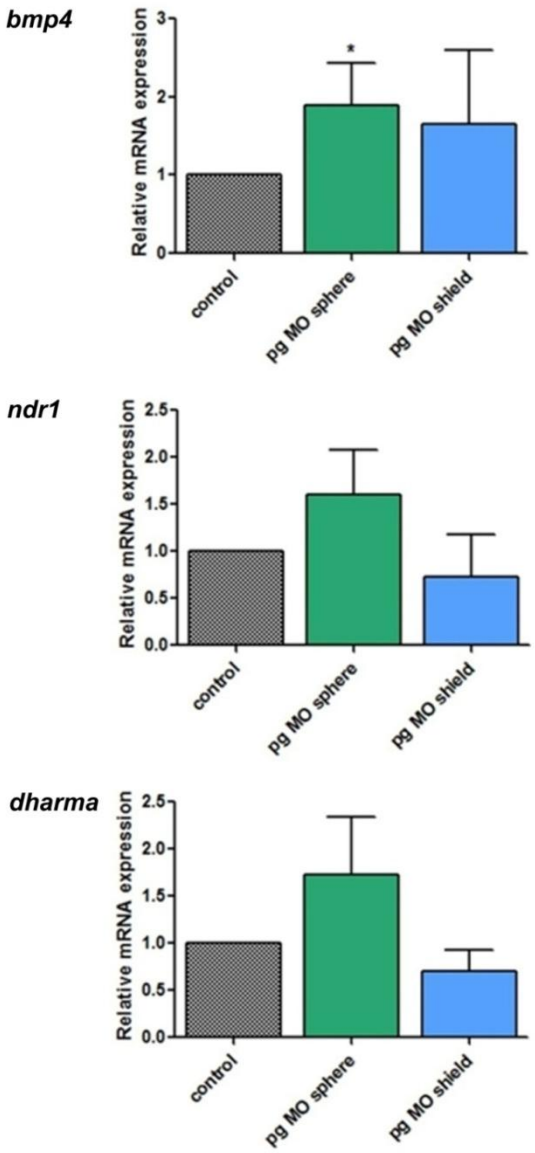

Figure 3.1 Expression of Wnt target genes in plakoglobin knockdown embryos at early stages of development.
mRNA expression of Wnt target genes *bmp4*, *ndr1* and *dharma* at sphere and shield stages of development; n=4. Data shown are means + s.d. **P*<0.05 vs control by paired *t*-test.

As *bmp4* expression was observed to have some tendency towards increased expression after zygotic transcription was initiated expression levels of *bmp4* at 48 hpf were then investigated in plakoglobin knockdown embryos. Levels of *bmp4* expression in morphants were similar to controls at this stage (Figure 3.2).

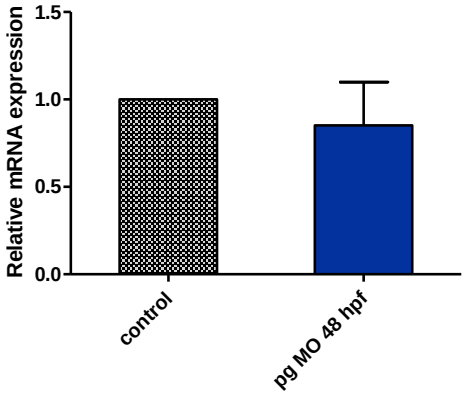

Figure 3.2 Expression of *bmp4* in 48 hpf plakoglobin morphant embryos.
mRNA expression of Wnt target gene *bmp4* in plakoglobin morphant embryos. Levels of *bmp4* expression in morphant embryos are similar to those of controls; n=3. Data shown are means + s.d. Data were analysed by paired *t*-test.

Examination of Wnt target gene expression pre-and post-MBT confirms and augments existing knowledge on the effect of plakoglobin knockdown on Wnt signalling. The tendency towards up-regulation of *dharma* and *ndr1* correlates with previously obtained data (Martin et al., 2009), with the supplementary information that *bmp4* expression is up-regulated significantly at the same stage. At the shield stage expression of both *ndr1* and *dharma* were observed to return to normal levels, indicating that loss of plakoglobin has only a transient effect on the expression of these genes, which occurs prior to the mid-blastula transition. Expression of *bmp4* appears to be affected both maternally and zygotically, however mRNA expression levels are normal at 48 hpf. As Martin et al., (2009) demonstrated expanded expression of cardiac *bmp4* at this stage of development it seems that loss of plakoglobin alters localisation but not expression at 48 hpf. Temporal gene expression is tightly regulated throughout development, hence it may be that the expanded expression patterns of Wnt target genes are transient and stage-dependent in the absence of plakoglobin, and discrete periods of over-expression are sufficient to perpetuate the severe developmental defects seen in the zebrafish plakoglobin knockdown phenotype.

3.1.2 Functional effects of Dickkopf-1 co-injection with plakoglobin morpholino

Further evidence for the role of plakoglobin as a negative regulator of Wnt signalling was provided by the ability of Wnt antagonist Dickkopf-1 (Dkk1) to rescue the gross phenotype observed in the absence of plakoglobin (Martin et al., 2009). It has not been shown to what extent this rescue can compensate for loss of plakoglobin, though embryos co-injected with the plakoglobin morpholino and Dkk1 appear phenotypically restored. However as plakoglobin morphant embryos also display functional and ultra-structural defects a more detailed investigation of these Dkk1 "rescue" embryos was conducted.

To test their functionality, heart rates of Dkk1-rescue embryos (where Dkk1 RNA was co-injected with plakoglobin morpholino) were compared to those of control and plakoglobin morphant embryos, and to those of embryos in which Dkk1 was over-expressed (i.e. Dkk1 RNA was co-injected with the control morpholino). Plakoglobin morphant embryos and those embryos over-expressing Dkk1 had significantly reduced heart-rates in comparison to wild type and control morpholino-injected embryos. Embryos "rescued" with Dkk1 RNA showed no significant difference compared to wild type and control embryos, thus indicating that this aspect of heart function is restored as a result of Dkk1 co-injection (Figure 3.3).

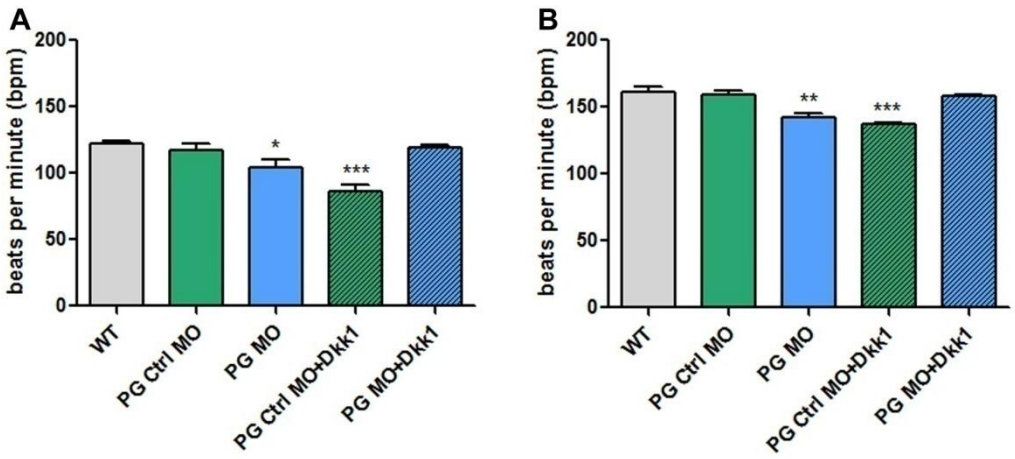

Figure 3.3 Co-injection of Dkk1 RNA with plakoglobin morpholino restores heart rate.
Heart rates were measured at both 48 hpf (A) and 72 hpf (B) in wild type, control morpholino, plakoglobin morpholino, control morpholino plus Dkk1 RNA (Dkk1 over-expression) and plakoglobin morpholino plus Dkk1 RNA (Dkk1 rescue) injected embryos. Plakoglobin knockdown embryos and Dkk1 over-expression embryos were found to have significantly lower heart rates than controls at both developmental stages investigated, whereas embryos injected with both the plakoglobin morpholino and Dkk1 RNA showed a restored heart rate that did not significantly differ from control embryos; n=3 in all groups. Data shown are means + s.d. **P*<0.05, ****P*<0.001 vs control morpholino group by one-way ANOVA with Dunnett's multiple comparison post-hoc test.

To investigate the effect of Dkk1 co-injection on patterning in the zebrafish heart semi-thin (1 µm) sections were examined by microscopy. The structure and patterning of control hearts was observed to be normal, while plakoglobin morphant hearts were smaller in size with pericardial oedema in keeping with the phenotype previously obtained. Embryos in which Dkk1 was over-expressed were also found to be abnormal, with a similar phenotype to plakoglobin morphants featuring altered heart size, patterning defects and obvious oedema. Embryos injected with a mixture of the plakoglobin morpholino and Dkk1 RNA ("rescue") had hearts of a normal size and pattern, indicating that Dkk1 can rescue the patterning defects that occur following loss of plakoglobin (Figure 3.4).

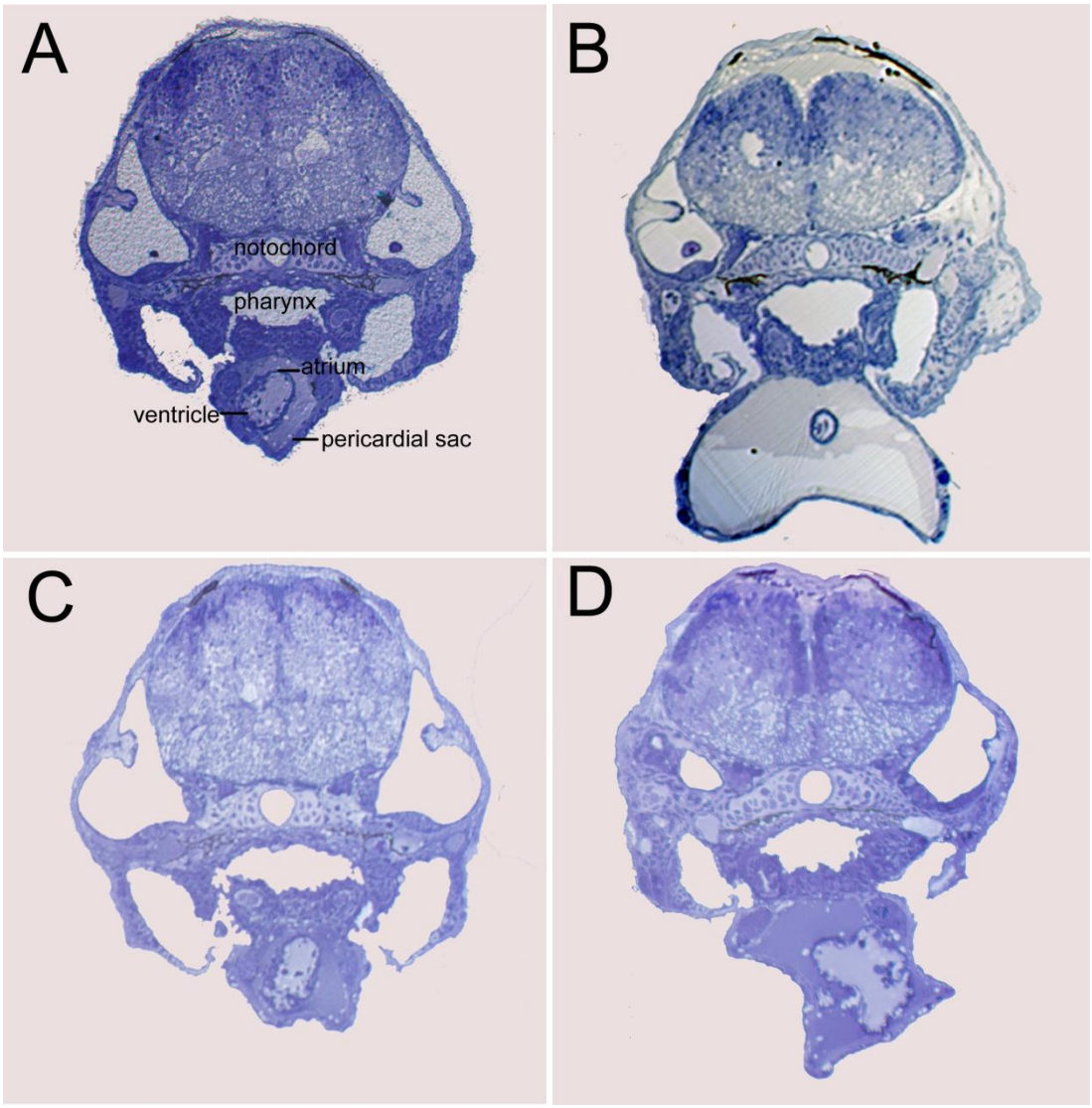

Figure 3.4 Dkk1 restores the structure of plakoglobin morphant hearts.
1 µm cross sections through 72 hpf embryos showing normal patterning of control (A) and "rescue" (C) hearts. Plakoglobin morphants (B) and embryos in which Dickkopf-1 has been over-expressed (D) had abnormal hearts with pericardial oedema and disrupted patterning; n=3.

To further examine the extent of the Dkk1 rescue on plakoglobin morphant embryos, ultra-thin cross sections were examined using Transmission Electron Microscopy (TEM). Both the pericardial epithelium and the intercalated disks were examined, and cell-cell junctions were quantified by counting desmosomes and adherens junctions at the cell-cell borders in ten randomly selected non-overlapping images from each of three biological repeats per treatment. Cell gap width was also measured in each of the images selected.

At the intercalated disks, adhesion was normal in plakoglobin control morpholino-injected samples with easily identifiable desmosomes often observed in series at cell-cell borders. As expected, plakoglobin morphants had significantly enlarged gaps between cells compared to their controls (Table 3.2) with desmosomes harder to distinguish and fewer in evidence. The number of junctions that could not be classified was also increased in these embryos. Surprisingly, Dkk1 "rescue" embryos (plakoglobin morpholino plus Dkk1 RNA) displayed a similar phenotype to the plakoglobin morphants, and the Dkk1 over-expression embryos (control morpholino plus Dkk1 RNA) had both an increased number of unclassified junctions and less desmosomes when compared to controls as well as significantly increased cell-cell gaps (Figure 3.5). These data, presented numerically in Tables 3.2 and 3.3, indicate that Dkk1 cannot compensate for the loss of the adhesion protein plakoglobin and does not restore full functionality to the morphant hearts.

The epithelium of the pericardial sac was also examined, and cell-cell junctions were quantified as before. It is noteworthy that defects in cell-cell junctions were observed in the pericardial epithelium of the plakoglobin morphant samples, as previous examinations of the knockdown failed to detect any impairment to the cell-cell junctions of the epithelium in the absence of plakoglobin. Overall, desmosome numbers and cell gap width repeated the trend observed at the intercalated disks (Figure 3.6), as can be seen from the quantitative data in Table 3.2 and Table 3.4.

Table 3.2 Cell gap width

Average Cell Gap Width (nm)				
	Control morpholino	**Plakoglobin morpholino**	**PG MO + Dkk1 ("Rescue")**	**Ctrl MO + Dkk1 (Over-expression)**
Intercalated discs	30.69	38.16	33.97	36.58
P-value		**	ns	*
Pericardial epithelium	31.43023	47.1046	45.65077	43.87433
P-value		***	***	**

n=30 images per group. *p<0.05, **p<0.005, ***p<0.001 vs control morpholino group by one-way ANOVA with Dunnett's multiple comparison post-hoc test.

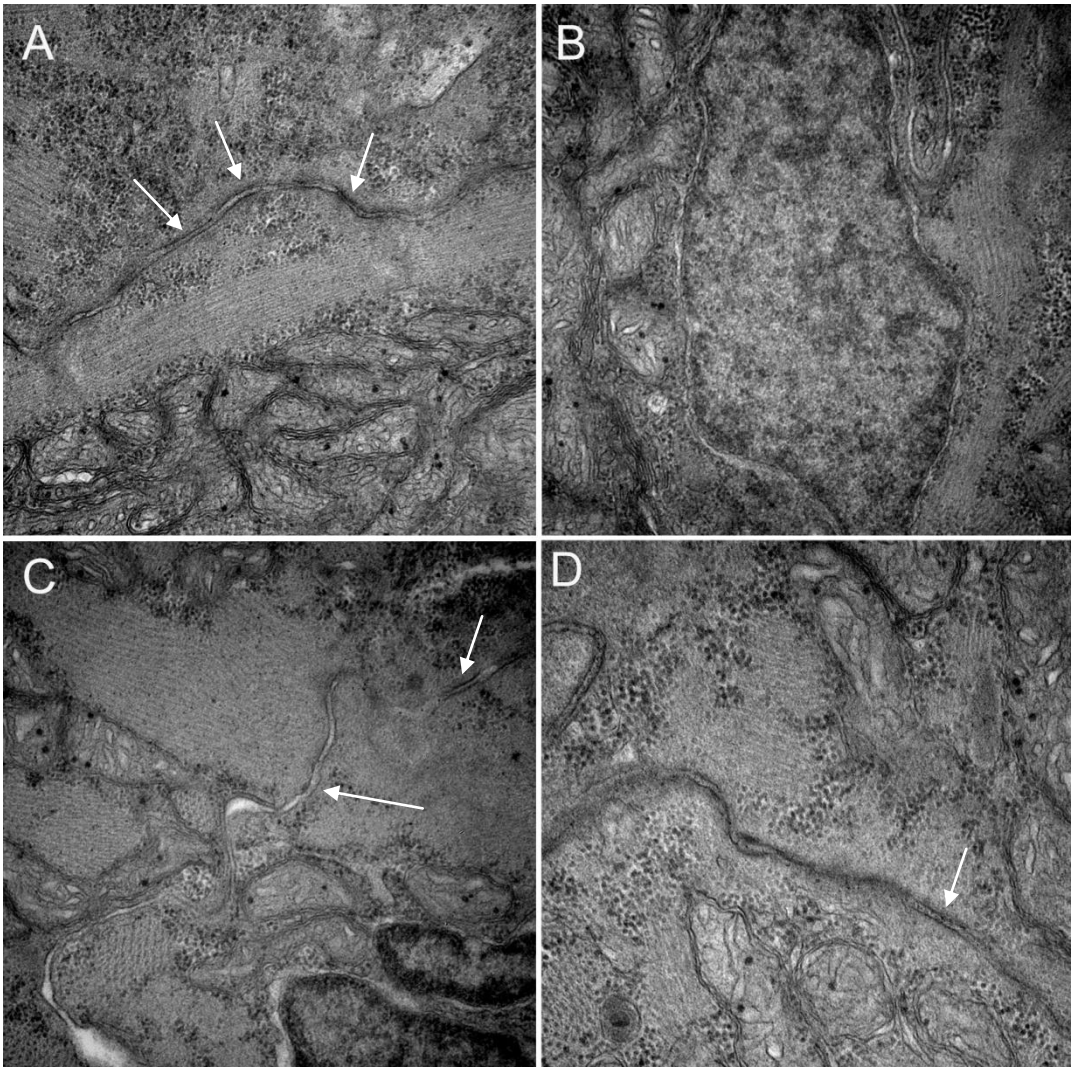

Figure 3.5 Ultra-structure of intercalated disks in 72 hpf embryos.
Transmission Electron Microscopy (TEM) images of cell-cell borders in the intercalated disks (magnification 40,000). Control (A) and Dkk1 over-expression (D) samples with normal adhesion, whereas plakoglobin morphants (B) and Dkk1 co-injected embryos (C) have enlarged cell-cell gaps and decreased numbers of desmosomes. Sample desmosomes are indicated by arrows; n=3.

Table 3.3 Cell-cell junctions in intercalated disks at 72 hpf

	Cell-cell borders	Desmosomes	Adherens Junctions	Unclassified
A- Control	33	55	1	2
B- Plakoglobin morphant	35	21	1	19
C- PG MO + Dkk1 RNA ("rescue")	34	18	0	21
D- Ctrl MO + Dkk1 RNA (over-expression)	34	15	0	14

n=3 embryos per group

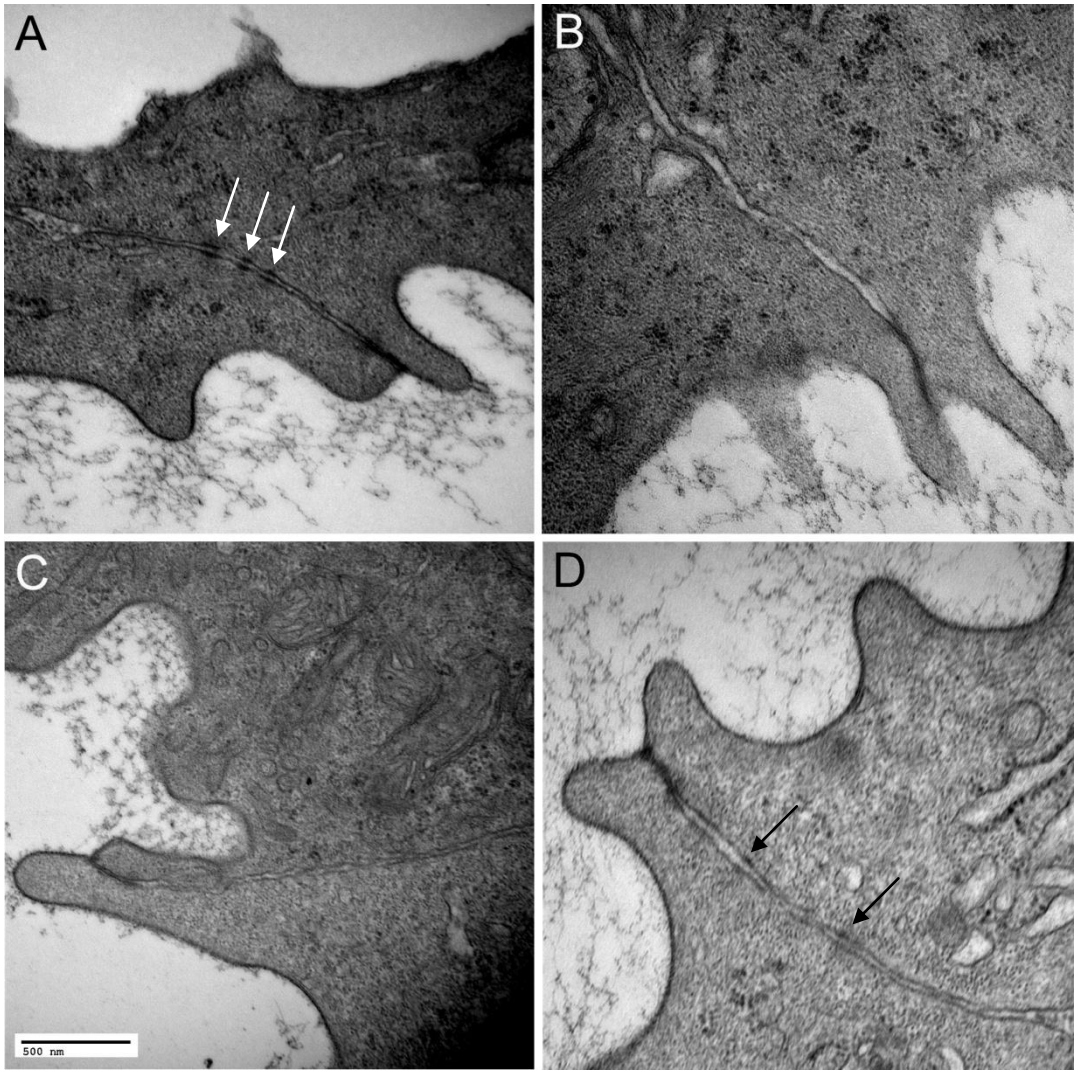

Figure 3.6 Ultra-structure of pericardial epithelium in 72 hpf embryos.
Transmission electron microscopy (TEM) images of cell-cell borders in cardiac epithelium (magnification 40,000). Control (A) and Dkk1 over-expression (D) samples display normal adhesion, whereas plakoglobin morphants (B) and Dkk1 co-injected embryos (C) show enlarged cell-cell gaps and decreased numbers of desmosomes. Arrows indicate sample desmosomes; n=3

Table 3.4 Cell-cell junctions in pericardial epithelium at 72 hpf

	Cell-cell borders	Desmosomes	Adherens Junctions	Unclassified
A- Control	32	48	16	7
B- Plakoglobin morphant	32	17	11	18
C- PG MO + Dkk1 ("rescue")	31	19	17	21
D- Ctrl MO + Dkk1 (over-expression)	31	21	24	38

n=3 embryos per group

3.2 The effect of plakophilin-2 knockdown on gene expression

An established link between the desmosomal protein plakoglobin and the Wnt signalling pathway led to the hypothesis that plakophilin-2 may be utilising the same signalling mechanism. Both plakoglobin and plakophilin-2 are desmosomal adhesion proteins of the armadillo family, and as both plakophilin-2 and plakoglobin knockdown in zebrafish induce similar cardiac phenotypes it was hypothesized that loss of plakophilin-2 could also result in disruption of the Wnt signalling pathway; hence the expression of Wnt target genes in plakophilin-2 knockdown embryos was investigated.

3.2.1 The effect of plakophilin-2 knockdown on Wnt target gene expression

Early-stage plakophilin-2 morphant embryos were harvested at sphere (pre-MBT) and shield (post-MBT) stages of development and *in situ* hybridisation experiments were performed to examine localisation of the selected genes of interest.

The initial experiment examined the expression pattern of *ndr1* at sphere and shield stages, and *bmp4* at shield. *Ndr1* expression was localised to the presumptive shield in all controls and 97% of morphant embryos at sphere, and staining appeared to be of equal intensity in both groups. At the shield stage all control embryos displayed faint expression across the marginal blastoderm. Of the morphant group, 96% exhibited an identical domain of expression, though intensity of staining appeared stronger in these plakophilin-2 knockdown embryos. *Bmp4* expression was present in the shield and extended approximately half-way across the germ ring in 72% of control samples, however 94% of morphant embryos appeared to have an increased domain and intensity of expression (Figure 3.7). Subsequent repeats of the *in situ* experiments displayed contradictory or indeterminate expression patterns (data not shown).

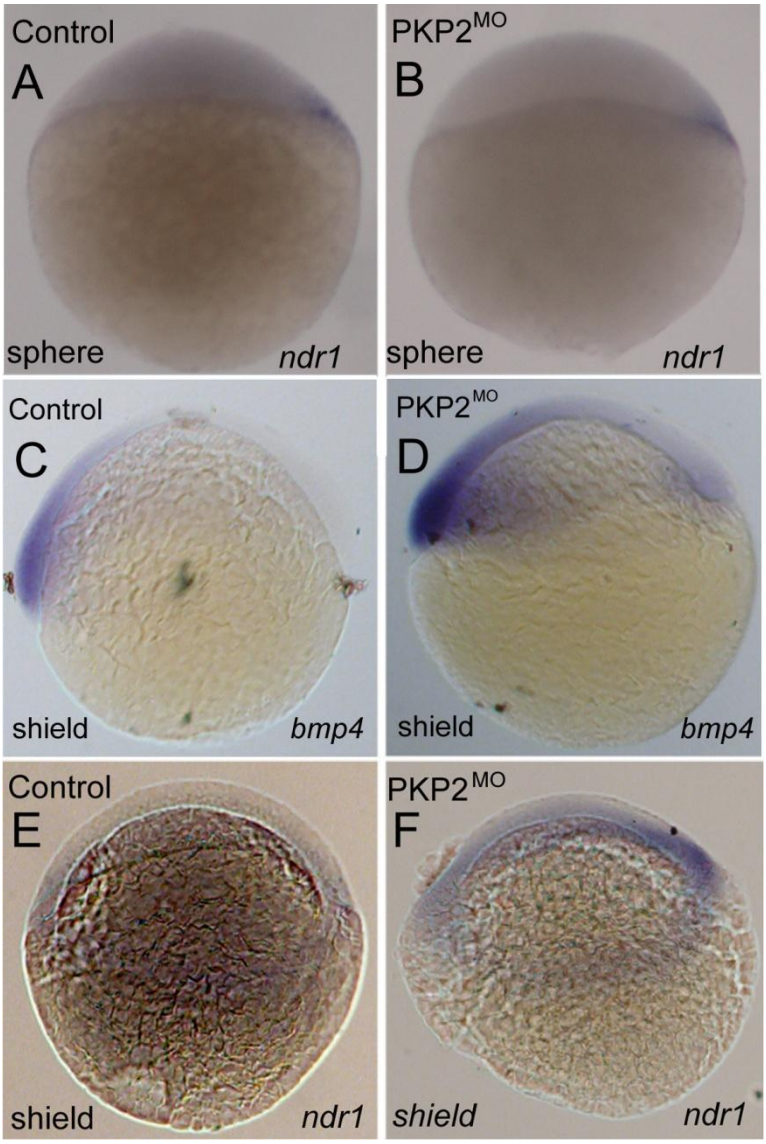

Figure 3.7 Wnt target gene expression in early stage plakophilin-2 morphant embryos. Expression of *ndr1* at sphere (A&B) and shield (E&F) and *bmp4* at shield (C&D). Total number of embryos with pattern shown were (A) 30/30, (B) 30/31, (C) 31/31, (D) 29/30, (E) 23/32 and (F) 30/32.

It had been hypothesized that plakophilin-2 plays a similar role to its desmosomal counterpart plakoglobin; however the inconsistencies between repeats made it impossible to glean any information on what effect, if any, the loss of plakophilin-2 was having on Wnt target genes. As expression domains and intensities varied between repeats, it was plausible that no significant effect on Wnt signalling was occurring, and the variation observed was due to the immense changes taking place within the developing embryo at the crucial developmental stages when the zygotic

genome activates. In order to confirm or reject this hypothesis a quantitative method was required to identify any changes in the expression level of these Wnt target genes, and so qPCR was used for further investigation.

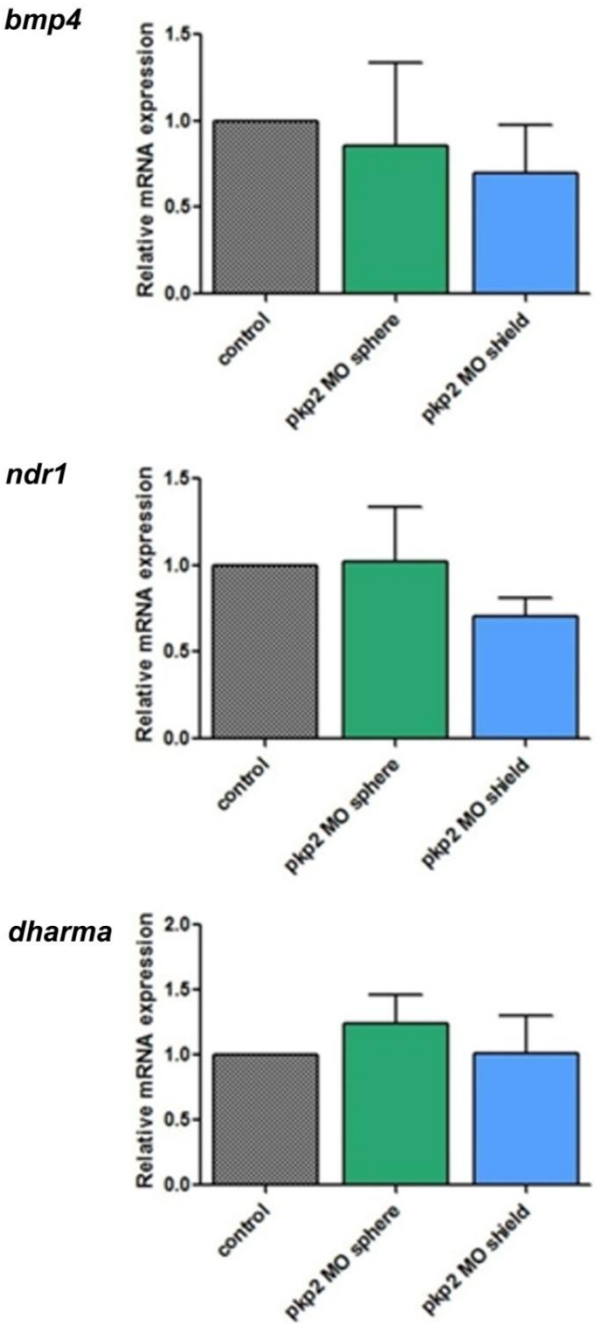

Figure 3.8 Expression of Wnt target genes in plakophilin-2 morphant embryos.
mRNA expression of Wnt target genes *bmp4* (A), *ndr1* (B) and *dharma* (C) is unaffected after loss of plakophilin-2; n=4. Data shown are means + s.d., analysed by paired *t*-test.

qPCR was used to investigate the mRNA expression of Wnt pathway genes *bmp4*, *nodal-related-1* and *dharma*. Expression of all Wnt target genes in plakophilin-2 morphants was similar to controls both pre-and post-MBT (Figure 3.8). These data indicate that plakophilin-2 knockdown does not affect the Wnt signalling pathway at early stages of development.

As bmp4 plays an important role in later stages of development the mRNA expression levels of this gene were examined at 48 hpf by qPCR. As in plakoglobin morphants, *bmp4* expression was found to be unaffected at this later stage of development in the plakophilin-2 morphant samples (Figure 3.9).

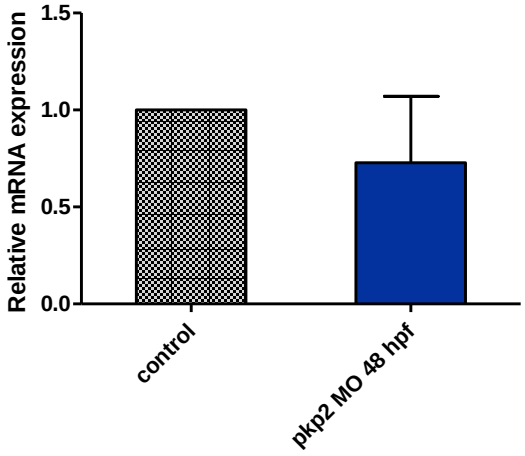

Figure 3.9 Expression of *bmp4* in 48 hpf plakophilin-2 morphant embryos.
mRNA expression of Wnt target gene *bmp4* in plakophilin-2 morphant embryos. Levels of bmp4 expression are normal in morphant embryos when compared to controls; n=3. Data shown are means + s.d., analysed by paired *t*-test.

3.2.2 The Effect of Plakophilin-2 Knockdown on the Nodal Signalling Pathway

In characterising the plakophilin-2 morphant phenotype previous work in our lab discovered expanded expression of heart domain marker *nkx2.5* at 24 hpf. Incomplete looping of the heart was also observed, and this was confirmed by examination of *cmlc2* and *vmhc* using whole-mount *in situ* hybridisation (Moriarty et al, 2012). These results indicated asymmetric patterning of the heart, as the looping mechanism appeared incomplete and the atrium was expanded in a number of plakophilin-2 morphants. A candidate for this defect in cardiac

patterning was predicted to lie within the Nodal signalling cascade and so cardiogenic markers from the Nodal pathway were examined both by qPCR and whole-mount *in situ* hybridisation.

Plakophilin-2 morphant embryos were harvested at the 18-22 somite stage and processed for whole-mount *in situ* hybridisation as previously described (Section 2.2.7). Nodal pathway genes *lefty1*, *bmp4*, *spaw* and *oep* demonstrated correct localisation with increased intensity of expression in plakophilin-2 morphant embryos when compared to control-injected embryos at equivalent stages. The most notable result however was the complete abolition of *lefty2* expression in the left cardiac field of plakophilin-2 morphant embryos (Figure 3.10).

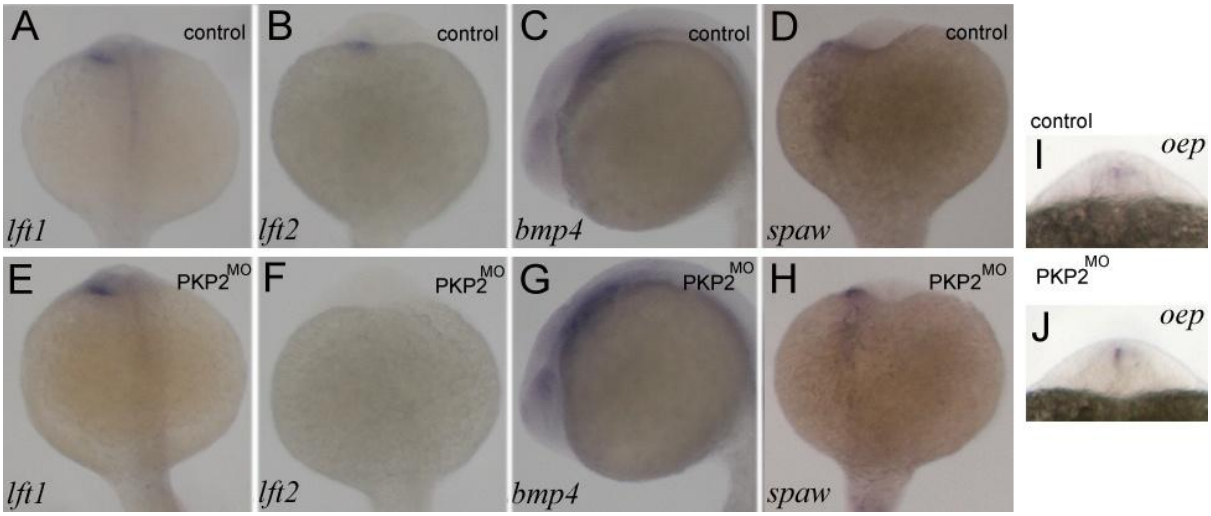

Figure 3.10 Loss of plakophilin-2 disrupts the spatial expression of Nodal signalling components.
Expression of cardiogenic marker genes in plakophilin-2 morphant and control morpholino-injected embryos. Whole-mount in-situ hybridisation lateral view of *bmp4* at the 18 somite stage, dorsal views of *lefty1* (*lft1*), *lefty2 (lft2*), *southpaw* (*spaw*) and *one-eyed pinhead* (*oep*) at the 18 somite stage. Expression of lefty 1 (A, E) was unaffected in morpholino injected embryos while the expression domain of *oep* (I,J) was expanded and intensity of *bmp4* (C, G) and *spaw* (D, H) was increased. *Lefty2* (B, F) expression was absent in plakophilin 2 morphant embryos compared to controls. Embryos with the displayed phenotype were as follows: 26/39 (*lft1* control), 44/54 (*lft1* morphant), 47/63 (*lft2* control), 28/34 (*lft2* morphant), 29/35 (*bmp4* control), 34/36 (*bmp4* morphant), 25/32 (*spaw* control), 50/57 (*spaw* morphant), 39/47 (*oep* control) and 42/48 (*oep* morphant).

Each of the genes examined by whole-mount *in situ* hybridisation was also examined by qPCR, as were *ndr1* and *pitx2c*. Embryos were harvested at the 18 somite stage and RNA was extracted and gene expression quantified by qPCR as previously described in Section 2.2.5. The mRNA expression levels of all genes were increased with the notable exception of *lefty2*, confirming the results obtained by qualitative analysis. qPCR examination of *lefty2* mRNA demonstrated an almost complete absence of expression in plakophilin-2 morphants (Figure 3.11).

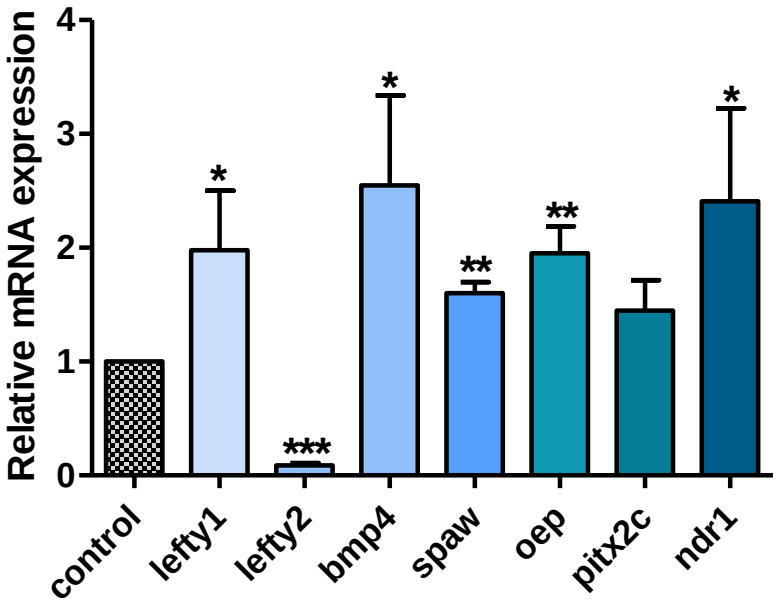

Figure 3.11 Loss of plakophilin-2 disrupts Nodal gene expression.
mRNA levels of Nodal target genes *lefty1, bmp4, spaw, oep* and *ndr1* were significantly up-regulated in plakophilin-2 knockdown embryos at the 18 somite stage. *Pitx2c* displayed a tendency towards increase, whereas *lefty2* expression was almost completely abolished in the morphant embryos. n=3. Data shown are means + s.d. **P*<0.05, ***P*<0.005, ****P*<0.0001 vs controls analysed by paired *t*-test.

3.2.3 The effect of plakophilin-2 knockdown on organ laterality

The disruption to important markers of cardiac asymmetry in plakophilin-2 morphant embryos led to the examination of neural structures to determine if the observed patterning defects extended outside the cardiac field. *Otx5* was chosen as a neural marker, to examine if symmetry of neural structures was affected in embryos lacking plakophilin-2.

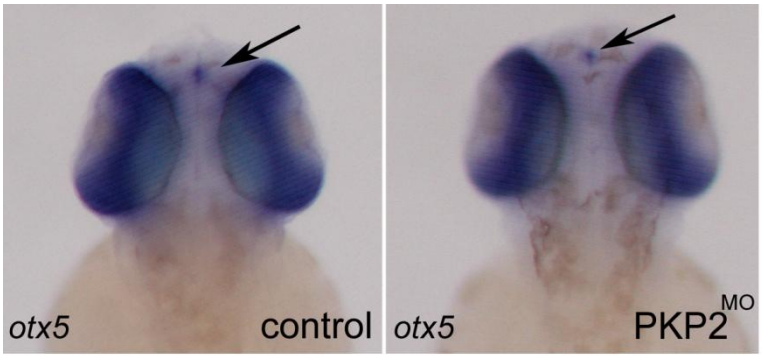

Figure 3.12 Laterality of neural structures is unaffected by loss of plakophilin-2.
Expression of neural marker *otx5* in the epiphysis is unaffected in plakophilin-2 morphants at 48 hpf. 98% of controls (59/60) and 93% of morphant embryos (53/57) displayed the expression phenotypes shown.

Whole-mount in-situ hybridisation showed symmetrical expression of *otx5* in the epiphysis of both control and plakophilin-2 morphant embryos (Figure 3.12) indicating that loss of plakophilin-2 does not affect the positioning of the neural structures and the patterning disruption seen in these morphant embryos does not extend beyond the cardiac field. Positioning of the gut could potentially be affected in plakophilin-2 knockdown embryos however gut laterality was not examined in this study.

3.3 Summary

Wnt antagonist Dkk1 is capable of rescuing the gross developmental defects caused by loss of plakoglobin (Martin et al., 2009). As plakoglobin is antagonistic to Wnt signalling, it follows that the defects resulting from loss of plakoglobin can be ameliorated by ectopic Dkk1 expression. Data presented in Section 3.1.2 indicates that Dkk1 cannot compensate for loss of plakoglobin in cell-cell junctions as the ultra-structure of Dkk1 “rescue” hearts is comparable to that of plakoglobin morphants, and so the phenotypic rescue achieved is probably due to the ability of Dkk1 to repress the up-regulation of Wnt signalling that occurs in the absence of plakoglobin.

Loss of either plakoglobin or plakophilin-2 disrupts cardiac development in the zebrafish (Martin et al., 2009; Moriarty et al., 2012). Loss of plakoglobin results in up-regulation of Wnt pathway target genes both at early and late stages of embryogenesis. Despite the similarities between plakoglobin and plakophilin-2, loss of plakophilin-2 did not affect Wnt signalling at any of the developmental stages examined, but resulted in significant disruption the Nodal signalling pathway during early cardiogenesis, with significant up-regulation of Nodal target genes *lefty1, bmp4, spaw, oep,* and *ndr1,* and complete ablation of *lefty2* expression.

3.4 Discussion

The process of vertebrate heart development is an extremely complex one, requiring the coordination of many molecular, temporal and spatial factors. The loss of one component can have far-reaching downstream effects resulting in cardiac disruption, as has been shown in zebrafish *in vivo* experiments i.e. loss of desmosomal proteins plakoglobin and plakophilin-2 (Martin et al., 2009; Moriarty et al., 2012). The signalling networks affected by the loss of these desmosomal proteins were examined, and results discussed below demonstrate the intricate nature of cardiac development as the divergent signalling effects of two structurally similar armadillo proteins are revealed.

Loss of either plakoglobin or plakophilin-2 disrupts cardiac development in the zebrafish (Martin et al., 2009; Moriarty et al., 2012). These proteins are important components of cell-cell junctions and as such are required for correct cell-cell adhesion in the skin and heart (reviewed by Garrod et al., 1996), however the requirement for these armadillo proteins extends beyond their structural role in cell-cell adhesion. Despite their similarities in structure and mechanical function, plakoglobin and plakophilin-2 have disparate effects on signalling. In this study, loss of plakoglobin results in up-regulation of Wnt pathway target genes both at early and late stages of embryogenesis, consistent with the postulated “waves” of Wnt signalling that occur throughout development, whereas loss of plakophilin-2 disrupts the Nodal signalling pathway during early cardiogenesis. Though Wnt inhibitor Dkk1 can restore the patterning defects that occur following loss of plakoglobin, it cannot structurally compensate for the loss of this protein at the desmosomes, and hence does not fully restore cardiac function in the absence of plakoglobin.

3.4.1 Plakoglobin and Wnt signalling

Loss of plakoglobin in the zebrafish embryo has already been shown to up-regulate Wnt signalling at selected early stages of development (Martin et al., 2009). Here it

is shown that of the Wnt target genes selected for investigation only *bmp4* demonstrates significant up-regulation pre-mid-blastula transition, with levels of zygotic transcripts still appearing aberrantly high at the shield stage, although the difference observed at this stage was not statistically significant. Both *ndr1* and *dharma* appeared transiently increased in plakoglobin morphant samples when compared to controls. Though the observed increase was not statistically significant, expression levels were more comparable between control and morphant samples at shield, indicating that a biologically significant change in expression may be occurring at the sphere stage in all the Wnt target genes examined. The requirement of *dharma* and *ndr1* for the formation of the zebrafish organiser (i.e. the shield) has previously been identified and this role may explain the early but transient disruption to expression of these genes. The dorsal organiser is first visible as a thickening of the germ ring, hence the "shield" nomenclature of this stage of gastrulation, which occurs at 6 hpf. *Dharma* mutants do not form this embryonic shield region, and have a wide variety of anterior deformities at later stages of development (Fekany et al., 1999). Expression of *dharma* and *ndr1* at late blastula and early gastrula stages is dependent on their own zygotic expression and subsequent expression of organiser genes *goosecoid* and *chordin* depends on correct expression of *dharma* and *ndr1*. Of even greater consequence is the severely ventralised phenotype of *dharma*:*ndr1* double-mutants, which is not seen in single mutants of the same gene, indicating that *dharma* and *ndr1* regulate the formation of the zebrafish dorsal organiser in a cooperative manner (Shimizu et al., 2000). Expression of *goosecoid (gsc)* and *chordin* is dependent on *dharma* and *ndr1*, and *bmp4* expression appears to inversely proportional to that of *gsc* and *chordin* (Sasai et al., 1994; Neave et al., 1997). Hence it is likely that the elevated transcript levels of *dharma* and *ndr1* are indirectly responsible for the increase in *bmp4* expression visible at both sphere and shield stages in plakoglobin morphant embryos.

The requirement of plakoglobin expression for normal Wnt signalling in the developing embryo has been substantiated by the ability of Wnt-inhibitor Dkk-1 to rescue the gross morphological defects that result from plakoglobin knockdown

(Martin et al., 2009). Here an extension of this study has provided more detailed information about the importance of plakoglobin and the relationship between this armadillo protein and Wnt signalling. Dkk1 was able to rescue not only the gross morphological defects but also normalised the cardiac patterning defects seen in plakoglobin morphant embryos, as semi-thin cross-sections through the heart were normal in both the control and "rescue" samples, and embryos co-injected with Dkk1 and the plakoglobin morpholino had comparable heart rates. Though Dkk1 "rescued" embryos appeared to be restored both functionally and at a gross anatomical level, ultra-structural analysis revealed that amelioration of the signalling defects induced by loss of plakoglobin cannot compensate for loss of the protein at the desmosomes, and hence the heart ultra-structure is not fully restored despite the ability of Dkk1 to correct gross patterning defects. These results highlight the importance of plakoglobin at cell-cell junctions. The transmission electron microscopy images also reveal for the first time a loss of desmosomes in the cardiac epithelium of plakoglobin morphant embryos. In the intercalated disks, plakoglobin morphants, Dkk-1 co-injected samples, and Dkk-1 over-expression samples had comparable numbers of desmosomes and unclassified junctions, with desmosome numbers overall greatly reduced when compared to control samples and a much greater number of unclassified junctions visible in all the treated samples. In all probability these ultra-structural defects are caused by the inability of desmosomes to form properly in the absence of plakoglobin or the presence of ectopic Dkk-1 expression. Despite the ability of Dkk-1 to rescue the gross morphological defects it seems that it cannot compensate for the loss of plakoglobin at the desmosomes, and the over-expression of Dkk-1 may be inhibiting adhesion via repression of Wnt signalling.

Similar defects in adhesion were observed in the pericardial epithelium, with desmosome numbers decreased and numbers of unclassified junctions increased in all samples compared to control embryos. Interestingly, the total number of junctions in the pericardial epithelium was not decreased in Dkk-1 over-expression samples, though the majority of junctions could not be classified. As these over-expression samples appeared to have enlarged cell-cell gaps and a dramatic

reduction in identifiable desmosome numbers it is evident that adhesion in the epithelium is also affected. As samples over-expressing Dkk-1 have disrupted adhesion with an increased number of unidentified junctions, it must be remembered that plakoglobin is present in these samples, and so the disruption to adhesion is caused not by the loss of this protein, but by the Wnt pathway inhibition mediated by ectopic Dkk-1 expression which likely prevents proper desmosome formation. Canonical Wnt signalling has been shown to have a direct role in the modulation of cell-cell adhesion, with Wnt1 expression resulting in accumulation of β-catenin and plakoglobin, and stabilisation of β-catenin-cadherin binding. This interaction between Wnt-1 and the armadillo proteins β-catenin and plakoglobin results in enhanced cell-cell adhesion (Hinck et al., 1994). As decreased Wnt signalling resulted in disrupted adhesion in this study it is possible that a decrease in canonical Wnt has the opposite effect, perhaps due to the destruction of β-catenin following inactivation of the Wnt pathway by Dkk1.

As the pericardial epithelium appears to have a greater number of total junctions than the myocardium in samples with surplus Dkk-1, the differences between epithelial and cardiac tissue must be considered. Additional desmosomal proteins plakophilin-1 and plakophilin-3 are not found in the cardiac tissue, but function in the epithelia (reviewed by Neuber et al., 2010). Little is known about the signalling functions of the plakophilin family, however it is possible that these proteins are unaffected by the signalling disruption caused by Dkk-1 over-expression (a theory strengthened by the data presented here as Wnt target genes appear unaffected in the plakophilin-2 knockdown). The presence of plakophilins 1 and 3 may be capable of alleviating the adhesion defects found in the skin to some extent, hence the increased number of “unclassified” junctions observed in the epithelium may be desmosomes that did not form correctly in the absence of plakoglobin. In the cardiac tissue these “attempted” desmosomes were not observed in the same numbers, likely due to the absence of plakophilins 1 and 3 in this tissue.

3.4.2 Plakophilin-2 and Wnt signalling

As a previous loss-of-function study on plakoglobin demonstrated up-regulation of Wnt target genes at early developmental stages (Martin et al., 2009) it was hypothesized that a loss of plakophilin-2 may result in similar signalling disruptions. As both desmosomal proteins share similarities in structure and function it seemed plausible that comparable signalling defects would exist in both loss-of-function models. Surprisingly, both quantitative and qualitative methods used to investigate Wnt target genes failed to expose any appreciable difference in gene expression between control and plakophilin-2 knockdown embryos. This lack of disruption to the Wnt pathway, combined with previously observed defects in cardiac left-right patterning in plakophilin-2 morphant embryos, led to the examination of another major signalling pathway, the Nodal cascade.

3.4.3 Plakophilin-2 and Nodal signalling

The expression levels and patterns of several cardiac marker genes were examined in plakophilin-2 morphant embryos at an early stage of cardiogenesis (the 18 somite stage) to elucidate what effect, if any, plakophilin-2 knockdown has on genes of the Nodal pathway. Expression of *lefty2* was completely ablated from the left cardiac field of plakophilin-2 morphant embryos, with expression of *bmp4*, *spaw*, *oep* and *lefty1* increased at this stage. qPCR also revealed a concomitant increase in expression of *ndr1*. As cardiac positioning and looping are affected in plakophilin-2 morphant embryos it is likely that these phenotypic defects are linked to these disturbances of the Nodal pathway.

The observed disruption of Nodal target genes at the 18 somite stage occurs at a key time-point for patterning events in the cardiac field (approximately 18 hpf), as the bilateral myocardial primordia begin merging to form the heart tube at 19 hpf (Stainier et al., 1993). Expression of *bmp4* is normal at early stages of development in plakophilin-2 morphants (Section 3.2.1), however up-regulation of *bmp4* thereafter is likely the cause of the increased expression of the other affected cardiogenic genes *lefty1* and *spaw*. The chirality of *bmp4* expression in the developing zebrafish heart has been directly linked to the subsequent direction of

cardiac jogging and looping and *bmp4* signalling has been shown to regulate cardiac laterality by controlling expression of *cyclops*, *spaw*, *lefty1* and *lefty2* during segmentation (Chen et al., 1997; Chocron et al., 2007). As later *bmp4* expression returns to normal levels it seems the critical time point occurs during late segmentation (approximately 18 hpf). Further evidence comes from mice homozygous for a mutation in Smad5, a component of BMP signalling. These mice have defects in heart development, particularly in cardiac looping. Smad5 mutant mice also have bilateral expression of Nodal, Lefty2 and Pitx2 with concomitant reduced or absent Lefty1 expression (Chang et al., 2000). Additionally, a study on *pitx2* has revealed two zebrafish isoforms, *pitx2a* and *pitx2c*. Several differences exist between these isoforms, including variation in initiation of expression, with *pitx2c* detectable at the dome stage whereas *pitx2a* expression appears not to initiate until bud stage. *Pitx2c* expression is lost in zebrafish *oep* mutants, indicating *oep* regulation of *pitx2c*, but not *pitx2a* (Essner et al., 2000), hence increased expression of *oep* seen in the plakophilin-2 knockdown may be responsible for the observed trend towards *pitx2c* up-regulation. Due to sequence similarities between the two isoforms it was not possible to design specific qPCR probes targeting *pitx2a*, however according to the Essner et al. study ectopic expression of *pitx2c* can induce *pitx2a* expression, and embryos with ectopic expression of *pitx2a* displayed decreased *lefty2*. *Pitx2a* is also strongly expressed in the anterior region of the cardiac field, a domain which includes the future atrium (Stainier and Fishman, 1992; Essner et al., 2000). As plakophilin-2 morphant embryos display enlarged atria in addition to cardiac looping defects it is plausible that an increase in the expression of *pitx2a* occurs and is linked to these defects.

Murine studies have suggested a role for Lefty2 as a feedback inhibitor of Nodal signalling. In the absence of Lefty2, Nodal (the murine equivalent of zebrafish *southpaw*) has been seen to diffuse over a large distance into the anterior LPM, and these Lefty2 mutant mice displayed gut and heart abnormalities. The striking loss of *lefty2* expression in our zebrafish plakophilin-2 knockdown model tallies with these data, particularly as Lefty2-deficient mice also displayed increased expression of Lefty1 and Pitx2 (Meno et al., 1999; Meno et al., 2001). Zebrafish data has also

demonstrated the ability of the lefty paralogs to negatively regulate each other (Bisgrove et al., 1999; Meno et al., 2001).

Of particular interest in this study is the up-regulation of the Nodal gene *southpaw*. In mice, Nodal is thought to directly induce expression of Pitx2 (Shiratori et al., 2001). In zebrafish southpaw is first expressed in the left lateral plate at the 10-12 somite stage, preceding asymmetric expression of lefty2 and pitx2 at the 17-22 somite stage. Loss of *southpaw* expression has also been shown to correlate with down-regulation of *lefty 1* and *pitx2,* and southpaw-deficient embryos exhibit severe disruption to L-R asymmetry of cardiac jogging and looping (Bisgrove et al., 1999; Essner et al., 2000; Long et al., 2003). Expression of *southpaw* coincides both temporally and proximally with *one-eyed pinhead* in the developing embryo from the 10-17 somite stage (Long et al., 2003). Interestingly, Lenhart et al. have recently described a novel role for *lefty2*, proposing a molecular model whereby *lefty2* expression functions as an "anterior barrier" in the left cardiac field, preventing the propagation of *southpaw* into the right LPM (Lenhart et al., 2011).

Collectively these data strongly support the signalling results obtained in this study for embryos lacking plakophilin-2, as the plakophilin-2 morphant phenotype exhibits incomplete cardiac looping and also displays increased expression of Nodal genes *lefty 1*, *one-eyed pinhead*, *pitx2c* and *southpaw*, with ablation of *lefty2*. These spatial and chronological relationships indicate that disruption to any of the Nodal genes may have a cascade effect, disrupting expression of other targets and co-factors through the pathway.

As signalling is tightly regulated in normal embryonic development it would be interesting to further investigate the extent of Nodal pathway disruption at different stages of development in plakophilin-2 morphants, and to examine Nodal target genes in early cardiogenesis in plakoglobin morphant embryos. As phenotypic similarities exist between these loss-of-function models it would be interesting to investigate what similarities in signalling, if any, exist between them.

As expression of many genes in the Nodal cascade was disrupted following loss of plakophilin-2, *otx5* was chosen as a marker to determine if the patterning

disruption occurring in the heart extended to the neural structures. Localisation of *otx5* was found to be normal in morphant embryos indicating that a selective disruption of patterning, localised to the cardiac field, is occurring in embryos lacking plakophilin-2 expression. A more thorough examination of internal organs, and in particular laterality of the gut, would be required to confirm the heart-specific nature of the patterning disruption occurring.

4 Molecular Analysis of Plakoglobin and Plakophilin-2 Morphant Embryos as Models for ARVC

4.1 Assessing the zebrafish knockdown models for ARVC-related defects

Genes implicated in the human congenital heart condition ARVC were examined in both the plakoglobin and plakophilin-2 knockdown models to determine if complete loss of these proteins rather than mutation was sufficient to replicate specific clinical features of the disease. The aim of these experiments was to investigate to what extent a complete knockdown could model diagnostic and molecular features associated with human desmosomal protein mutations.

Mutations in genes that encode cell-cell adhesion proteins cause ARVC, including mutations in *plakoglobin*, *plakophilin-2*, *desmoplakin*, *desmocollin-2* and *desmoglein-2* (Protonotarios et al., 1986; McKoy et al., 2000; Rampazzo et al., 2002; Gerull et al., 2004; Pilichou et al., 2006). Despite the number of causative genes, ARVC variants share some common pathological and molecular features. Confocal immunofluorescence microscopy has shown that in all cases of ARVC the immunoreactive signal for plakoglobin is decreased at the intercalated disks, and connexin 43 is frequently reduced. Changes in localisation of other desmosomal proteins such as plakophilin-2 and desmocollin vary from patient to patient depending on the causative mutation; however N-cadherin levels are consistently unaffected (Kaplan et al., 2004a; Kaplan et al., 2004b; Asimaki et al., 2007; Tandri et al., 2008; Asimaki et al., 2009; Gehmlich et al., 2011). These findings dictated the genes and proteins selected for investigation in this study, and provided criteria by which to assess our plakoglobin and plakophilin-2 knockdowns as zebrafish models for ARVC.

The resulting changes in expression of genes linked to ARVC (e.g. *desmoplakin-a* and *connexin 43*) following loss of plakoglobin or plakophilin-2 will be presented in this chapter. Additionally, expression of selected genes in APC mutant embryos will be compared to their expression in plakoglobin morphant embryos. As fibro-fatty replacement of the ventricle is a key diagnostic feature of ARVC, the resulting changes in adipogenic genes will also be presented. Assessment of both plakoglobin and plakophilin-2 morphant embryos as zebrafish models for ARVC will be based upon this cumulative data.

4.1.1 mRNA expression levels of ARVC-related genes in plakoglobin knockdown embryos

Plakoglobin morpholino-injected embryos were harvested at 48 and 72 hpf and processed for qPCR as previously described in Section 2.2.5. mRNA levels of *desmoplakin-a*, *connexin 43* and *β-catenin* were then examined.

mRNA expression of gap-junction protein *connexin 43* was significantly down-regulated at both 48 and 72 hpf. mRNA expression of desmosomal plaque protein, desmoplakin, was also significantly decreased in plakoglobin knockdown embryos, with a tendency towards decrease evident at 48 hpf becoming statistically significant by 72 hpf (Figure 4.1).

β-catenin, an armadillo protein and integral component of the Wnt signalling pathway, was found to have a similar mRNA expression profile to desmoplakin-a in plakoglobin knockdown embryos with a significant decrease evident at 72 hpf (Figure 4.1).

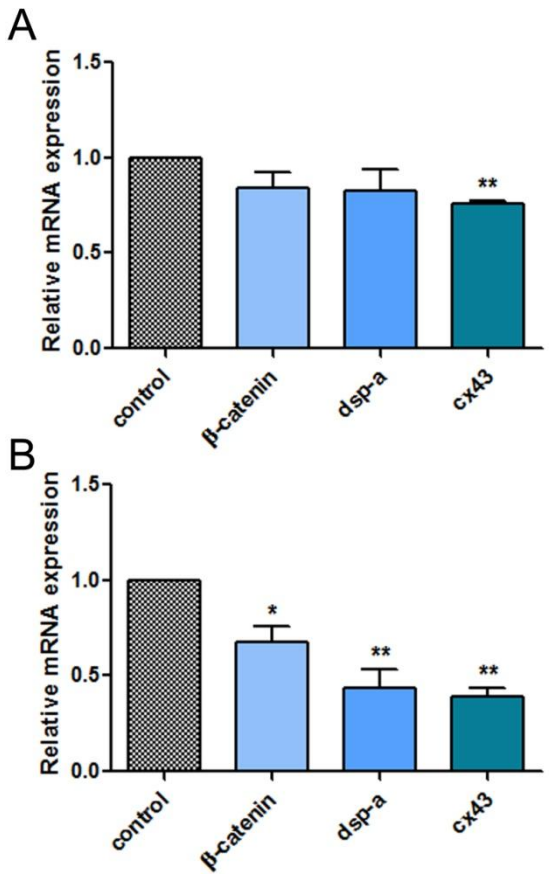

Figure 4.1 mRNA expression of ARVC-related genes in plakoglobin knockdown embryos. Expression of ARVC-related genes *β-catenin*, *desmoplakin-a* (dsp-a) and *connexin 43* (cx43) at 48 hpf (A) and 72 hpf (B) in plakoglobin knockdown samples. By 72 hpf all genes show significant down-regulation in plakoglobin morphant samples compared to controls; n=3. Data are means +s.d. **P*<0.05, ***P*<0.005 vs controls by paired *t*-test.

Wnt1 has previously been implicated in cell culture experiments as a positive regulator of connexin 43 (van der Heyden et al., 1998; Ai et al., 2000) and as levels of connexin 43 mRNA expression were found to be decreased in the plakoglobin morphant embryos, expression of Wnt1 was investigated. Embryos lacking plakoglobin protein have decreased levels of Wnt1 mRNA (Figure 4.2), further corroborating the data obtained for connexin 43 expression.

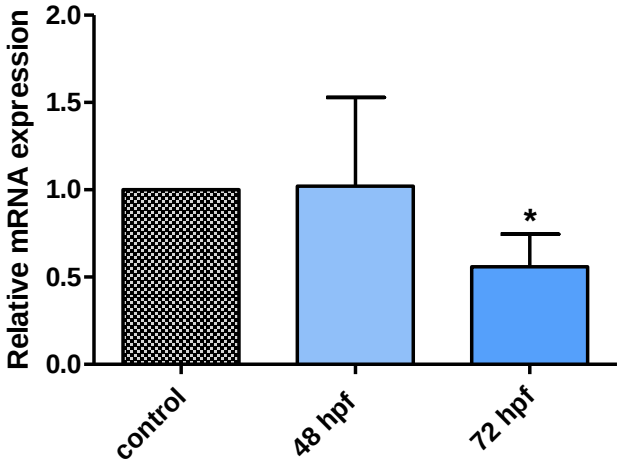

Figure 4.2 Wnt1 mRNA expression in plakoglobin morphant embryos at 48 and 72 hpf. Expression of Wnt1 was unaffected at 48 hpf and decreased significantly in plakoglobin knockdown samples at 72 hpf when compared to control morpholino samples; n=3. Data are means + s.d.* *P*<0.05 vs control by paired *t*-test.

4.1.2 mRNA expression levels of ARVC-related genes in APC mutant embryos

The plakoglobin knockdown phenotype is similar to the cardiac phenotype observed in APC mutant embryos, hence gene expression in this transgenic line was examined to determine if comparable signalling defects existed. The disruption to Wnt/β-catenin signalling that characterises the APC mutant line results in pericardial oedema, cardiac malformation and blood pooling, along with a host of other developmental defects (Hurlstone et al., 2003). Thus, this line presented an ideal opportunity to compare signalling defects in embryos with similar cardiac defects stemming from different causative genes.

Before the APC embryos were harvested for gene expression studies, heart rates were recorded and compared with those of wild-type AB embryos at the same developmental stage. APC mutants (as expected) had significantly reduced heart rates (Figure 4.3) and obvious looping defects when compared to those of wild-type controls (phenotype not shown, see Hurlstone et al.,(2003)).

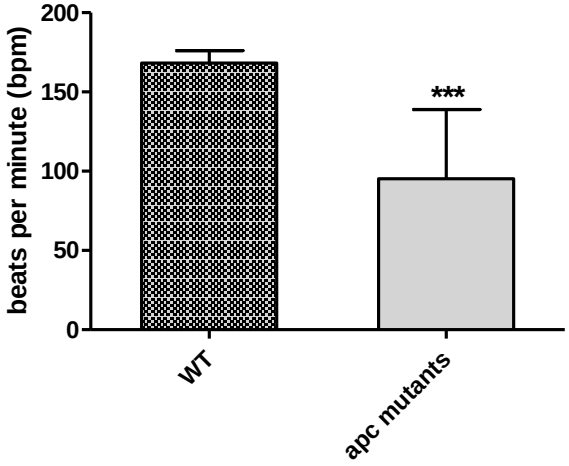

Figure 4.3 APC mutant heart rates measured at 72 hpf.
APC mutant embryos had deceased heart rates compared to wild-type embryos at the same developmental stage. Data shown are means + s.d. ***P<0.001 vs wild-type by un-paired t-test; n=10.

Expression levels of *plakoglobin*, *connexin 43* and *Wnt1* were examined in both 48 and 72 hpf *apc* mutant samples, with same stage wild-type AB embryos used for controls. Expression levels of *plakoglobin* were of particular interest as mutation of APC constitutively activates the Wnt pathway and loss of plakoglobin is thought to up-regulate Wnt target genes (Martin et al., 2009). Plakoglobin morphant embryos have significantly down-regulated expression of *connexin 43* and *Wnt1* (Section 4.1.1) hence their expression in APC mutant embryos was examined. Additionally, Wnt1 has recently been linked to premature myocardial infarction (Goliasch et al., 2012), so it would be most interesting to see if embryos with similar cardiac defects stemming from different molecular causes have the common feature of decreased Wnt1 expression.

At 48 hpf all three genes of interest were significantly down-regulated, whereas at 72 hpf only *connexin 43* and *Wnt1* mRNA levels were significantly decreased (Figure 4.4). *Plakoglobin* expression was also examined in sphere stage APC mutants; however mRNA expression was unaffected at this stage (data not shown), indicating that a cascade of events in early embryogenesis is required to induce a change in *plakoglobin* mRNA expression at later stages of development.

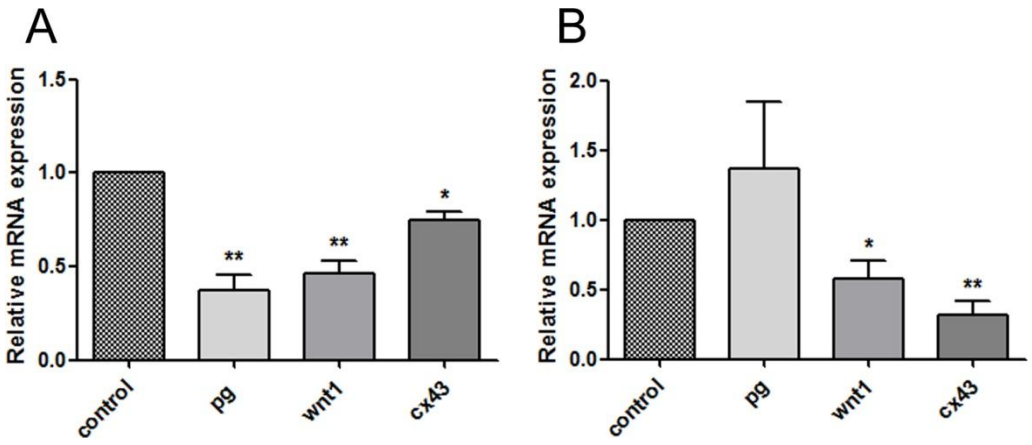

Figure 4.4 mRNA expression in APC mutant embryos.
Expression levels of *plakoglobin* (plakoglobin), *Wnt1* and *connexin 43* (cx43) levels at 48 hpf (A) and 72 hpf (B) in apc mutant embryos compared to those of wild-type AB fish at the same developmental stages. Data shown are means + s.d.**P*<0.05, ***P*<0.005 vs wild-type controls by paired *t*-test; n=3.

4.1.3 mRNA expression levels of ARVC-related genes in plakophilin-2 knockdown embryos

Relative transcript levels of *connexin 43*, *desmoplakin-a*, *β-catenin* and *plakoglobin* were then examined in plakophilin-2 morphant embryos at 72 hpf. mRNA expression was found to be unaffected in each case (Figure 4.5), indicating that none of the genes examined interact directly with plakophilin-2.

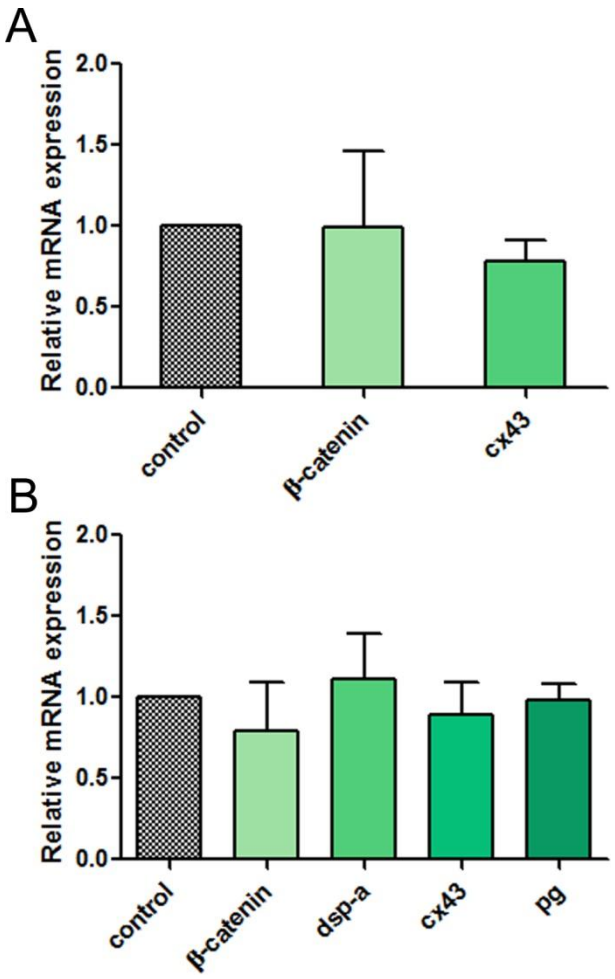

Figure 4.5 Loss of plakophilin-2 does not affect mRNA expression of ARVC-related genes. Expression of ARVC-related genes *β-catenin*, *desmoplakin-a* (dsp-a), *connexin 43* (cx43) and *plakoglobin* (pg) at 48 hpf (A) and 72 hpf (B) in plakophilin-2 knockdown samples. There was no significant effect on mRNA expression of any of the genes examined in the plakophilin-2 knockdown in comparison to control levels by paired *t*-test; n=3. Data shown are mean + s.d.

4.1.4 Expression levels of ARVC-related proteins in plakoglobin and plakophilin-2 knockdown embryos

Altered localisation of both gap-junction protein connexin 43 and plakoglobin at the intercalated disks of ARVC patients is reported to be a hallmark of ARVC, regardless of the causative gene mutated (Asimaki et al., 2007; Asimaki et al., 2009). An initial examination of connexin 43 localisation in zebrafish at 72 hpf showed that comparative immunofluorescence would not be possible due to the extremely low level of detectable connexin 43 in the zebrafish heart at this embryonic stage (data

not shown). Hence, total protein levels of connexin 43 and plakoglobin were examined by SDS-PAGE and Western blotting.

Expression of connexin 43 protein was examined in plakoglobin morphant embryos at 72 hpf. Though densitometric analysis of three independent biological repeats showed a slight decrease in all plakoglobin morphant samples, the level of decrease was not consistent enough to be of statistical significance (Figure 4.6).

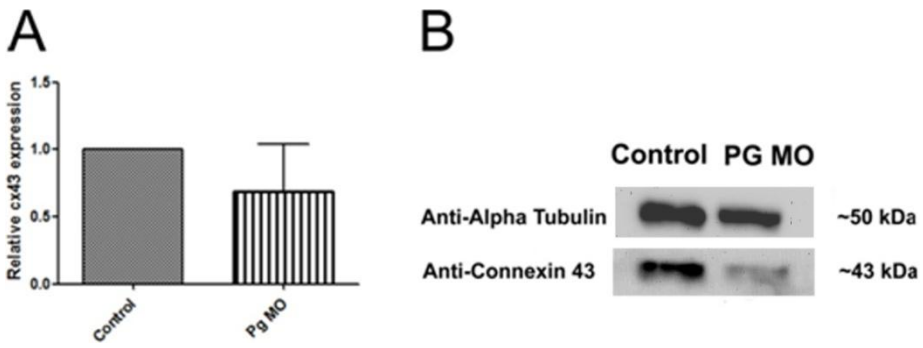

Figure 4.6 Expression of connexin 43 protein in plakoglobin knockdown embryos at 72 hpf.
(A) Western blot analysis of connexin 43 protein expression in control and plakoglobin (PG) knockdown embryos. Connexin 43 was detected at 43 kDa. α-tubulin was used as a loading control. (B) Densitometric analysis of connexin 43 expression in plakoglobin morphant embryos compared to control morpholino embryos at the same developmental stage. Data are means + s.d. , analysed by paired *t*-test; n=3.

Expression of plakoglobin and connexin 43 total protein was examined in plakophilin-2 knockdown samples harvested at 72 hpf. Expression levels were comparable between control and plakophilin-2 morphant samples, with no significant change in either of the proteins of interest (Figure 4.7).

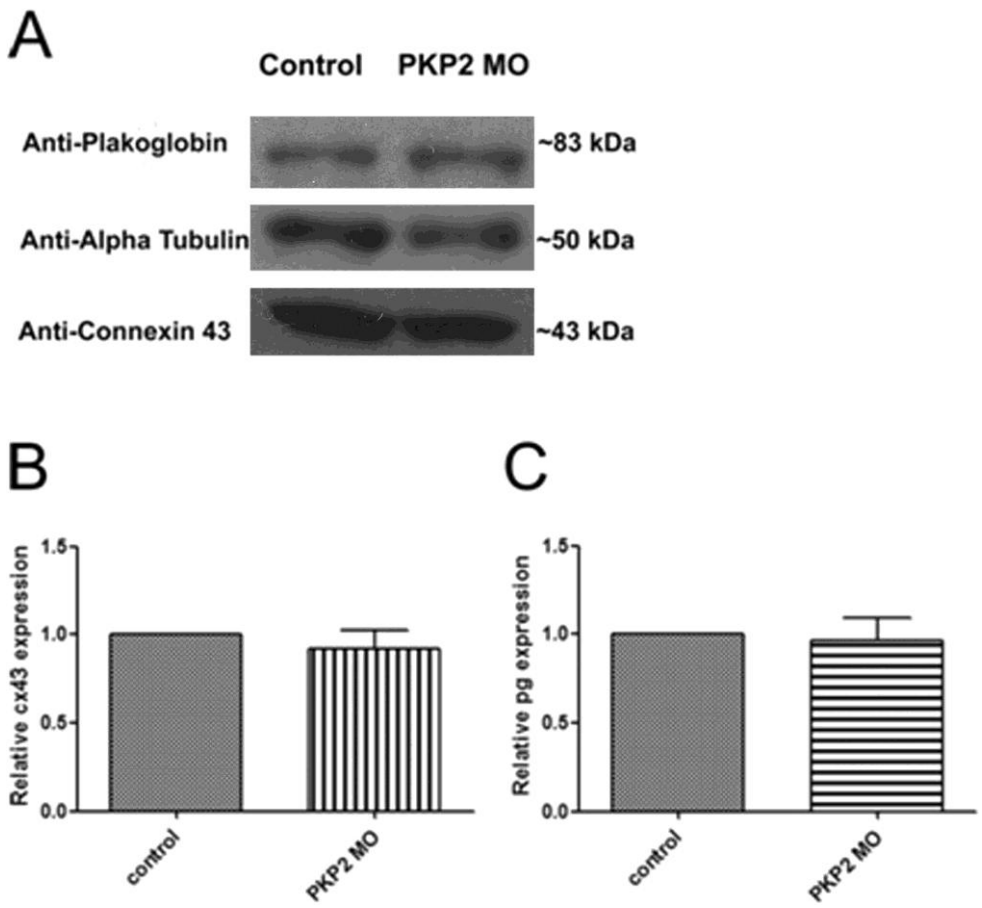

Figure 4.7 ARVC-related protein expression in 72 hpf plakophilin-2 knockdown embryos. (A) Western blot analysis of connexin 43 and plakoglobin protein expression in control and plakophilin-2 (PKP2) knockdown embryos. Connexin 43 was detected at approximately 43 kDa and plakoglobin was detected at approximately 83 kDa. α-tubulin was used as a loading control. (B & C) Densitometric analysis showed no appreciable difference in expression of either connexin 43 (B) or plakoglobin (C) in plakophilin-2 knockdown embryos when protein levels were compared to those of control morpholino-injected embryos at the same stage. Data shown are means + s.d., analysed by paired *t*-test; n=3.

4.1.5 The effect of plakoglobin and plakophilin-2 knockdown on adipogenic gene expression

One of the most distinct symptoms of ARVC is the fibro-fatty replacement of cardiomyocytes. To investigate if loss of plakoglobin or plakophilin-2 in the morphant embryos may have disruptive effects on the signalling components of adipogenesis, expression of two representative adipogenic genes was examined.

Adipogenic transcription factor *Wnt5b* and adipogenic marker *PPAR-γ* were selected as representative adipogenic genes, and mRNA expression of these genes was examined by qPCR. Interestingly, both *Wnt5b* and *PPAR-γ* were significantly down-regulated in plakoglobin morphant samples harvested at 72 hpf. However in plakophilin-2 knockdown samples there was no appreciable difference between morphant and control samples (Figure 4.8).

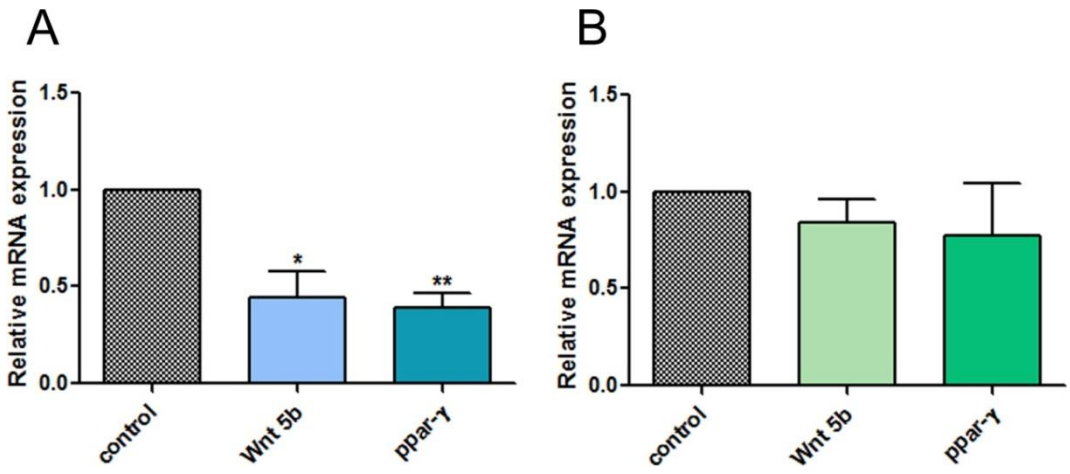

Figure 4.8 Adipogenic gene expression in plakoglobin and plakophilin-2 knockdown embryos.
Expression of adipogenic genes Wnt5b and PPAR-γ is decreased in 72 hpf plakoglobin morphant embryos (A), but unaffected in plakophilin-2 morphant embryos at the same developmental stage (B). Data shown are means + s.d. **P*<0.05, ***P*<0.005 vs control by paired *t*-test; n=3.

4.2 Summary

An examination of some of the molecular aspects of ARVC in plakoglobin and plakophilin-2 morphant embryos has yielded novel information that is of use when

evaluating these morphant embryos as models for the signalling defects associated with the human congenital heart condition.

Plakoglobin morphant embryos have decreased expression of all relevant genes examined. Genes strongly associated with ARVC, such as *desmoplakin-α* and *connexin 43*, as well as several genes that participate in Wnt signalling (*β-catenin, Wnt1*) and genes required for adipogenesis (*Wnt5b*, *PPAR-γ*) are all significantly down-regulated in plakoglobin morphant embryos. Total connexin 43 protein is however unaffected. Decreased levels of *desmoplakin-α* and *connexin 43* mRNA are favourable aspects of the plakoglobin knockdown as a model for ARVC. However the down-regulation of adipogenic genes, and the consistency of connexin 43 total protein levels between control and morphant embryos are not representative of the human condition and do not satisfy the requirements of a good animal model for this disease.

Results from the APC mutant line are similar to those achieved with plakoglobin morphant embryos. All genes examined were down-regulated in comparison to control samples, and at similar levels to those observed in plakoglobin morphant embryos. Additionally, expression of plakoglobin was also decreased in *apc* mutant embryos.

Expression of ARVC-related and adipogenic genes was also examined in plakophilin-2 morphant embryos, as was expression of plakoglobin. None of the genes examined were significantly affected, nor was the total protein expression of connexin 43 or plakoglobin.

4.3 Discussion

Experiments in this chapter aimed to evaluate zebrafish embryos lacking plakoglobin and plakophilin-2 as models for ARVC by examining characteristic signalling elements of the human condition in the zebrafish knockdown models. Overall, neither morphant provides an authentic model for the congenital heart defect, however loss of plakoglobin appears to have some more desirable consequences for a signalling model than loss of plakophilin-2. In addition to their notable cardiac defects, plakoglobin morphant embryos show significantly decreased expression of ARVC-related genes *connexin 43* and *desmoplakin-a,* and disruption to adipogenic genes *Wnt5b* and *PPAR-γ*. Plakophilin-2 however does not appear to have any of the posited effects of a true model for ARVC. This is not entirely unexpected, as already demonstrated in Chapter 3, loss of plakophilin-2 appears to operate via an entirely separate signalling pathway to plakoglobin.

4.3.1 Molecular features of ARVC

Patients with the N-terminal mutation form of plakoglobin-related ARVC have less plakoglobin, desmoplakin and connexin 43 proteins at the intercalated disks in cardiomyocytes, whereas distribution of plakophilin-2 and N-cadherin is unaffected (Asimaki et al., 2007). Similarly, samples from Naxos Disease patients display decreased levels of connexin 43 at the intercellular junctions of both ventricles, and abnormal localisation of the mutant plakoglobin at the intercalated disks, yet plakophilin-2, desmoplakin and other desmosomal proteins are unaffected (Kaplan et al., 2004b).

In excess of 200 pathogenic plakophilin-2 mutations have been identified to date with associated structural and cardiac abnormalities, and 131 of these are linked to ARVC (van der Zwaag et al., 2009; Roberts et al., 2012), yet little is known of the molecular role played by this armadillo protein. A decrease in junctional plakoglobin is thought to be a consistent feature in all diagnosed cases of ARVC, including those caused by mutations in the plakophilin-2 gene (Asimaki et al., 2009). A mouse model lacking plakophilin-2 has been reported as embryonic lethal due to distortions in cardiac development (altered cardiac morphogenesis, blood leakage

and cardiac rupture), with molecular defects distinct from those of a murine plakoglobin mutant, particularly with regard to desmoplakin localisation which is unaffected in plakoglobin-deficient murine hearts but strikingly absent from adherens junctions in plakophilin-null embryos. Desmoplakin is also seen to co-localise extensively with other desmosomal proteins (including plakoglobin, N-cadherin, β-catenin, plakophilin-2 and desmoglein-2) in wild-type embryos, yet this co-localisation fails to occur in plakophilin-2 knock-out embryos (Ruiz et al., 1996; Grossmann et al., 2004).

4.3.2 Molecular aspects of the plakoglobin knockdown model

Given the existence of these common molecular features across various desmosomal cardiomyopathies the expression levels of desmoplakin-a, connexin 43, and plakoglobin were selected as criteria by which to assess the signalling compatibility of the plakoglobin and plakophilin-2 loss-of-function models with human ARVC. Plakoglobin knockdown samples displayed decreased expression of connexin 43 and desmoplakin mRNA at 72 hpf, indicating that loss of plakoglobin in zebrafish affects expression of those genes identified as disrupted in human patients. Studies using human tissue samples have failed to detect any appreciable difference in connexin 43 total protein, or have reported only mild decreases (Kaplan et al., 2004a; Tandri et al., 2008; Gehmlich et al., 2011). These data are supportive of the results shown in this study, where Western blot analysis of connexin 43 total protein in plakoglobin morphant embryos showed no significant difference in comparison to control embryo samples, as it is quite likely that the decreased localisation reported in many studies is not due to a lack of protein, but a failure of the components to assemble correctly at cell-cell junctions, resulting in a change in localisation patterns and ultimately a failure in adhesion.

Increased levels of β-catenin protein have previously been associated with loss of plakoglobin (Martin et al., 2009; Li et al., 2011a), however data presented in Section 4.1.1 shows a small but significant decrease in β-catenin mRNA expression in plakoglobin morphant embryos. Examination of murine data may help clarify these

apparently conflicting results. Using a tissue-specific knock-out of plakoglobin, mRNA expression of β-catenin appeared unaffected when examined by qPCR, yet protein samples exhibited an unequivocal increase in β-catenin protein expression (Li et al., 2011a). These data, together with our own, indicate that a post-transcriptional increase in β-catenin expression occurs in the absence of plakoglobin.

Interestingly, the effect of ectopic desmoplakin expression on desmosomal components has recently been investigated in human lung cancer cell lines, where expression of desmoglein 1-3, desmocollin 1-3, plakophilin 1-3 and plakoglobin was examined. Expression of plakoglobin mRNA and protein was found to be up-regulated in the wake of desmoplakin over-expression, with a coincident decrease in levels of β-catenin and down-regulation of Wnt/β-catenin target genes Axin2 and MMP14. Conversely, desmoplakin knockdown resulted in decreased plakoglobin, increased β-catenin and an increase in MMP14 expression, whereas expression of plakophilins 1-3 was unaffected (Yang et al., 2012). In this study levels of *desmoplakin-a* mRNA were decreased in plakoglobin morphant samples, correlating with the results discussed above.

4.3.3 Further evidence for the role of plakoglobin in Wnt signalling gleaned from the APC mutant line

The results obtained with material extracted from APC mutant embryos are of great relevance to this study. Adenomatous polyposis coli (APC) is an integral component of the axin destruction complex required for the phosphorylation and subsequent ubiquitination and degradation of β-catenin, and truncation of APC activates the Wnt/β-catenin pathway (Fodde et al., 2001). In zebrafish, truncation of APC results in a myriad of gross developmental defects, of which cardiac malformation is the earliest detectable. Mutant hearts have normal morphology, positioning and chamber specification at 36 hpf, but by 80 hpf the heart has ceased to beat and blood circulation is absent. Similarly, plakoglobin knockdown causes increased Wnt signalling, but also a cardiac malformation phenotype (Martin et al., 2009). It is quite interesting to see that in APC mutant embryos with up-regulated Wnt

signalling mRNA expression of plakoglobin is reduced. This evidence further clarifies the role of plakoglobin as a constituent of the Wnt pathway, where it can regulate or be regulated by canonical Wnt signalling, and acts downstream of APC.

Similarly, in plakoglobin morphant embryos expression of *connexin 43* and *Wnt1* are found to be reduced, an effect mirrored in the APC mutant embryos. The consistency of these data gives further credence to previous studies that propose a relationship between plakoglobin and the Wnt/β-catenin pathway.

4.3.4 Molecular aspects of the plakophilin-2 knockdown model

Mutations in plakophilin-2 have been reported with attendant effects on plakoglobin, desmoplakin and connexin 43 localisation at the intercalated disks (Grossmann et al., 2004; Asimaki et al., 2009); hence these were selected as candidates likely to be affected by loss of plakophilin-2 in zebrafish. mRNA and protein levels of plakoglobin and connexin 43 were unaffected in the plakophilin-2 morphant samples, as were desmoplakin mRNA levels. These data are consistent with findings presented earlier in this study, where loss of plakophilin-2 had no effect on target genes of the Wnt pathway at early stages of development. It seems that ablation of plakophilin-2 protein in zebrafish embryos has completely different molecular consequences to those occurring in the absence of fellow armadillo protein plakoglobin, or as a result of mutated plakophilin-2 as in ARVC.

4.3.5 Connexin 43 and the Wnt signalling pathway

Connexin 43 is the major gap junction protein in the heart (Verheule et al., 1997) and has a previously identified relationship with the Wnt signalling pathway. *In vitro* studies have demonstrated that increased levels of Wnt1 can specifically up-regulate connexin 43 mRNA and protein expression, cause increased cell-cell adhesion and increase levels of plakoglobin protein. Increased levels of Wnt1 (coupled with the resulting increase in connexin 43) also induced increased contraction in cultured cardiomyocytes (Bradley et al., 1993; van der Heyden et al., 1998). *In vivo* a murine cardiomyopathy model has demonstrated concordant dysregulation of β-catenin and connexin 43 (Swope et al., 2012a). These data

further substantiate the results obtained in the zebrafish plakoglobin knockdown model where loss of plakoglobin results in decreased levels of canonical Wnt mRNAs, decreased *connexin 43* and *β-catenin* mRNA expression and a decreased heart rate.

Though the majority of publications point to a proportional relationship between connexin 43 and Wnt signalling, an opposing role has also been reported in an *in vitro* study on human colon cancer cells. Transient transfection of connexin 43 into human colon carcinoma cells reduced TCF-mediated gene transcription by 10% (as measured by luciferase assay) with an associated increase in apoptotic cell death (Sirnes et al., 2012). This observation is not unique, as a recent publication on malignant glioma stem cells (GSCs) has provided further insight into the underlying mechanism for this apparent discrepancy in signalling roles for connexin 43. Treatment with connexin 43 inhibited self-renewal, proliferation, invasiveness and tumorigenicity of the GSCs, via a Cx43/E-cadherin complex that formed following the up-regulation of the E-cadherin protein. As expression of Wnt/β-catenin downstream target genes was inhibited in the treated samples it is likely the E-cadherin/Cx43 protein complex interferes with expression of Wnt/β-catenin target genes and thus decreases the malignancy of the GSCs. These data indicate a unique signalling role for connexin 43 in the presence of malignant cell types, with the authors hypothesizing that over-expression of Cx43 may specifically affect the so-called “stemness” genes that are direct targets of the Wnt/β-catenin pathway (Yu et al., 2012). These results are of particular interest as previous experimental work on plakoglobin morphant embryos combined with data presented here shows increased localisation of E-cadherin and β-catenin, with decreased mRNA expression of connexin 43, and an increase in expression of Wnt target genes (such as bmp4, dharma and ndr1) at early stages, yet a member of the canonical Wnt pathway, Wnt1, is decreased in later stage embryos. The discrepancies between this study and previously published results may be attributed to the fact that work presented here focuses on an *in vivo* model, and other data is based on *in vitro* assays which utilise refined cell populations. Connexin 43 may have distinct roles depending on the tissue type in which it is expressed, and hence changes in

signalling detected in cell culture experiments may not match those from whole tissue models such as ours.

Interestingly, a recent publication has identified a link between Wnt-1 and myocardial infarction. Serum levels of Wnt-1 and Dkk-1 were examined in young patients who had survived myocardial infarction. Wnt-1 levels were found to be significantly lower in these patients compared to control subjects, and levels of Dkk-1 were increased (Goliasch et al., 2012). These data further substantiate results presented in Sections 4.1.1 and 4.1.2. Plakoglobin morphant embryos and APC mutant embryos have obvious cardiac defects (Hurlstone et al., 2003; Martin et al., 2009) and significantly decreased expression levels of *Wnt1* mRNA.

4.3.6 Desmosomal protein knockdown and adipogenic gene expression

An *in vitro* assay following the differentiation of pre-adipocytes has examined the relationship between PPAR-γ and β-catenin, and demonstrates that post-transcriptional suppression of β-catenin correlates with increased expression of PPAR-γ protein (Moldes et al., 2003). Similarly, Wnt5b has previously been shown *in vitro* to inhibit the canonical Wnt/β-catenin signalling pathway with associated promotion of adipogenesis (Kanazawa et al., 2005). As it has previously been shown that loss of plakoglobin results in increased expression of β-catenin, (Martin et al., 2009) and qPCR results discussed here (Section 4.1.1) indicate this increase occurs post-transcriptionally, this may explain why plakoglobin knockdown embryos display decreased expression of *PPAR-γ* and *Wnt5b* mRNA.

An ideal model for ARVC would demonstrate the fibrous/fatty replacement of cardiac tissue that is associated with the disease, yet examination of such progressive defects is beyond the scope of morpholino-based studies, as the effects of the morpholino knockdown are transient. Even without the limitations of the morpholino it must be remembered that ARVC is primarily an adult-onset disease, and clinical features are often undetectable until final stages, hence our embryonic zebrafish model did not provide a good candidate for a pathological model in this respect. An up-regulation of adipogenic genes might still be expected at early

stages if excessive adipogenesis were to occur, however our data indicates the contrary hence there is no indication that complete loss of plakoglobin results in adipogenic replacement of cardiac tissue.

Prior studies have also failed to recapitulate the adipogenic characteristic of ARVC in animal models other than zebrafish. A previous murine study closely related to our research overcame the problematic embryonic lethality associated with murine plakoglobin knock-out by adopting a cardiac-specific knock-out (CKO) approach. CKO mice displayed loss of myocytes with ancillary fibrotic replacement, thinning of the myocardial wall and decreased expression of desmosomal proteins desmoglein, plakophilin-2 and desmoplakin. However adipocytes were not seen in the myocardium and lipid accumulation was not increased in the plakoglobin CKO mice (Li et al., 2011a). A recent publication presents a murine double knock-out (DKO) model lacking plakoglobin and β-catenin specifically in the heart, and replicates many of the diagnostic features desirable for an animal model of cardiac disease. These DKO mice exhibit cardiomyopathy, fibrosis throughout the myocardium, enlarged ventricles and conductional defects that result in sudden cardiac death in 100% of DKO animals between 3 and 5 months, but no increase in adipocytes (Swope et al., 2012a). This double knock-out model represents the most comprehensive physiological animal model for ARVC that has been generated to date and further demonstrates the functional overlap of β-catenin and plakoglobin. Though it recapitulates the disease features successfully, this DKO is limited as it does not model the underlying cause of the human condition and hence does not contribute to a better understanding of the mechanism of disease.

There is a potential explanation for this inability to replicate the adipogenic aspect of ARVC in current models. Lombardi et al., (2009) propose that nuclear plakoglobin may function in the capacity of a transcriptional regulator, suppressing canonical Wnt signalling, and as such is required for the trans-differentiation of a cardiac progenitor into an adipocyte (Lombardi et al., 2009). If so, the complete ablation of plakoglobin currently used to model ARVC may not allow the generation of a model

that is fully faithful to the human condition, and hence the answer may lie in more recent advances in targeted mutation techniques, such as zinc-finger nucleases or transcription activator-like effector nucleases.

4.3.7 Plakoglobin and plakophilin-2 knockdowns as zebrafish models for ARVC

As a zebrafish model for ARVC, the plakoglobin knockdown has several desirable features, including defects in heart morphogenesis and changes in the mRNA expression of genes reported to be affected in samples from human ARVC patients, such as connexin 43 and desmoplakin. It is surprising that no significant change in connexin 43 protein was detectable, given the significant reduction in expression of *connexin 43* mRNA seen in the plakoglobin morphant samples. Changes in phosphorylation status of the protein have been reported in some studies (Gehmlich et al., 2011; Gehmlich et al., 2012), though not examined here. Defects in skin, such as blistering, have been reported in a study of plakoglobin-deficient mice, which tallies well with the palmoplantar keratoderma that is a defining feature of Naxos disease. No such defects were visible in the zebrafish knockdown, however for the first time this study reports defects in adhesion in the cardiac epithelium of zebrafish plakoglobin morphants (Chapter Three, Section 3.1.2).

A clinical feature of ARVC is the replacement of the right ventricle with fibrotic and fatty tissue. *PPAR-γ* and *Wnt5b* are adipogenic genes and we would have expected an increase in expression of these genes if fibro-fatty replacement was occurring in plakoglobin knockdown embryos. Adipogenic genes investigated were found to be significantly down-regulated in plakoglobin knockdown samples, thus failing to match the human symptom of increased adipogenesis in the heart. The fact that fibro-fatty replacement is a late-stage feature of a progressive, generally adult-onset disease, and the short-term knockdown incurred by morpholino injection may simply be too short a time-frame in which to achieve a model with such an advanced element of ARVC. It is more likely, however, that the loss of plakoglobin does not provide a good model for ARVC, as it fails to replicate the majority of the signalling aspects of the disease, and does not recapitulate the important feature of increased adipogenesis. The relationship between plakoglobin and the Wnt/β-

catenin pathway connects the various signalling defects seen in plakoglobin morphant embryos throughout development in this study, from early stage embryos where Wnt target gene expression has previously been shown to be altered (Martin et al., 2009) to the later stage effects on ARVC-related and adipogenic genes, highlighting the importance of plakoglobin as a modulator of Wnt signalling in zebrafish development, and also clarifying that complete loss of plakoglobin protein cannot be used to generate an accurate zebrafish model for ARVC.

The plakophilin-2 knockdown overall seems even less representative of the human condition than the plakoglobin knockdown. Heart defects are present but with no detectable change in ARVC-related protein or gene expression the complete loss of plakophilin-2 does not seem to mirror the effects of plakophilin-2 mutations as reported in human patients (Asimaki et al., 2009). Though loss of plakophilin-2 results in heart defects in zebrafish it is disappointing that no molecular aspects of ARVC have been detectable in the plakophilin-2 morphant zebrafish as yet, particularly when the high incidence of documented plakophilin-2 mutations in ARVC is considered. As in the previous chapter, it seems that although loss of plakoglobin or plakophilin-2 causes similar cardiac phenotypes these desmosomal proteins are operating by entirely divergent mechanisms and neither knockdown provides a comprehensive model for ARVC.

5 Heritable targeting of zebrafish plakoglobin using customised TAL-effector nucleases

5.1 Heritable gene targeting using customized TAL-effector nucleases

The use of TAL-effector nucleases (TALENs) for customizable gene targeting is a new technique. Transcription activator-like effectors isolated from the plant pathogenic bacterium *Xanthomonas* have been shown to be readily manipulable to bind almost any DNA sequence (Boch et al., 2009; Christian et al., 2010; Morbitzer et al., 2010). Recent developments in the technology that fuse these proteins to the cleavage domain of FokI have been used to successfully engineer mutations in a variety of organisms including yeast, *Drosophila*, zebrafish and human cell lines (Huang et al., 2011; Li et al., 2011c; Miller et al., 2011; Sander et al., 2011; Liu et al., 2012).

The transient nature of morpholino knockdown is the major limiting factor of the technique, and off-target effects are a continual concern in the characterisation of morphant phenotypes. Hence, it was decided to develop a plakoglobin mutant using TALEN targeting to generate an alternative zebrafish model of ARVC.

5.1.1 Design and synthesis of TALEN constructs targeting plakoglobin

Arrythmogenic right ventricular cardiomyopathy has several pathogenic plakoglobin-induced variants (discussed in Section 1.6.2), however two specific variants are of particular interest due to their distinctive phenotypes caused by mutations at opposing ends of the protein; an N-terminal mutation resulting in the insertion of an additional serine at position 39, causing the classical form of ARVC (Asimaki et al., 2007) and a two base-pair deletion at the C-terminal which causes truncation of the protein and manifests as Naxos disease, which has associated cardiac and cutaneous defects (McKoy et al., 2000). TALEN pairs were designed to target similar regions in the zebrafish genome and hence create the most faithful replication of the causative mutations possible. The plakoglobin protein sequence is highly conserved between zebrafish and humans, with over 79% similarity between the central arm domain of human and zebrafish plakoglobin, though similarity at the tail domains is considerably lower (42% at the N-terminal and a mere 9% at the C-terminal) (Cerda et al., 1999). Conserved loci between the human and zebrafish sequences enabled the identification of sites within the N- and C- termini of

zebrafish plakoglobin that were comparable to those mutations identified in ARVC (Figure 5.1).

The TALEN Targeter (available at https://boglab.plp.iastate.edu/node/add/talen-old) was used to design arrays for the TAL-effector nucleases targeting these regions of interest in the plakoglobin gene. Although zebrafish plakoglobin has a high degree of similarity to the human protein, the exact locations of the human mutation were unsuitable for TALEN-targeting due to limitations such as exon length and base composition in those regions. Cermak et al. (2011) have published a comprehensive analysis of naturally occurring TAL-effectors and binding sites, and have refined these data to provide a set of design criteria for successful and efficient TALEN targeting. TALEN binding sites should be preceded by a 5' T, with no T at position 1, no A at position 2 and binding sites should end with a T. In addition to this, the base composition of the target sites should be within two standard deviations of the following: 31±16% A, 37±13% C, 9±8% G and 22±10% T. Though it was hoped to target the exact sites of the plakoglobin ARVC mutations described above, these regions did not conform to the criteria for TALEN biding sites. Proximal locations adhering to these criteria were chosen for targeting using the Targeter program and are shown relative to the sites in zebrafish plakoglobin that correspond to human ARVC mutations in Figure 5.1.

A

```
zebrafish       -MEMHMGEAPGSVKVTEWQQSYYGTDSGIHSGATTVRS---------DDD---GTEYSSKK 48
human           MEVMNLMEQP--IKVTEWQQTYT-YDSGIHSGANTCVPSVSSKGIMEEDEACGRQYTLKK 57
                   *:: * *  :********:*   *********.*  .         ::*   * :*: **

zebrafish       -FTYTTTFTENPAEVESQLN-MTRAQRVRAAMFPETVMEG-SVIHSTQIDPSQQTNVQKL 105
human           TTTYTQGVPPSQGDLEYQMSTTARAKRVREAMCPGVSGEDSSLLLATQVEG-QATNLQRL 116
                  ***  .. . .::* *:.  :**:*** ** * .  *. *:: :**::  * **:*:*

zebrafish       AEPSQQLKAAIVHLINYQDDAELATRAIPELTKLLNDEDQLVVNKAAMIVNQLTRKEASR 165
human           AEPSQLLKSAIVHLINYQDDAELATRALPELTKLLNDEDPVVVTKAAMIVNQLSKKEASR 176
                ***** **:*******************:*********** :**.*********::*****
```

B

```
zebrafish       LDNVKRVAAGVLCELALDKQSAEIIDAEGASAPLMELLHSSNEGIATYAAAVLYRTAEDK 644
human           VENIQRVAAGVLCELAQDKEAADAIDAEGASAPLMELLHSRNEGTATYAAAVLFRISEDK 656
                ::*::*********** **::*: ********************* *** *********:* :***

zebrafish       NPDYKKRVSVELTHSLFKHDPEAWEMAHNTV-MDPVLGDEELDGYGPAGYGGYADG---M 700
human           NPDYRKRVSVELTNSLFKHDPAAWEAAQSMIPINEPYGDDMDATYRPMYSSDVPLDPLEM 716
                ****:*********:******** *** *:. : ::   **:    * *   .. . .   *

zebrafish       HMDPLDPEMQDDYRGGM--PYNSMARVYHDY 729
human           HMDMDGDYPIDTYSDGLRPPYPTADHMLA-- 745
                ***  .    * * .*:  ** :  ::
```

C

Exon 4

```
211 TCCATTCAGGAGCCACTACTGTTCGCTCAGATGATGATGGAACAGAGTACAGCTCT----------AAGAAA
    TTCACCTACACCACCACATTCACAGAGAACCCTGCAGAGGTGGAGTCTCAGTTAAACATGACTCGTGCTC
    AGCGTGTGAGGGCGGCCATGTTTCCTGAGACTGTGATGGAGGGATCGGTCATTCATTCTACACAGATCG
    ATCCATCCCAGCAGACCAATGTACAAAAGCTGGCCGAACCATCTCAGCAGCTCAAAGCTGCCATCGTTCA
    CCTCATCAACTACCAGGACGACGCTGAACTCGCCACACGCGCCATCCCAGAGCTCACCAAACTCCTCAAC
    GATGAAGACCAGTTGGTTGTGAACAAAGCCGCTATGATCGTGAACCAACTGACCCGCAAGGAGGCATCC
677 CGCAGGGCTCTTATGCAGTCCCCGCAGATGGTGGCCGCTGTAGTGAGAGCCATGCAGAACACGACCGAC
```

Exon 15

```
2101 GCTGTTCTCTACAGAACTGCTGAGGACAAAAACCCAGACTATAAGAAAAGAGTTTCAGTAGAACTCACAC
     ACTCACTCTTCAAACACGACCCTGAGGCTTGGGAAATGGCACACAACACTGTGATGGATCCCGTCCTTGG
     CGATGAAGAGCTTGATGGCTACGGTCCTGCAGGATACGGTGGATATGCTGATGGCATGCATATGGATCCT
     CTAGATCCAGAAATGCAAGACGATTATAGGGGCGGCATGCCCTACAACTCCATGGCCAGAGTCTACCATG
     ATTACTAACAGCCTGACGGTCAACTGACCTCCACTGGAAGAGGATTATCAAAAACACAAGAGACCTAATC
     TTCTGGCAAAGTGTTTTGTTTTGTTTTCCATTGCTGGGTGCCTGTGGTCCATTTCTCAGTAAACACACACAC
6304 ACACACACACTGACACTGTTGTAATATATGCAATTCTCACTTCTGGGGGAGGCAGAAGCCTTGAGCGC
```

Figure 5.1 Proximity of TALEN sites to ARVC mutations

TALEN and ARVC mutation regions shown in both plakoglobin protein and DNA sequences. (A) and (B) show alignment of human and zebrafish plakoglobin protein, with the N-terminal mutation site shown in green (A) and the C-terminal site in yellow (B). In the DNA sequence (C) exon regions are underlined, and the locations corresponding to the predicted serine insertion (exon 4) and 2-base-pair deletion (exon 15) are shown in red. The spacer region (where non-specific FokI cleavage will occur) for each TALEN is shown in blue in all panels.

The final TALEN constructs selected for assembly are shown within the sequence of their respective exons in Figure 5.2, with the full TALEN pairs shown on either side of the spacer region where FokI is predicted to cleave. The natural DNA repair process resulting from this non-specific cleavage is likely to result in small insertions or deletions due to its imperfect nature; hence mutations that occur as a result of TALEN targeting will occur in the spacer region.

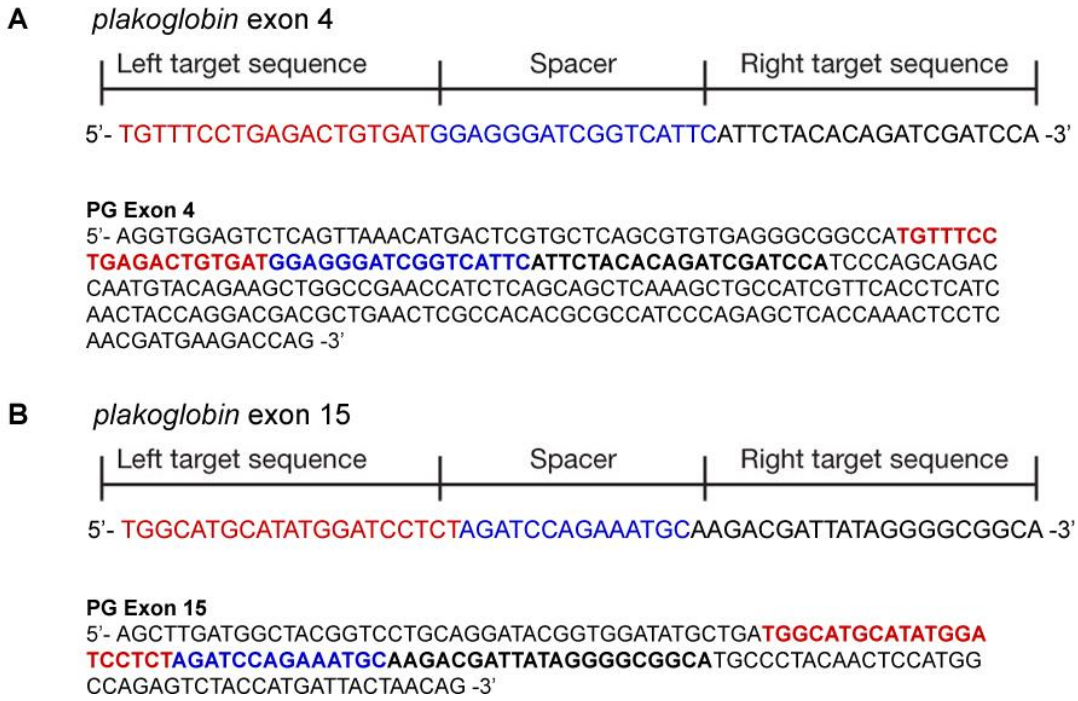

Figure 5.2 Targeted genome editing of plakoglobin using TAL-effector nucleases
TALEN target sites for exon 4 (A) and exon 15 (B) of the zebrafish plakoglobin sequence. Target sequences for TALEN pairs are shown in boldface type with left TALEN shown in red, spacer region in blue, and right TALEN in black.

TALEN pairs were then synthesized using the previously described protocol (Section 2.2.9) adapted from Cermak *et al.,* (2001). Colony PCR was used to check final constructs, with correct clones showing the characteristic "smear-and-ladder" effect when examined under UV light on an agarose gel (Figure 5.3). As several clones showed the correct pattern when examined by agarose gel electrophoresis, one clone for each TALEN (i.e. PG exon4 TAL1(a), PG exon4 TAL2(a), PG exon15 TAL1(a) and PG exon15 TAL2(a)) were selected and cultured, and sequencing of the plasmid DNA was used to confirm the final constructs. This plasmid DNA was then

linearised and transcribed to generate 5' capped mRNA for microinjection. The forward and reverse TALEN pairs for each gene were mixed in a 1:1 ratio and a 100 pg dose of this mixture was delivered by micro-injection to wild-type zebrafish embryos at the 1-cell stage, hereafter referred to as F_0 or founder fish.

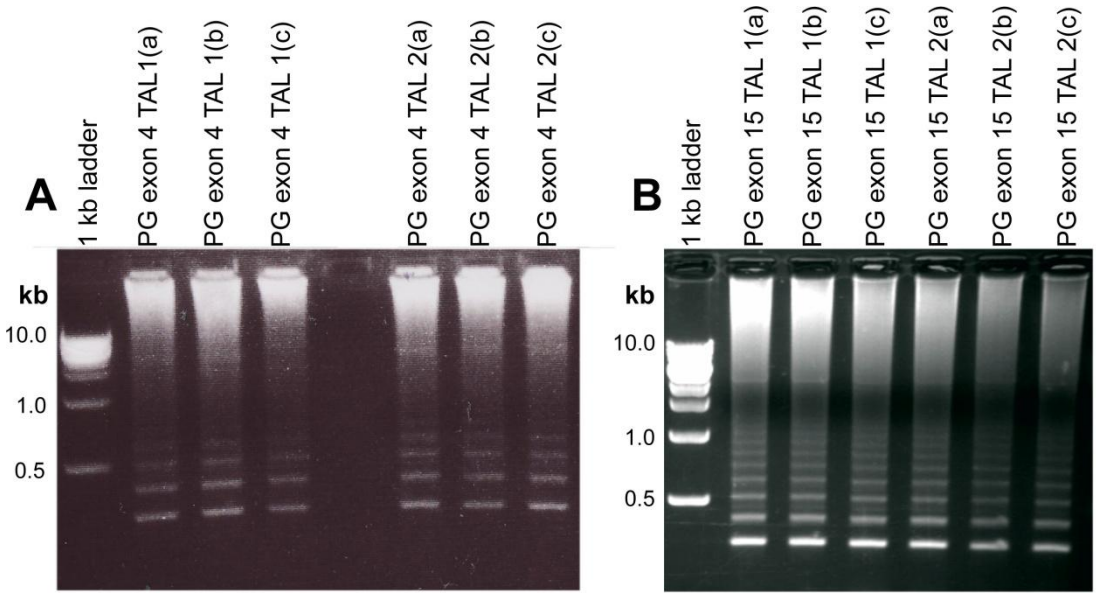

Figure 5.3 Final TALEN constructs
Colony PCR samples of TALEN constructs targeting plakoglobin exon 4 (A) and exon 15 (B), with a-c for each TALEN representing multiple clones. TAL1 and TAL2 refer to left- and right- binding TALENs respectively.

5.1.2 Genotyping of TALEN-induced somatic mutations

Following micro-injection of 100 pg of each TALEN at the 1-cell stage, 24 hpf zebrafish embryos were harvested and genomic DNA was extracted. Wild-type sibling embryos were used as controls in all cases, and injected embryos were grouped into normal or deformed embryos (Table 5.1).

Table 5.1 Classification of TALEN-injected embryos[1]

Exon 4 TALEN		**Exon 15 TALEN**	
Unfertilised	5	Unfertilised	3
Dead	9	Dead	4
Deformed	4	Deformed	3
Normal	12	Normal	20

[1]TALEN-injected embryos were classified at 24 hpf
n=30 for each TALEN construct injected.

Deformities observed included anopthalmia, shortened anterior-posterior body axis, enlarged yolk, developmental retardation and fragility of the chorion. Embryos in the deformed group were sacrificed after 24 hpf as they were unlikely to survive due to toxicity. Those injected embryos not showing defects were selected for genomic DNA extraction and harvested at 24 hpf. The genomic DNA extracted was then used as template for high-resolution melt analysis (HRMA) to determine if mutations had been induced. Primers were designed on either side of the targeted region to produce a small amplicon of less than 150 base-pairs. Differences in the melting temperature of this amplicon would indicate the presence of a mutation in the region. Genotyping of the injected embryos using HRMA showed that the TALEN pair targeting exon 15 did not induce any detectable mutations, however 75% of embryos (8/12) injected with the TALEN pair targeting exon 4 had an irregular melt curve compared to wild-type control siblings (Figure 5.4). The TALEN pair targeting exon 4 successfully induced mutations with a high level of efficiency (75%).

A small number of very low peaks were observed in HRMA of both the exon 4 and exon 15 TALEN injected embryos. The melting curve for exon 15 displayed four of these peaks (three of which were wild type embryos, and one a TALEN-injected embryo) and the melting curve for exon 4 displayed three (all TALEN-injected embryos). These diminutive peaks (visible in Figure 5.4) are assumed to have occurred as a result of very low concentration or poor quality of the template genomic DNA as they were observed in both wild-type and TALEN-injected samples with almost equal frequency. If there was an absence of template DNA in these wells it is likely that a by-product of primer-dimer may have occurred if the primers used self-annealed. As the desired amplicon was of such a short length (approximately 100 base-pairs) and the primers were themselves approximately 20 base-pairs in length each these peaks seem to be in the appropriate range one might expect if hybridisation of the primers was occurring, hence this is the most likely explanation.

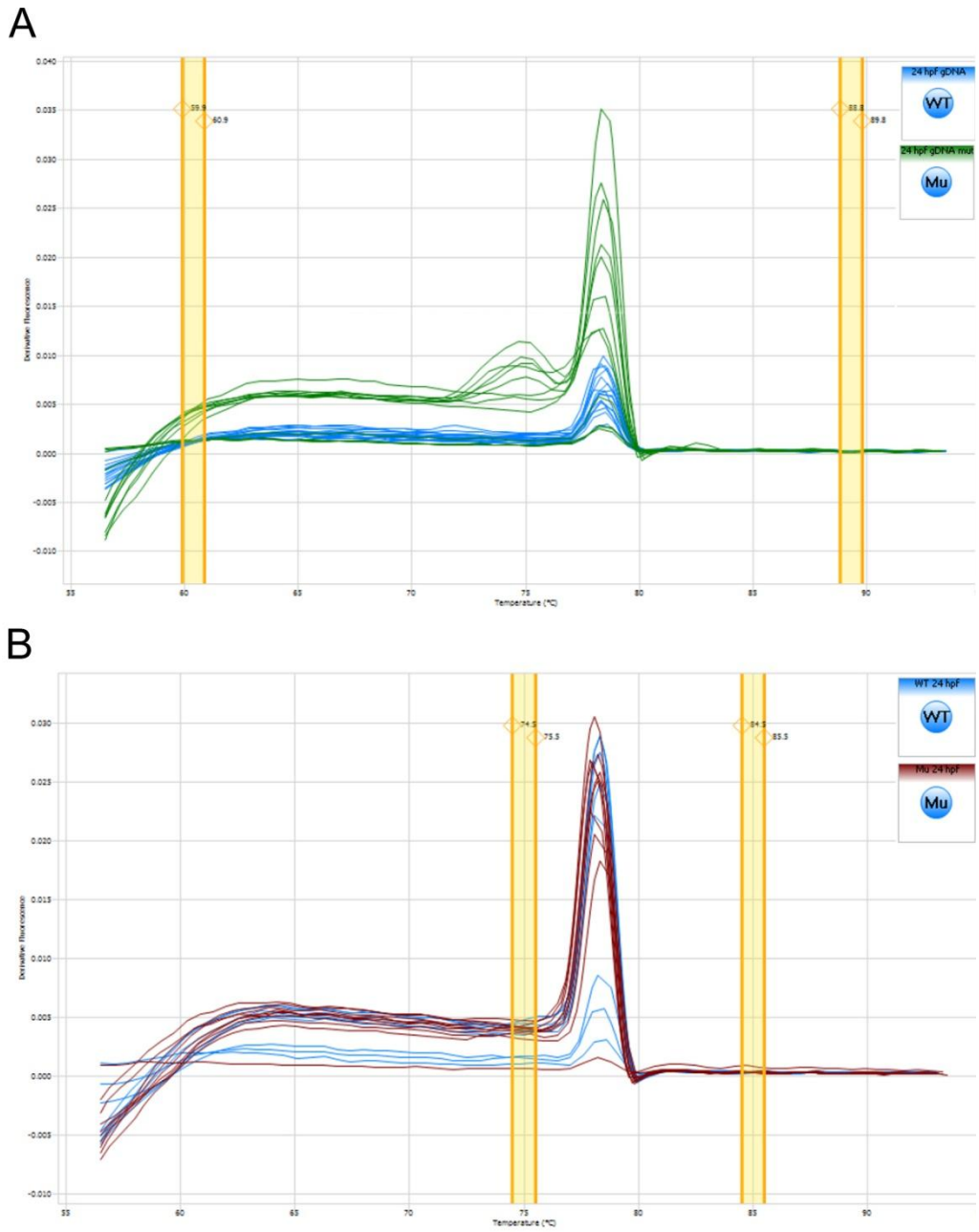

Figure 5.4 HRMA of genomic DNA samples extracted from 24 hpf TALEN-injected embryos
(A) TALEN targeting exon 4 of plakoglobin. WT samples (n=16) are shown in blue, and TALEN injected samples (n=12) are shown in green. (B) TALEN targeting exon 15 of plakoglobin. WT samples (n=8) are shown in blue, and TALEN injected samples (n=10) are shown in red. Yellow bars indicate fluorescence thresholds.

5.1.3 Germline transmission of a plakoglobin mutation

Embryos injected with the TALEN constructs targeting plakoglobin exon 4 were cultivated to maturity and then out-crossed with wild-type AB fish. The adult founder fish, and their resulting F_1 progeny were then screened for indels in the targeted region of plakoglobin. Adult founder fish were screened for somatic

mutations in the targeted region of plakoglobin exon 4, and F1 progeny were also screened to determine if germline transmission of the mutation had occurred. The TALEN-targeted region of plakoglobin exon 4 was amplified by PCR and sequenced. Sequence analysis revealed mutations in both the TALEN-injected founder adults and their progeny. Mutations were detected in 80% of founders (4/5) and all F_1 embryos from successful founders (20/20) (Figure 5.5).

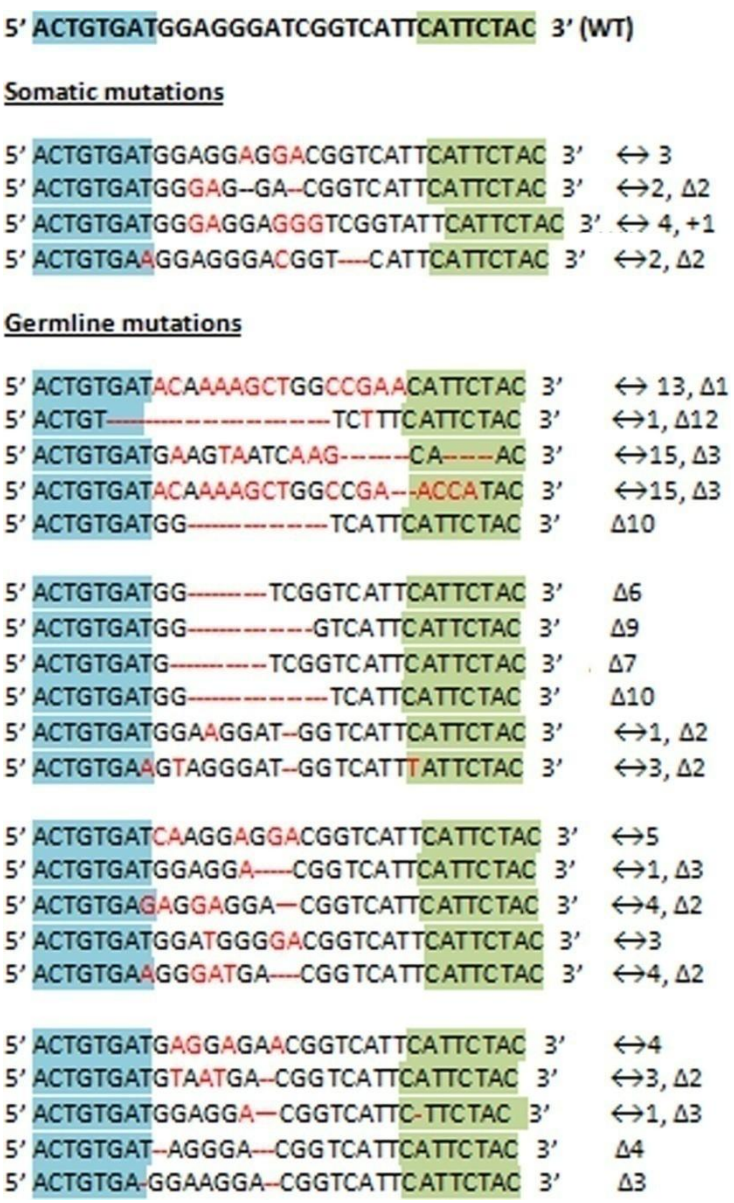

Figure 5.5 Somatic and germline mutations in plakoglobin exon 4 TALEN mutant embryos. Wild-type sequence with spacer region (flanked by blue and green shading) and sequences showing somatic and germline mutations (insertions, deletions and exchanges shown in red). ↔ indicates base-pair exchange followed by the number of bases exchanged, Δ deletions and + insertions.

Sequence analysis of mutated founder fish revealed that all mutations were predicted to cause altered protein composition and induce a premature stop codon, which could result in a truncated form of the protein. The mutated sequences were predicted to encode truncated proteins ranging from 126 to 148 amino acids (compared to wild type plakoglobin, 728 amino acids), depending on the founder fish (Figure 5.6)

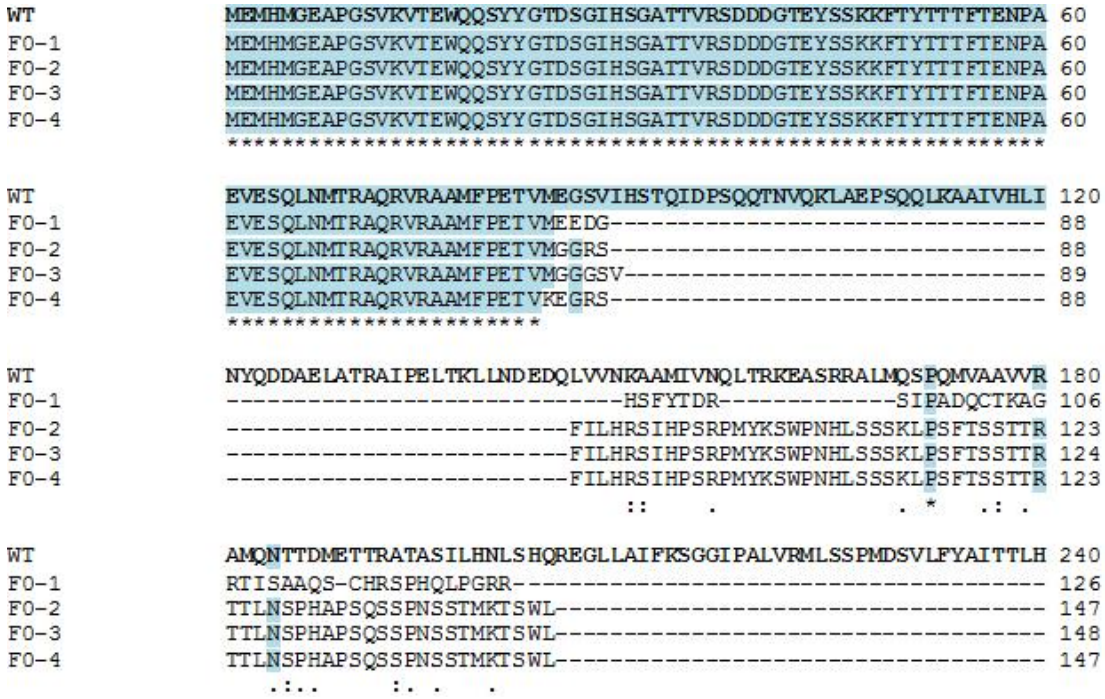

Figure 5.6 Predicted sequences of plakoglobin mutant proteins
Predicted protein sequences for plakoglobin TALEN mutant founder fish (F_0). Regions of alignment are indicated in blue shading and with an asterisk (*). Groups with strongly similar properties are indicated with a colon (:) and groups with weakly similar properties are indicated with a full stop (.).

5.1.4 Phenotypic analysis of TALEN mutant embryos

The four TALEN-injected adult fish (F_0) with confirmed mutations in plakoglobin were out-crossed with wild-type adults and the F_1 progeny were screened for phenotypic defects. Embryos were classified depending on their phenotype as normal, mild, intermediate or severely affected, based on the criteria previously published for plakoglobin morphant phenotypes (Martin et al., 2009). No embryos with a phenotype corresponding to the "mild" classification were observed. Embryos with pericardial oedema, a decreased heart rate, abnormalities in yolk sac

extension, and abnormal body curvature were classified as “intermediate”. Embryos in the “severe” category had more extreme cardiac defects (including enlarged atria and looping defects, blood pooling, and a decreased heart rate), developmental delay, enlarged yolks and more closely recapitulated the phenotype of plakoglobin morphant embryos as they also had kinked tails. A small proportion of embryos had very extreme developmental and cardiac defects that did not correspond to the previous criteria used for plakoglobin morphant embryos, and classification was expanded to include an additional “very severe” classification for these plakoglobin TALEN mutants. “Very severe” embryos had kinked tails, abnormal body curvature, extreme pericardial oedema, blood pooling, and an absence of blood in a heart that failed to form chambers or loop (i.e. heart string) and had a very slow and arrhythmic heart beat. These “very severe” embryos also had abnormal pericardial epithelium, with small sac or blister-like structures present in this area. The distribution of phenotypes was observed to be the same at both 48 and 72 hpf. The percentage of embryos with each phenotype at is shown in Figure 5.7, and the number of embryos in each group is shown in Table 5.2.

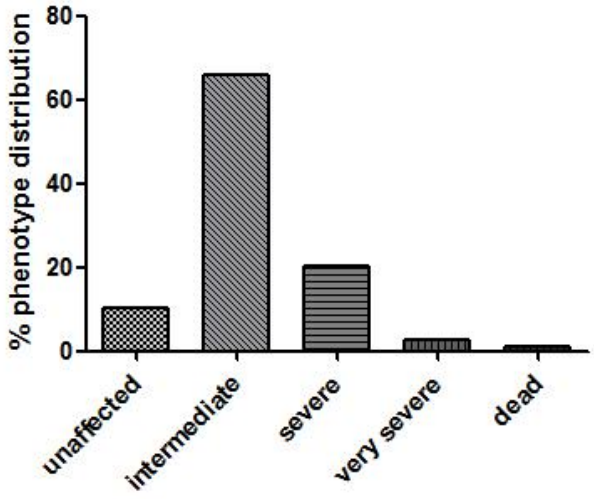

Figure 5.7 Phenotype distribution (%) in plakoglobin TALEN mutants
Embryos were examined for developmental and cardiac defects and classified accordingly. Phenotype distribution was identical at 48 and 72 hpf.

Table 5.2 Phenotype distribution in plakoglobin TALEN mutants

48 hpf						
Total viable embryos		Unaffected	Intermediate	Severe	Very Severe	Dead
108		11	71	22	3	1
72 hpf						
Total viable embryos		Unaffected	Intermediate	Severe	Very Severe	Dead
107		11	71	21	3	1

At 48 hpf the majority of TALEN mutant embryos had cardiac defects, with only 11.875% of embryos unaffected. Intermediately affected embryos accounted for 65% of embryos screened. 20% of embryos were classified as “severe” and 3.125% of embryos had a “very severe” developmental and cardiac phenotype (Figure 5.8).

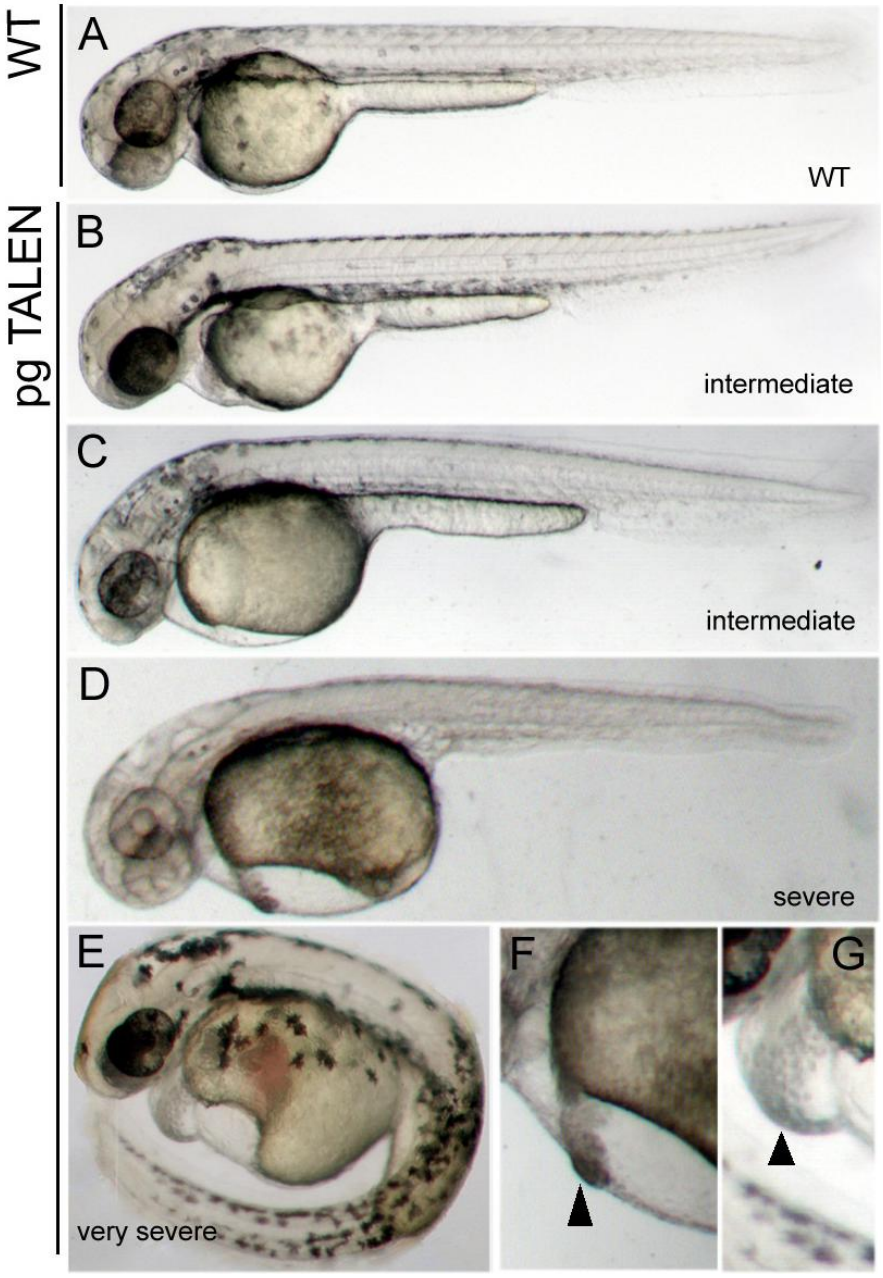

Figure 5.8 Plakoglobin TALEN mutant phenotypes at 48 hpf
Lateral views of WT (A) and TALEN mutant phenotypes (B-G) at 48 hpf. Embryos were classified as intermediate (B&C), severe (D) or very severe (E). Defects in the pericardial epithelium were observed in very severely affected embryos (F&G, arrows).

At 72 hpf the majority of embryos in the intermediate category appeared to recover from the abnormalities in body curvature that were observed at 48 hpf, however those embryos with kinked tails in the severe group did not. Very severely affected

embryos did not recover, and pericardial oedema was, in general, observed to worsen over time in this small population. Epithelial defects were still evident at 72 hpf (Figure 5.9).

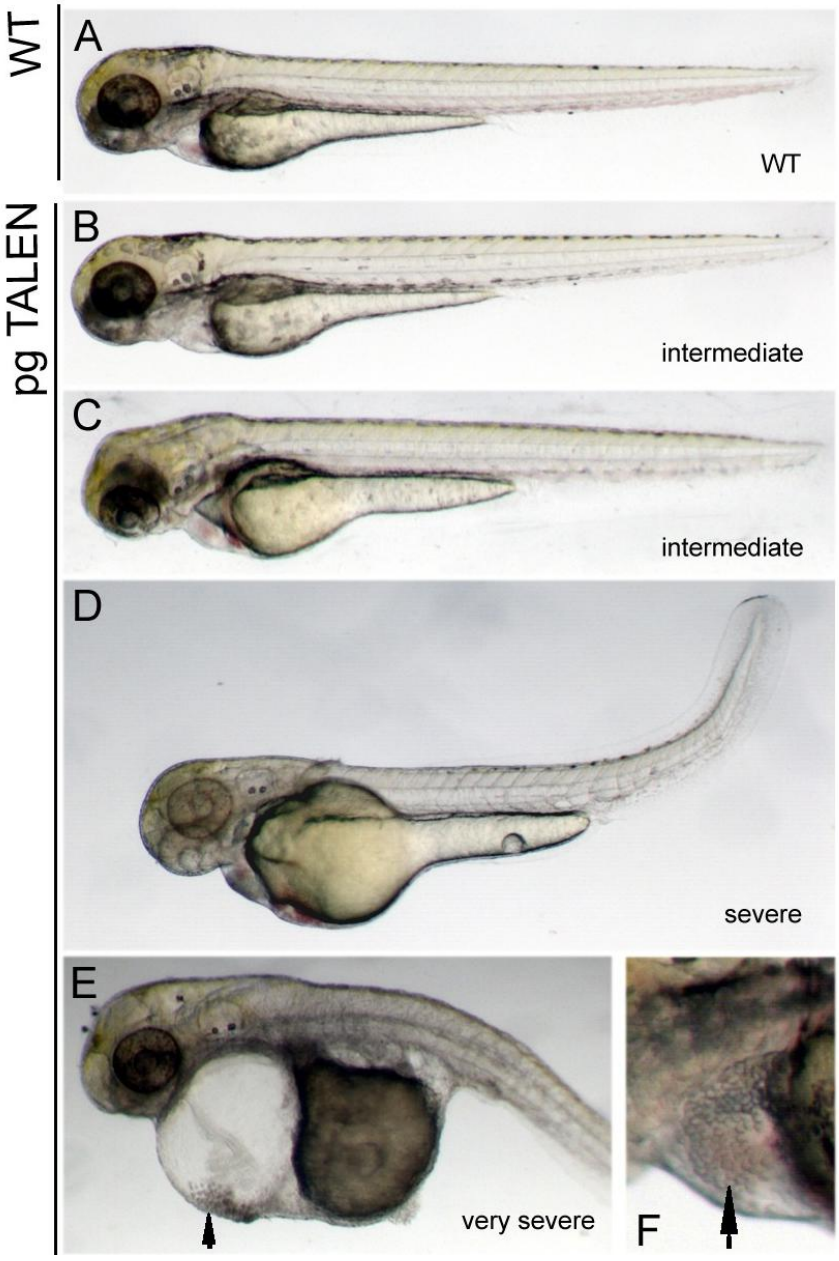

Figure 5.9 TALEN phenotypes at 72 hpf
Lateral views of WT (A) and TALEN mutant phenotypes (B-F) at 72 hpf. Embryos were classified as intermediate (B&C), severe (D) or very severe (E). Defects in the pericardial epithelium were still evident in very severely affected embryos at this stage (E&F, arrows).

At 72 hpf intermediate and severely affected embryos had cardiac defects as at 48 hpf, with failure of the heart to loop correctly now evident in over 60% of all embryos. The ventricle appeared enlarged in all affected embryos apart from those in the very severe category (Figure 5.10). Very severely affected embryos (3.125%) typically did not form distinct chambers, nor did the heart loop, and no blood was observed to move through the heart. Necrosis was observed in the yolk tissue of these very severe embryos at 72 hpf, though the heart was still beating and some motility was detectable. F_0 TALEN fish were outcrossed with Tg (cmlc2:eGFP) adults to enable visualisation of the very severely affected hearts (Figure 5.10).

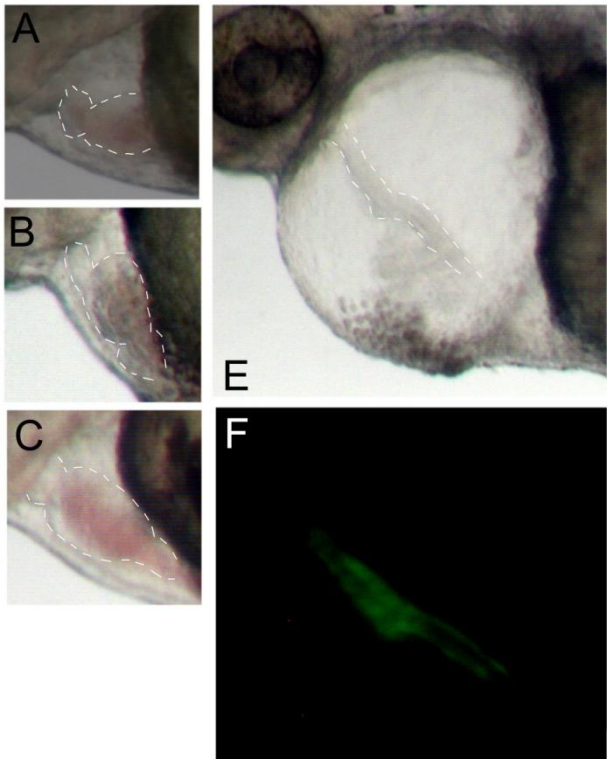

Figure 5.10 Cardiac phenotypes of plakoglobin TALEN mutant embryos at 72 hpf
WT (A) and plakoglobin TALEN mutant hearts (B-F). TALEN hearts failed to loop correctly (B-F) and had enlarged ventricles. Very severely affected embryos typically did not form chambers (E), most clearly visible in (F) where the Tg cmlc2:egfp line was used to visualise the heart. No blood was observed circulating through the heart in very severely affected embryos (E).

Heart rates of TALEN mutants were measured and recorded at 48 and 72 hpf, and were significantly lower than those of wild-type siblings at both developmental stages examined (Figure 5.11).

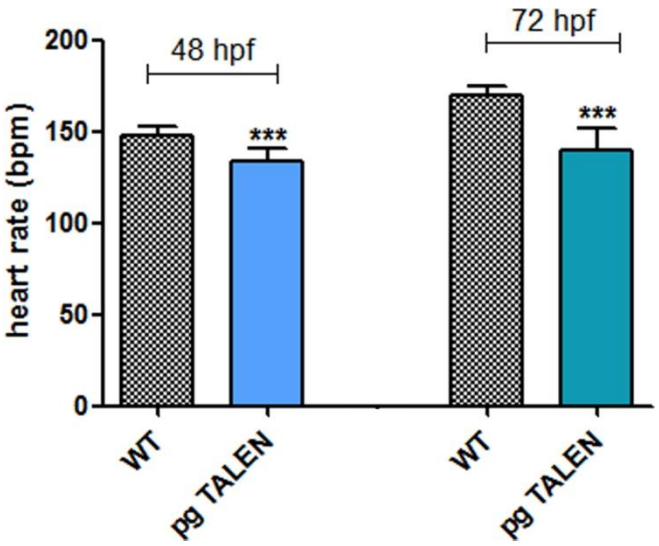

Figure 5.11 Plakoglobin TALEN mutant heart rates
Plakoglobin TALEN mutants (pg TALEN) have significantly decreased heart rates compared to wild-type sibling controls (WT) at both 48 and 72 hpf; n=10. Data are means + s.d.. ***P<0.0001 vs wild-type controls by unpaired t-test.

TALEN F_0 mutant embryos and wild-type siblings were monitored between days 1 and 7 post-fertilisation to assess the death rate in the respective groups. TALEN mutants had a much lower survival rate than their wild-type controls, which increased in a proportional manner with age, indicating that mutations in the plakoglobin gene decrease the viability of zebrafish embryos (Figure 5.12).

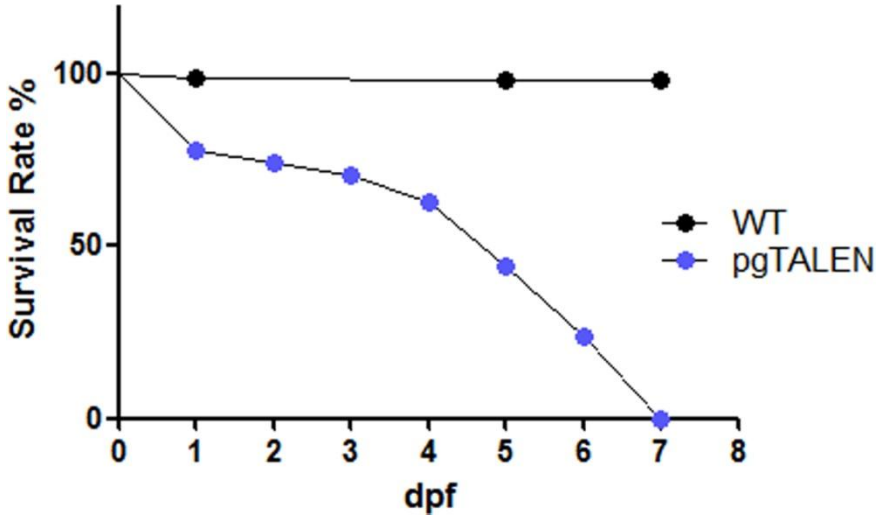

Figure 5.12 Viability of plakoglobin TALEN mutants
Survival rates (%) of wild type (WT) and plakoglobin TALEN mutants (pg TALEN) from 1 dpf to 7 dpf (WT n=86, pg TALEN n= 118).

5.1.5 Gene expression in plakoglobin mutant embryos

qPCR as described previously (Section 2.2.5) was used to investigate gene expression in TALEN mutant embryos (F_1). As 90% of plakoglobin TALEN mutant embryos had cardiac and developmental defects, it was expected that genes affected in plakoglobin morphant embryos (Sections 4.1.1 and 4.1.5) would also show altered expression levels in the plakoglobin mutant embryos (F_1).

Expression levels of *β-catenin*, *connexin 43* and *Wnt1* were significantly down-regulated in 72 hpf plakoglobin TALEN mutants (F_1) (Figure 5.13). *Desmoplakin-a* expression was reduced in all samples, although the variation between repeats did not allow for statistical significance there was a discernible trend, with a *P*-value of 0.0932. Adipogenic transcription factor *Wnt5b* was significantly down-regulated in the mutant embryos, but interestingly, *PPAR-γ* showed a high level of variation between samples, with the three replicates showing increased, decreased and unaffected expression respectively.

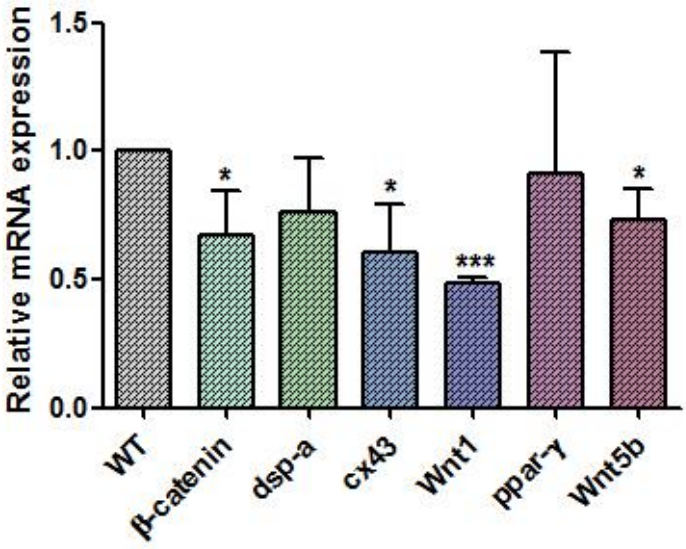

Figure 5.13 Gene expression in plakoglobin TALEN mutant embryos
Relative mRNA expression levels of *β-catenin*, *desmoplakin-a* (dsp-a), *connexin 43* (cx43), *Wnt1*, *PPAR-γ* and *Wnt5b* at 72 hpf. WT siblings were used as controls. Data are means + s.d.* *P*<0.05, ****P*<0.001 vs wild-type controls by paired *t*-test; n=3.

In plakoglobin knockdown embryos mRNA expression levels of *β-catenin* and *connexin 43* were down-regulated at comparable levels to those seen in the

plakoglobin TALEN mutants (Section 4.1.1). Plakoglobin morphant embryos also showed concordant down-regulation of adipogenic genes *Wnt5b* and *PPAR-γ* (Section 4.1.5), though this was not observed in the plakoglobin TALEN mutants. It is most interesting to note the continued association between connexin 43 and Wnt1. Expression of these genes has been shown to be concomitantly down-regulated in plakoglobin morphant embryos (Section 4.1.1), APC mutant embryos (Section 4.1.2), and now in plakoglobin mutant embryos (Figure 5.13).

5.2 Discussion

As an emerging technique there are varying reports regarding the efficiency of TALENs and several different methods have already been developed for the synthesis of custom TALENs. Here the Golden Gate cloning method of TALEN assembly as reported by Cermak et al.,(2011) has been used to target two regions of plakoglobin, exons 4 and 15, in an attempt to mimic mutations reported to cause the congenital heart defect ARVC in humans.

5.2.1 Targeted genome editing can be achieved with high efficiency using TALEN constructs

TALEN constructs were designed and synthesised to target opposing ends of the plakoglobin sequence, and high-resolution melt analysis (HRMA) determined successful genome editing had occurred in 75% of those embryos injected with the TALEN construct targeting exon 4. HRMA is a sensitive PCR-based method suitable for detecting any newly-introduced polymorphisms, as the presence of TALEN-induced polymorphisms results in the presence of heteroduplex molecules in addition to homoduplex molecules, which can be detected due to differences in thermostability of the products (Dahlem et al., 2012). There has been much variation in the reported efficiency of TALENs in zebrafish. Efficiency of achieved mutations in injected founder fish (F_0) has been reported from 16% to 100% (Bedell et al., 2012; Cade et al., 2012; Dahlem et al., 2012; Moore et al., 2012). Though two TALEN pairs were designed to target the zebrafish plakoglobin gene, mutations were only successfully detected with the TALEN designed to target exon 4. As yet there is only anecdotal evidence as to why some TALEN constructs are not successful, with increased methylation towards the 3' end of the gene suggested to interfere with TALENs that target this region. There is however no published data to support this theory.

5.2.2 High rates of germline transmission can be achieved using TALEN technology

Genotypic analysis of F_1 embryos from TALEN-injected founder fish revealed a mutation in all samples sequenced. Phenotypic analysis of siblings to these F_1

progeny confirmed a high rate of germline transmission, with over 60% of embryos observed to have cardiac defects. These values are in keeping with published results. Dahlem *et al*., report that 77 – 100% of F_1 embryos carried mutations (depending on the gene mutated), while Cade *et al*., report more modest success rates of 25 – 75%. Both publications note that though almost all (90-100%) of the founder fish with confirmed mutations transmit these to the next generation, the efficiency with which polymorphisms are transmitted can vary. The variation between detected mutations in the F1 progeny (i.e. germline mosaicism) indicates numerous independent repair events are occurring due to inherited TALEN targeting through the germline, resulting in slight differences in the achieved mutation.

5.2.3 Targeted mutation of plakoglobin exon 4 causes cardiac defects

Loss of plakoglobin has previously been shown to disrupt cardiac development and Wnt signalling in zebrafish embryos (Martin et al., 2009), and Asimaki et al., (2007) have identified a mutation in the N-terminal of human plakoglobin that causes ARVC. Though this exact mutation could not be replicated in this study, mutations were induced in a proximal region, 36 amino acids down-stream of the corresponding region in the zebrafish protein (Section 5.1.1). The resulting mutant embryos had a range of cardiac and signalling defects.

Though the region chosen for targeting was based upon a human mutation known to cause heart defects, no functional domains could be identified in this exact region of the protein in human or zebrafish sequences. The human plakoglobin protein consists of 13 armadillo repeats (beginning at residue 109) and *in vitro* studies using human cell lines have identified functional domains within these repeats that are required for the interaction of plakoglobin with α-catenin and the desmosomal cadherins. The first three armadillo repeats are required for interaction with desmosomal cadherins (Troyanovsky et al., 1996), and repeats 6, 7 and 8 are required for plakoglobin to associate with N-cadherin and α-catenin (Sacco et al., 1995), and repeat 1 is also thought to be important for plakoglobin/α-catenin interaction (Witcher et al., 1996). Though plakoglobin interacts with

numerous adhesion proteins via these armadillo repeat domains, they all occur downstream of both the human mutation identified in ARVC and the targeted zebrafish mutation induced in this study.

Sequence analysis of the mutated founder fish predicted that the mutations identified in the F_1 generation could all potentially introduce premature stop codons, resulting in truncation of the plakoglobin protein after the first ARM repeat. If these theoretical truncations did occur then the requisite binding sites for α-catenin and N-cadherin would all be absent as they occur downstream of the predicted truncations. This analysis is presumptive, yet it provides the most likely explanation for the defects observed in the TALEN mutant embryos. The germline mosaicism that features in the TALEN mutants may foster such a wide variety of mutations that the possibility of some mutations not resulting in protein truncation must also be considered.

The serine insertion detected by Asimaki et al. (2007) occurs between residues 39 and 40 of the plakoglobin protein. The destruction box phosphorylated by GSK is located proximally (residues 23-36), and so this adjacency may provide an alternative explanation for the observed cardiac defects in that study as the serine addition could give rise to increased GSK phosphorylation. Asimaki et al. utilised additional data from a yeast-two-hybrid screen to provide an alternative explanation of the observed defects in human ARVC patients carrying the plakoglobin mutation. Mutant plakoglobin was observed to bind two additional proteins, Histidine-Rich Ca^{2+} Binding Protein (HRC-BP) and TT virus-derived apoptosis-inducing protein (TAIP-2) (Asimaki et al., 2007).

HRC-BP is found in the sarcoplasmic reticulum (SR) of heart and skeletal muscle cells, and has been implicated in the regulation of Ca^{2+} release into the SR. In the presence of these elevated Ca^{2+} levels in the SR, the density and binding kinetics of the ryanodine receptor (RYR)/Ca^{2+} release channel were slightly reduced (Kim et al., 2003). *RYR2*, the gene that encodes the cardiac ryanodine receptor, was one of the initial genes to be implicated in ARVC, and mutations in the *RYR2* gene are thought to trigger arrhythmias by allowing the leakage of Ca^{2+} into the cytoplasm (Laitinen

et al., 2001; Tiso et al., 2001). The observed interaction between mutant plakoglobin and the sarcoplasmic reticulum protein HRC-BP may simply result from the altered distribution of plakoglobin and have no direct relationship to ARVC. However, the results obtained by Asimaki et al., may also indicate a role for this interaction in the regulation of Ca^{2+} homeostasis and hence promote myocyte injury or contribute to electrical instability. Transfection of the mutated protein into a human cell line revealed ubiquitination of the mutant protein and increased cytoplasmic localisation, suggesting that the increased association between mutant plakoglobin and the degradation machinery forces the protein away from the cell junctions and into the cytoplasm (Asimaki et al., 2007).

5.2.4 TALEN mutants recapitulate many aspects of the plakoglobin morphant phenotype

TALEN mutants typically had a range of cardiac and developmental defects, with incomplete cardiac looping, decreased heart rate, enlarged ventricles and pericardial oedema most commonly observed. Blood pooling and kinked tails were also observed in a smaller proportion of embryos.

It has previously been established that loss of plakoglobin (via morpholino knockdown) during development results in cardiac defects (including reduced heart size, decreased heart rate, cardiac oedema, looping defects and reflux of blood between the atrium and ventricle), and a kinked tail (Martin et al., 2009).

This study presents evidence that use of TALEN targeting to generate heritable mutations in plakoglobin can recapitulate many of the defects characteristic of morpholino knockdown. Plakoglobin TALEN mutants also had a number of the cardiac defects seen in plakoglobin morphants (i.e. failure of the heart to loop correctly, decreased heart rate, oedema) and “severely” affected TALEN mutants also had kinked tails, though this was less common (20% of all mutant embryos).

Classification of plakoglobin morphant phenotypes identified a high percentage (19.65%) of “severe” defects at 72 hpf (Martin, 2008). Morphant embryos classified

as “severe” had extreme oedema, an absence of blood in the heart and a reduced heart rate, in addition to tail defects. In this study, a similar population of severely affected embryos was observed (20%), but an additional group of embryos (3%) had such extreme cardiac defects that they transcended those published for severely affected morpholino-injected embryos and had to be classified independently as “very severely” affected.

There was no obvious reduction in heart size in the majority of TALEN mutant embryos compared to wild-type controls (with the exception of very severe embryos displaying “heart string” phenotypes), nor was blood reflux between the chambers observed. Martin *et al.,* previously identified defects in valvulogenesis as the cause of blood reflux in plakoglobin morphant embryos, with valve-specific genes *bmp4* and *notch1b* failing to restrict to the valve forming regions in embryos lacking plakoglobin. Examination of the valvulogenic genes was beyond the scope of this study, yet theoretically it is possible that a complete loss of plakoglobin has a more disruptive effect on the Wnt signalling pathway than a mutation does. If so, expression of *bmp4* and *notch1b* may not be affected to the same extent in the mutant embryos and so defects in valvulogenesis, if any, may not be sufficient to allow blood reflux. The achieved mutations in plakoglobin are predicted to severely truncate the protein, preventing translation of the central arm repeat domains and the C-terminal. As the C-terminal of plakoglobin is thought to be essential for interaction with TCF/LEF (Maeda et al., 2004) it seems logical that complete ablation of plakoglobin and truncation should have similar effects on Wnt signalling, but further analysis (both of the cardiac ultra-structure, the mutated protein and Wnt target gene expression) would be required to confirm the exact mechanism by which the phenotype of the TALEN mutant embryos is occurring.

5.2.5 Plakoglobin mutants as a model for ARVC

As a model for ARVC, the TALEN mutants have many desirable features, most importantly the cardiac defects discussed in Section 5.1.3.

In addition to the cardiac defects, the plakoglobin TALEN mutant line shows some other promising characteristics as a model. The observed significant decreases in

expression of *connexin 43*, *β-catenin* and *Wnt1* indicate potential for the TALEN mutant embryos as a molecular model for ARVC. Expression of *desmoplakin-a* was decreased in all samples tested, unfortunately the variation in magnitude did not allow for statistical significance yet it is worth noting that the observed decrease in expression ranged from 5-47% between three samples tested. *PPAR-γ* expression also varied between replicates, however expression of another adipogenic gene, *Wnt5b*, was consistently and significantly decreased. Germline mosaicism may hold the key to elucidating the variation between these samples, as discussed before the incidence of different mutations may have a range of signalling consequences as well as phenotypes.

Defects in the pericardial epithelium were observed in a small number of embryos, presenting as what appeared to be blistering on the epithelial surface, which may be representative of the dermal abnormalities associated with ARVC. Bierkamp *et al.,* have reported skin blistering in a murine model that occurs due to acantholysis, and concurrent epithelial detachment, though this defect is more discernible and consistent within their plakoglobin knockout model than the rare incidences reported here for plakoglobin mutant zebrafish. Viability of embryos was observed to decrease with age, with death rates increasing over time from 24 hpf to 7 dpf. Though some embryos survived past this stage, the proportional relationship between age and viability may be reflective of the progressive nature of ARVC. As the effects of gene knockdown with morpholino are transient and so can only be assessed to about 72 hpf it is not possible to compare the viability of these TALEN mutant embryos with the plakoglobin knockdown.

It was hoped that the induced mutations would provide an improved model for ARVC, however limitations within the plakoglobin sequence prevented TALEN targeting of the conserved locations where human mutations occur. As a result, it seems that though TALEN mutant embryos have a number of cardiac defects they do not present any significant improvement on the existing plakoglobin knock-down as a model for ARVC. The convenience of a heritable mutation that eliminates the need for morpholino micro-injection, and can be studied beyond three days

post-fertilisation is an important advance however, and will greatly facilitate further study.

5.2.6 Advantages and disadvantages of plakoglobin TALEN mutants and plakoglobin morphants

Both morpholino oligonucleotides and TALEN targeting are powerful tools for genetic manipulation, but there are advantages and disadvantages to both with respect to the study of plakoglobin in zebrafish development.

As discussed (Section 5.2.3) plakoglobin TALEN mutants phenocopy plakoglobin morphant embryos, though the distribution of phenotypes observed is different. In particular, Martin et al., (2009) reported a "mild" phenotype, consisting of embryos that had oedema, kinked tails and reduced heart rate, yet no such classification was observed in this study. Interestingly, though plakoglobin TALEN mutant embryos with mild phenotypic defects were not observed, an extremely severe cardiac phenotype with defects far in excess of those observed previously in the plakoglobin morphant embryos was seen in a small percentage of the plakoglobin TALEN mutant embryos, and required separate classification as "very severe". As yet, no off-target effects have been reported with TALEN-targeting; hence it may be that the small minority observed to be very severely affected are harbouring more disruptive mutations than sibling mutant embryos. The occurrence of germline mosaicism in TALEN mutant lines supports this theory, and also identifies a significant limiting factor of the TALEN technology. Though the exact location of the TALEN target site can be selected, the exact nature of the resulting mutation cannot, nor can the mutation be predicted in resulting progeny. The possibility of a wide range of mutations presents a wide range of consequences, ranging from point mutations which may have no effect to larger insertions or deletions that could result in frame-shifts or premature truncations.

Morpholino knockdown of plakoglobin also results in a range of phenotypes, yet the method is consistent for all of them, complete loss of the plakoglobin protein in each embryo. A more general comparison of TALEN targeting versus morpholino knockdown is continued in Section 5.2.7, however with regard to this particular

study it appears that TALEN targeting has potential to provide an excellent substitute for morpholino-based knockdown of plakoglobin.

5.2.7 TALEN targeting as a strategy for genome editing in the zebrafish

Targeted genome editing using TALEN technology has now been reported in a variety of model species, with several publications confirming its success in targeting the zebrafish genome (Bedell et al., 2012; Cade et al., 2012; Dahlem et al., 2012; Joung and Sander, 2012; Moore et al., 2012).

Generation of TALEN constructs is both quick and straightforward, and they can be tested for efficacy as early as the 256-cell stage, less than three hours after initial delivery (Bedell et al., 2012). Reagents and plasmids required for TALEN targeting are readily available and cost-effective, and can be used to generate an almost limitless number of constructs that are easily customisable. Once a successful TALEN has been confirmed in the F_0 fish the waiting period for these fish to mature to breeding age is certainly comparable to the time required for the design, testing and dose-response studies needed for morpholino-based knockdown. Specificity of the TALEN can be easily confirmed by sequence analysis and no toxicity has been reported for TALEN in any model system to date. For research purposes, the heritable quality of the mutation induced by TALEN-targeting is an extremely useful feature. Morpholino knockdown is comparatively very labour-intensive and time-consuming, as both embryos and controls must be injected individually. This is particularly relevant in the case of gene or protein expression studies where relatively large numbers of embryos are required. These advantages, combined with the recapitulation of knockdown phenotypes observed in this study and others (Bedell et al., 2012), recommend TALEN above morpholino knockdown for future work.

The negative aspects of TALEN must also be considered. Not all TALENs are effective, as presented in Section 5.1.3. A success rate of 50% was observed here with the TALEN constructs tested; however the small sample size of two is not sufficient to give a valid overview of the general efficacy of TALENs. Though existing publications report efficiency rates of successful TALEN constructs it is not

possible to discern the overall success rate as only those TALENs seen to accomplish induction of mutations are discussed.

Synthesis of TALEN constructs is quick and straightforward, but after verification of a successful TALEN the original injected fish (F_0) must be carefully maintained and cultured to adulthood before the benefits of heritability can be realised. This can take between six and ten weeks before the fish are of an age to breed, which is in excess of the length of time required to design, test and determine a dose for a morpholino.

Additionally, as it is not possible to exactly predict the final indels that will occur after TALEN targeting and design guidelines can limit the exact location of target sites. This inability to predict the exact final mutation represents a significant disadvantage and may render TALEN targeting unsuitable for studies where precise replication of an existing mutation is desirable. For applications such as these morpholinos in conjunction with techniques such as site-directed mutagenesis, or TILLING may still have precedence.

Morpholino oligonucleotides have the advantage of being extremely well established. They are simple to design, and on a small scale (e.g. if only one gene is to be targeted) they are comparable in cost to the reagents required for TALEN targeting. Unlike TALEN targeting, with morpholino knockdown a dose-response is required, and this can be time-consuming and require a large number of embryos to confirm effective knockdown with no off-target effects, as unlike TALENs toxicity is a constant source of concern with morpholinos. The resulting inhibition of translation achieved with morpholino knockdown is consistent, but transient.

In conclusion it seems the utility of TALEN targeting, like any method, is entirely dependent on the needs of the researcher. The use of TALENs can certainly alleviate the limitations associated with morpholino knockdown, but has limitations of its own. The advent of TALENs does not automatically replace existing strategies for genome editing, and as always, the question to be answered will dictate the method to be used.

6 Discussion

It has been well-established that desmosomal proteins are required structurally for correct formation of the desmosomes and subsequent cell-cell adhesion. This study aimed to further investigate the signalling roles of two of these proteins, plakoglobin and plakophilin-2. Though these proteins have a high degree of structural similarity, here data is presented that indicates highly divergent signalling roles and temporal requirements for these armadillo proteins during heart development. Loss-of-function morpholino knockdown models were used to study the signalling activity of plakoglobin and plakophilin-2, and the value of these morphant embryos as models for the human congenital heart defect ARVC was also assessed. Finally, an alternative to the plakoglobin morpholino knockdown model was developed using TALEN targeted genome editing.

There is conflicting evidence regarding the role of plakoglobin in the Wnt signalling pathway, which seems to implicate a requirement for multi-phasic activity by Wnt signalling during development. In zebrafish, the effect of loss of plakoglobin on Wnt signalling in early stage embryos and the ability of Wnt-inhibitor Dkk-1 to rescue the plakoglobin morphant phenotype has identified a role for plakoglobin as a negative regulator of the canonical Wnt pathway (Martin et al., 2009). Plakoglobin has also been shown to have an antagonistic effect on the Wnt pathway *in vitro* (Miravet et al., 2002).

However, Maeda et al., (2004) report increased transcriptional activity in a β-catenin deficient cell line following co-transfection of plakoglobin with TCF4 or LEF, and decreased transcriptional activity after knockdown of endogenous plakoglobin (Maeda et al., 2004). These results are strongly indicative of an agonistic role for plakoglobin in Wnt/β-catenin signalling. Overall however, the role of plakoglobin as a regulator of Wnt signalling appears to be variable and dependent on several factors, including cell and tissue type, and developmental stage.

The use of atrial myocytes to generate an *in vitro* model for ARVC has had most interesting results. Suppression of desmoplakin using siRNA led to nuclear localization of plakoglobin, and a resulting 2-fold decrease in canonical Wnt/β-

catenin signalling (Garcia-Gras et al., 2006), hence their data also supports a role for plakoglobin as a Wnt pathway antagonist.

Conversely, plakoglobin morphant embryos and plakoglobin TALEN mutants had decreased expression of *Wnt1*, *Wnt5b* and *β-catenin* mRNAs at 72 hpf (Sections 4.1.1, 4.1.5 and 5.1.6). Additionally expression of plakoglobin was decreased in APC mutant embryos, as was *Wnt1* expression (Section 4.1.2). It remains difficult to delineate the specific interactions that are occurring between plakoglobin and β-catenin to suppress Wnt signalling, yet results obtained in this study are consistent between several signalling models investigated (plakoglobin morphant embryos, TALEN mutants and *apc* mutant embryos), suggesting a potential role for plakoglobin as a positive regulator of Wnt signalling in late stage zebrafish embryos. Ueno et al., (2007) propose that Wnt/β-catenin expression prior to gastrulation promotes cardiac differentiation, whereas expression during gastrulation is inhibitory, with this bi-phasic process regulated by a feedback loop involving β-catenin and other canonical Wnt pathway members (Ueno et al., 2007). Such a system within the Wnt pathway may explain the apparent discrepancy between the role of plakoglobin as a Wnt inhibitor at early developmental stages and a Wnt agonist later in development.

Overall however it seems there is more evidence for an antagonistic role for plakoglobin in the regulation of the Wnt pathway. Dkk-1 is capable of restoring the patterning defects caused by loss of plakoglobin, up-regulation of Wnt target genes occurs following plakoglobin knockdown, and *plakoglobin* mRNA expression is decreased in APC mutant embryos.

Despite being the most widely distributed member of the plakophilin family (Mertens et al., 1996; Mertens et al., 1999; Borrmann et al., 2000; Akat et al., 2003; Borrmann et al., 2006; Franke et al., 2006; Akat et al., 2008) little is known about the signalling roles of plakophilin-2. Loss of plakophilin-2 has been linked to sodium current deficits (Sato et al., 2009; Deo et al., 2011; Sato et al., 2011; Cerrone et al., 2012) and one study in colon carcinoma cells has shown an ability for plakophilin-2 to associate with β-catenin and up-regulate Wnt signalling (Chen et al., 2002). As

information regarding the molecular function of this armadillo protein remains scarce the signalling events that link plakophilin-2 to ARVC remain to be elucidated.

Plakoglobin and plakophilin-2 are similar in protein structure and function, and knockdown results in similar cardiac phenotypes in zebrafish embryos (Martin et al., 2009; Moriarty et al., 2012). With this in mind it seemed likely that they may also have a similar mechanism of action, and so initial experiments focused on expression of Wnt target genes in plakophilin-2 embryos. Surprisingly, Wnt signalling was unaffected at all stages examined, however examination of Nodal pathway genes proved more fruitful. Loss of plakophilin-2 causes substantial disruption to several signalling components of the Nodal pathway at an important stage in cardiogenesis, including a striking loss of Lefty2 expression at the 18 somite stage. These results indicate divergent signalling activities for plakoglobin and plakophilin-2, and are the first report of any interaction between plakophilin-2 and the Nodal signalling pathway.

As morpholino knockdown of plakoglobin and plakophilin-2 results in serious cardiac malformation and ultra-structural defects reminiscent of the human congenital heart condition it was hoped that molecular aspects would also be recapitulated, providing greater insights into the processes responsible for ARVC.

Plakoglobin morphant embryos overall had a more promising molecular profile, however it seems the complete loss of plakoglobin is not sufficient to replicate the most distinctive diagnostic feature of adipogenic and fibrogenic replacement of the myocardial tissue. This is potentially due to the short span of the morpholino-based experiment, limited by the transient nature of the knockdown and hence incapable of recapitulating such a progressive disease feature. A more likely reason may be that a complete blockade of plakoglobin protein translation does not accurately mirror the initial molecular events required for the disease phenotype. Garcia-Gras et al., (2006) have shown that translocation of the plakoglobin protein to the nucleus is required for the subsequent up-regulation of adipogenic and fibrogenic genes, hence a model based upon complete loss of plakoglobin may be incapable of mimicking this particular aspect of the disease.

Plakophilin-2, as before, appears to operate via a completely different mechanism to plakoglobin, with no desirable qualities for a molecular model of ARVC identified in the plakophilin-2 knockdown. Mutations in plakophilin-2 are the most common cause of ARVC, and have been reported at all regions of the protein, yet complete loss of the protein fails to recapitulate many elements of the disease. Though a poor model for ARVC, loss of plakophilin-2 has provided some exciting new insights into its function and signalling interactions.

As molecular models for ARVC it seems that neither knockdown provides an ideal system, however plakoglobin morphant embryos have several signalling defects of interest. Importantly, these models have provided a wealth of information about the molecular functions and interactions of the proteins. The conserved decrease in Wnt1 expression across the various models (plakoglobin knockdown, TALEN mutants and apc mutants) may even propose Wnt1 as a novel candidate for a molecular marker of cardiac defects. Collectively the data obtained regarding plakoglobin and plakophilin-2 are of great benefit as they demonstrate that structural similarity does not always imply functional parity.

The successful generation of a plakoglobin mutant line using TALEN targeting has provided an exciting avenue by which to pursue the study of cardiac development in the zebrafish. Further analysis of the TALEN mutant fish will provide greater insight into the role plakoglobin plays in development. If analysis of plakoglobin protein in TALEN mutants confirms the truncation predicted by analysis of the mutated sequences, there is potential to further explore what functional domains lie in the upstream portion of the sequence.

TALEN mutants generally demonstrated both phenotypic and molecular similarities to plakoglobin morphant embryos, thus confirming the specificity of both the TALEN mutant and the morpholino knockdown. Preliminary results indicate potential for plakoglobin TALEN mutants to provide a somewhat improved model for ARVC in comparison to the plakoglobin morphant model. A small proportion of TALEN mutant embryos were observed to have epithelial defects which have not been observed in the existing plakoglobin knockdown model. Examination of the

ultra-structure of mutant hearts and protein localisation within these embryos, in addition to the ability to observe adult hearts in later developmental stages present exciting projects for the future and may reveal a refined zebrafish model for ARVC that models the progressive aspects of the disease.

7 Future Work

As plakophilin-2 morphant embryos show such significant disruption to selected genes from the Nodal signalling pathway, it would be interesting to examine the expression profile of these genes during early cardiogenesis in plakoglobin morphants, and plakoglobin TALEN mutants to determine if these signalling defects are the product of a unique interaction between plakophilin-2 and the Nodal pathway, or occur commonly in embryos with cardiac defects irrespective of the pathogenesis.

Further analysis of the TALEN plakoglobin mutants is required to determine the full extent of the cardiac defects, including confocal microscopy to examine localisation of the mutant plakoglobin in TALEN embryos, and TEM to see if desmosome structure is altered.

Cermak et al., (2011) have provided design guidelines for successful and efficient TALEN targeting, however more recent publications suggest that not all of these must be applied. With this in mind, design of a new TALEN to target the exact regions of human ARVC mutations in the zebrafish plakoglobin sequence could provide a better animal model for ARVC. Current research projects in our group are focused on developing a refined ARVC-model using co-injection of a mutant plakoglobin mRNA with plakoglobin morpholino. An alternative would be to attempt TALEN-targeting in a more 5' location to generate a plakoglobin-null mutant line, thus reducing the need for co-injection. If generation of a plakoglobin-null mutant using TALEN targeting was successful, injection of mutated plakoglobin mRNA into these TALEN embryos has the potential to create a more refined and accurate zebrafish model for ARVC.

8 Bibliography

ABU-ISSA, R.;SMYTH, G.;SMOAK, I.;YAMAMURA, K. & MEYERS, E. N. 2002. Fgf8 is required for pharyngeal arch and cardiovascular development in the mouse. *Development,* 129**,** 4613-25.

ACEHAN, D.;PETZOLD, C.;GUMPER, I.;SABATINI, D. D.;MULLER, E. J.;COWIN, P. & STOKES, D. L. 2008. Plakoglobin is required for effective intermediate filament anchorage to desmosomes. *J Invest Dermatol,* 128**,** 2665-75.

AI, D.;FU, X.;WANG, J.;LU, M. F.;CHEN, L.;BALDINI, A.;KLEIN, W. H. & MARTIN, J. F. 2007. Canonical Wnt signaling functions in second heart field to promote right ventricular growth. *Proc Natl Acad Sci U S A,* 104**,** 9319-24.

AI, Z.;FISCHER, A.;SPRAY, D. C.;BROWN, A. M. & FISHMAN, G. I. 2000. Wnt-1 regulation of connexin43 in cardiac myocytes. *J Clin Invest,* 105**,** 161-71.

AKAT, K.;BLECK, C. K.;LEE, Y. M.;HASELMANN-WEISS, U. & KARTENBECK, J. 2008. Characterization of a novel type of adherens junction in meningiomas and the derived cell line HBL-52. *Cell Tissue Res,* 331**,** 401-12.

AKAT, K.;MENNEL, H. D.;KREMER, P.;GASSLER, N.;BLECK, C. K. & KARTENBECK, J. 2003. Molecular characterization of desmosomes in meningiomas and arachnoidal tissue. *Acta Neuropathol,* 106**,** 337-47.

ALCALAI, R.;METZGER, S.;ROSENHECK, S.;MEINER, V. & CHAJEK-SHAUL, T. 2003. A recessive mutation in desmoplakin causes arrhythmogenic right ventricular dysplasia, skin disorder, and woolly hair. *J Am Coll Cardiol,* 42**,** 319-27.

ASIMAKI, A.;SYRRIS, P.;WICHTER, T.;MATTHIAS, P.;SAFFITZ, J. E. & MCKENNA, W. J. 2007. A novel dominant mutation in plakoglobin causes arrhythmogenic right ventricular cardiomyopathy. *Am J Hum Genet,* 81**,** 964-73.

ASIMAKI, A.;TANDRI, H.;HUANG, H.;HALUSHKA, M. K.;GAUTAM, S.;BASSO, C.;THIENE, G.;TSATSOPOULOU, A.;PROTONOTARIOS, N.;MCKENNA, W. J.;CALKINS, H. & SAFFITZ, J. E. 2009. A new diagnostic test for arrhythmogenic right ventricular cardiomyopathy. *N Engl J Med,* 360**,** 1075-84.

BAO, B.;ZHANG, L.;HU, H.;YIN, S. & LIANG, Z. 2012. Deletion of a single-copy DAAM1 gene in congenital heart defect: a case report. *BMC Med Genet,* 13**,** 63.

BARRON, M.;GAO, M. & LOUGH, J. 2000. Requirement for BMP and FGF signaling during cardiogenic induction in non-precardiac mesoderm is specific, transient, and cooperative. *Dev Dyn,* 218**,** 383-93.

BASS-ZUBEK, A. E.;HOBBS, R. P.;AMARGO, E. V.;GARCIA, N. J.;HSIEH, S. N.;CHEN, X.;WAHL, J. K., 3RD;DENNING, M. F. & GREEN, K. J. 2008. Plakophilin 2: a critical scaffold for PKC alpha that regulates intercellular junction assembly. *J Cell Biol,* 181**,** 605-13.

BASSO, C.;CORRADO, D.;MARCUS, F. I.;NAVA, A. & THIENE, G. 2009. Arrhythmogenic right ventricular cardiomyopathy. *Lancet,* 373**,** 1289-300.

BASSO, C.;FOX, P. R.;MEURS, K. M.;TOWBIN, J. A.;SPIER, A. W.;CALABRESE, F.;MARON, B. J. & THIENE, G. 2004. Arrhythmogenic right ventricular cardiomyopathy causing sudden cardiac death in boxer dogs: a new animal model of human disease. *Circulation,* 109**,** 1180-5.

BEDELL, V. M.;WANG, Y.;CAMPBELL, J. M.;POSHUSTA, T. L.;STARKER, C. G.;KRUG, R. G., 2ND;TAN, W.;PENHEITER, S. G.;MA, A. C.;LEUNG, A. Y.;FAHRENKRUG, S. C.;CARLSON, D. F.;VOYTAS, D. F.;CLARK, K. J.;ESSNER, J. J. & EKKER, S. C.

2012. In vivo genome editing using a high-efficiency TALEN system. *Nature,* 491**,** 114-8.

BEHRENS, J.;VON KRIES, J. P.;KUHL, M.;BRUHN, L.;WEDLICH, D.;GROSSCHEDL, R. & BIRCHMEIER, W. 1996. Functional interaction of beta-catenin with the transcription factor LEF-1. *Nature,* 382**,** 638-42.

BEIMAN, M.;SHILO, B. Z. & VOLK, T. 1996. Heartless, a Drosophila FGF receptor homolog, is essential for cell migration and establishment of several mesodermal lineages. *Genes Dev,* 10**,** 2993-3002.

BEIS, D.;BARTMAN, T.;JIN, S. W.;SCOTT, I. C.;D'AMICO, L. A.;OBER, E. A.;VERKADE, H.;FRANTSVE, J.;FIELD, H. A.;WEHMAN, A.;BAIER, H.;TALLAFUSS, A.;BALLY-CUIF, L.;CHEN, J. N.;STAINIER, D. Y. & JUNGBLUT, B. 2005. Genetic and cellular analyses of zebrafish atrioventricular cushion and valve development. *Development,* 132**,** 4193-204.

BELEMA BEDADA, F.;TECHNAU, A.;EBELT, H.;SCHULZE, M. & BRAUN, T. 2005. Activation of myogenic differentiation pathways in adult bone marrow-derived stem cells. *Mol Cell Biol,* 25**,** 9509-19.

BIERKAMP, C.;MCLAUGHLIN, K. J.;SCHWARZ, H.;HUBER, O. & KEMLER, R. 1996. Embryonic heart and skin defects in mice lacking plakoglobin. *Dev Biol,* 180**,** 780-5.

BISGROVE, B. W.;ESSNER, J. J. & YOST, H. J. 1999. Regulation of midline development by antagonism of lefty and nodal signaling. *Development,* 126**,** 3253-62.

BISGROVE, B. W.;ESSNER, J. J. & YOST, H. J. 2000. Multiple pathways in the midline regulate concordant brain, heart and gut left-right asymmetry. *Development,* 127**,** 3567-79.

BOCH, J. & BONAS, U. 2010. Xanthomonas AvrBs3 family-type III effectors: discovery and function. *Annu Rev Phytopathol,* 48**,** 419-36.

BOCH, J.;SCHOLZE, H.;SCHORNACK, S.;LANDGRAF, A.;HAHN, S.;KAY, S.;LAHAYE, T.;NICKSTADT, A. & BONAS, U. 2009. Breaking the code of DNA binding specificity of TAL-type III effectors. *Science,* 326**,** 1509-12.

BOGDANOVE, A. J.;SCHORNACK, S. & LAHAYE, T. 2010. TAL effectors: finding plant genes for disease and defense. *Curr Opin Plant Biol,* 13**,** 394-401.

BONNE, S.;VAN HENGEL, J.;NOLLET, F.;KOOLS, P. & VAN ROY, F. 1999. Plakophilin-3, a novel armadillo-like protein present in nuclei and desmosomes of epithelial cells. *J Cell Sci,* 112 (Pt 14)**,** 2265-76.

BOOKOUT, A. L.;CUMMINS, C. L.;MANGELSDORF, D. J.;PESOLA, J. M. & KRAMER, M. F. 2006. High-throughput real-time quantitative reverse transcription PCR. *Curr Protoc Mol Biol,* Chapter 15**,** Unit 15 8.

BORRMANN, C. M.;GRUND, C.;KUHN, C.;HOFMANN, I.;PIEPERHOFF, S. & FRANKE, W. W. 2006. The area composita of adhering junctions connecting heart muscle cells of vertebrates. II. Colocalizations of desmosomal and fascia adhaerens molecules in the intercalated disk. *Eur J Cell Biol,* 85**,** 469-85.

BORRMANN, C. M.;MERTENS, C.;SCHMIDT, A.;LANGBEIN, L.;KUHN, C. & FRANKE, W. W. 2000. Molecular diversity of plaques of epithelial-adhering junctions. *Ann N Y Acad Sci,* 915**,** 144-50.

BRADLEY, R. S.;COWIN, P. & BROWN, A. M. 1993. Expression of Wnt-1 in PC12 cells results in modulation of plakoglobin and E-cadherin and increased cellular adhesion. *J Cell Biol,* 123**,** 1857-65.

BUSSMANN, J.;BAKKERS, J. & SCHULTE-MERKER, S. 2007. Early endocardial morphogenesis requires Scl/Tal1. *PLoS Genet,* 3**,** e140.

CABRAL, R. M.;LIU, L.;HOGAN, C.;DOPPING-HEPENSTAL, P. J.;WINIK, B. C.;ASIAL, R. A.;DOBSON, R.;MEIN, C. A.;BASELAGA, P. A.;MELLERIO, J. E.;NANDA, A.;BOENTE MDEL, C.;KELSELL, D. P.;MCGRATH, J. A. & SOUTH, A. P. 2010. Homozygous mutations in the 5' region of the JUP gene result in cutaneous disease but normal heart development in children. *J Invest Dermatol,* 130**,** 1543-50.

CABRERA, C. V.;ALONSO, M. C.;JOHNSTON, P.;PHILLIPS, R. G. & LAWRENCE, P. A. 1987. Phenocopies induced with antisense RNA identify the wingless gene. *Cell,* 50**,** 659-63.

CADE, L.;REYON, D.;HWANG, W. Y.;TSAI, S. Q.;PATEL, S.;KHAYTER, C.;JOUNG, J. K.;SANDER, J. D.;PETERSON, R. T. & YEH, J. R. 2012. Highly efficient generation of heritable zebrafish gene mutations using homo- and heterodimeric TALENs. *Nucleic Acids Res,* 40**,** 8001-10.

CADIGAN, K. M. & NUSSE, R. 1997. Wnt signaling: a common theme in animal development. *Genes Dev,* 11**,** 3286-305.

CARVAJAL-HUERTA, L. 1998. Epidermolytic palmoplantar keratoderma with woolly hair and dilated cardiomyopathy. *J Am Acad Dermatol,* 39**,** 418-21.

CERDA, J.;REIDENBACH, S.;PRATZEL, S. & FRANKE, W. W. 1999. Cadherin-catenin complexes during zebrafish oogenesis: heterotypic junctions between oocytes and follicle cells. *Biol Reprod,* 61**,** 692-704.

CERMAK, T.;DOYLE, E. L.;CHRISTIAN, M.;WANG, L.;ZHANG, Y.;SCHMIDT, C.;BALLER, J. A.;SOMIA, N. V.;BOGDANOVE, A. J. & VOYTAS, D. F. 2011. Efficient design and assembly of custom TALEN and other TAL effector-based constructs for DNA targeting. *Nucleic Acids Res,* 39**,** e82.

CERRONE, M.;NOORMAN, M.;LIN, X.;CHKOURKO, H.;LIANG, F. X.;VAN DER NAGEL, R.;HUND, T.;BIRCHMEIER, W.;MOHLER, P.;VAN VEEN, T. A.;VAN RIJEN, H. V. & DELMAR, M. 2012. Sodium current deficit and arrhythmogenesis in a murine model of plakophilin-2 haploinsufficiency. *Cardiovasc Res,* 95**,** 460-8.

CHANG, H.;ZWIJSEN, A.;VOGEL, H.;HUYLEBROECK, D. & MATZUK, M. M. 2000. Smad5 is essential for left-right asymmetry in mice. *Dev Biol,* 219**,** 71-8.

CHATTERJEE, B.;CHIN, A. J.;VALDIMARSSON, G.;FINIS, C.;SONNTAG, J. M.;CHOI, B. Y.;TAO, L.;BALASUBRAMANIAN, K.;BELL, C.;KRUFKA, A.;KOZLOWSKI, D. J.;JOHNSON, R. G. & LO, C. W. 2005. Developmental regulation and expression of the zebrafish connexin43 gene. *Dev Dyn,* 233**,** 890-906.

CHEN, C. & SHEN, M. M. 2004. Two modes by which Lefty proteins inhibit nodal signaling. *Curr Biol,* 14**,** 618-24.

CHEN, J. N.;VAN EEDEN, F. J.;WARREN, K. S.;CHIN, A.;NUSSLEIN-VOLHARD, C.;HAFFTER, P. & FISHMAN, M. C. 1997. Left-right pattern of cardiac BMP4 may drive asymmetry of the heart in zebrafish. *Development,* 124**,** 4373-82.

CHEN, X.;BONNE, S.;HATZFELD, M.;VAN ROY, F. & GREEN, K. J. 2002. Protein binding and functional characterization of plakophilin 2. Evidence for its diverse

roles in desmosomes and beta -catenin signaling. *J Biol Chem,* 277**,** 10512-22.

CHENG, S. K.;OLALE, F.;BRIVANLOU, A. H. & SCHIER, A. F. 2004. Lefty blocks a subset of TGFbeta signals by antagonizing EGF-CFC coreceptors. *PLoS Biol,* 2**,** E30.

CHIN, A. J.;TSANG, M. & WEINBERG, E. S. 2000. Heart and gut chiralities are controlled independently from initial heart position in the developing zebrafish. *Dev Biol,* 227**,** 403-21.

CHOCRON, S.;VERHOEVEN, M. C.;RENTZSCH, F.;HAMMERSCHMIDT, M. & BAKKERS, J. 2007. Zebrafish Bmp4 regulates left-right asymmetry at two distinct developmental time points. *Dev Biol,* 305**,** 577-88.

CHRISTIAN, M.;CERMAK, T.;DOYLE, E. L.;SCHMIDT, C.;ZHANG, F.;HUMMEL, A.;BOGDANOVE, A. J. & VOYTAS, D. F. 2010. Targeting DNA double-strand breaks with TAL effector nucleases. *Genetics,* 186**,** 757-61.

DAHLEM, T. J.;HOSHIJIMA, K.;JURYNEC, M. J.;GUNTHER, D.;STARKER, C. G.;LOCKE, A. S.;WEIS, A. M.;VOYTAS, D. F. & GRUNWALD, D. J. 2012. Simple methods for generating and detecting locus-specific mutations induced with TALENs in the zebrafish genome. *PLoS Genet,* 8**,** e1002861.

DEJMEK, J.;SAFHOLM, A.;KAMP NIELSEN, C.;ANDERSSON, T. & LEANDERSSON, K. 2006. Wnt-5a/Ca2+-induced NFAT activity is counteracted by Wnt-5a/Yes-Cdc42-casein kinase 1alpha signaling in human mammary epithelial cells. *Mol Cell Biol,* 26**,** 6024-36.

DELVA, E.;TUCKER, D. K. & KOWALCZYK, A. P. 2009. The desmosome. *Cold Spring Harb Perspect Biol,* 1**,** a002543.

DEN HAAN, A. D.;TAN, B. Y.;ZIKUSOKA, M. N.;LLADO, L. I.;JAIN, R.;DALY, A.;TICHNELL, C.;JAMES, C.;AMAT-ALARCON, N.;ABRAHAM, T.;RUSSELL, S. D.;BLUEMKE, D. A.;CALKINS, H.;DALAL, D. & JUDGE, D. P. 2009. Comprehensive desmosome mutation analysis in north americans with arrhythmogenic right ventricular dysplasia/cardiomyopathy. *Circ Cardiovasc Genet,* 2**,** 428-35.

DEO, M.;SATO, P. Y.;MUSA, H.;LIN, X.;PANDIT, S. V.;DELMAR, M. & BERENFELD, O. 2011. Relative contribution of changes in sodium current versus intercellular coupling on reentry initiation in 2-dimensional preparations of plakophilin-2-deficient cardiac cells. *Heart Rhythm,* 8**,** 1740-8.

DOHN, T. E. & WAXMAN, J. S. 2012. Distinct phases of Wnt/beta-catenin signaling direct cardiomyocyte formation in zebrafish. *Dev Biol,* 361**,** 364-76.

DOREY, K. & HILL, C. S. 2006. A novel Cripto-related protein reveals an essential role for EGF-CFCs in Nodal signalling in Xenopus embryos. *Dev Biol,* 292**,** 303-16.

DOYON, Y.;MCCAMMON, J. M.;MILLER, J. C.;FARAJI, F.;NGO, C.;KATIBAH, G. E.;AMORA, R.;HOCKING, T. D.;ZHANG, L.;REBAR, E. J.;GREGORY, P. D.;URNOV, F. D. & AMACHER, S. L. 2008. Heritable targeted gene disruption in zebrafish using designed zinc-finger nucleases. *Nat Biotechnol,* 26**,** 702-8.

DRAPER, B. W.;MCCALLUM, C. M.;STOUT, J. L.;SLADE, A. J. & MOENS, C. B. 2004. A high-throughput method for identifying N-ethyl-N-nitrosourea (ENU)-induced point mutations in zebrafish. *Methods Cell Biol,* 77**,** 91-112.

DRAPER, B. W.;MORCOS, P. A. & KIMMEL, C. B. 2001. Inhibition of zebrafish fgf8 pre-mRNA splicing with morpholino oligos: a quantifiable method for gene knockdown. *Genesis,* 30**,** 154-6.

ENGLER, C.;GRUETZNER, R.;KANDZIA, R. & MARILLONNET, S. 2009. Golden gate shuffling: a one-pot DNA shuffling method based on type IIs restriction enzymes. *PLoS One,* 4**,** e5553.

ENGLER, C.;KANDZIA, R. & MARILLONNET, S. 2008. A one pot, one step, precision cloning method with high throughput capability. *PLoS One,* 3**,** e3647.

ERTER, C. E.;SOLNICA-KREZEL, L. & WRIGHT, C. V. 1998. Zebrafish nodal-related 2 encodes an early mesendodermal inducer signaling from the extraembryonic yolk syncytial layer. *Dev Biol,* 204**,** 361-72.

ESSNER, J. J.;BRANFORD, W. W.;ZHANG, J. & YOST, H. J. 2000. Mesendoderm and left-right brain, heart and gut development are differentially regulated by pitx2 isoforms. *Development,* 127**,** 1081-93.

FABRITZ, L.;HOOGENDIJK, M. G.;SCICLUNA, B. P.;VAN AMERSFOORTH, S. C.;FORTMUELLER, L.;WOLF, S.;LAAKMANN, S.;KREIENKAMP, N.;PICCINI, I.;BREITHARDT, G.;NOPPINGER, P. R.;WITT, H.;EBNET, K.;WICHTER, T.;LEVKAU, B.;FRANKE, W. W.;PIEPERHOFF, S.;DE BAKKER, J. M.;CORONEL, R. & KIRCHHOF, P. 2011. Load-reducing therapy prevents development of arrhythmogenic right ventricular cardiomyopathy in plakoglobin-deficient mice. *J Am Coll Cardiol,* 57**,** 740-50.

FEKANY, K.;YAMANAKA, Y.;LEUNG, T.;SIROTKIN, H. I.;TOPCZEWSKI, J.;GATES, M. A.;HIBI, M.;RENUCCI, A.;STEMPLE, D.;RADBILL, A.;SCHIER, A. F.;DRIEVER, W.;HIRANO, T.;TALBOT, W. S. & SOLNICA-KREZEL, L. 1999. The zebrafish bozozok locus encodes Dharma, a homeodomain protein essential for induction of gastrula organizer and dorsoanterior embryonic structures. *Development,* 126**,** 1427-38.

FELDMAN, B.;GATES, M. A.;EGAN, E. S.;DOUGAN, S. T.;RENNEBECK, G.;SIROTKIN, H. I.;SCHIER, A. F. & TALBOT, W. S. 1998. Zebrafish organizer development and germ-layer formation require nodal-related signals. *Nature,* 395**,** 181-5.

FODDE, R.;SMITS, R. & CLEVERS, H. 2001. APC, signal transduction and genetic instability in colorectal cancer. *Nat Rev Cancer,* 1**,** 55-67.

FONTAINE, G.;GUIRAUDON, G.;FRANK, R.;VEDEL, J.;GROSGOGEAT, Y.;CABROL, C. & FACQUET, J. 1977. *Stimulation studies and epicardial mapping in ventricular tachycardia: study of mechanisms and selection for surgery,* Lancaster, MTP Press Limited.

FOX, P. R.;MARON, B. J.;BASSO, C.;LIU, S. K. & THIENE, G. 2000. Spontaneously occurring arrhythmogenic right ventricular cardiomyopathy in the domestic cat: A new animal model similar to the human disease. *Circulation,* 102**,** 1863-70.

FRANKE, W. W.;BORRMANN, C. M.;GRUND, C. & PIEPERHOFF, S. 2006. The area composita of adhering junctions connecting heart muscle cells of vertebrates. I. Molecular definition in intercalated disks of cardiomyocytes by immunoelectron microscopy of desmosomal proteins. *Eur J Cell Biol,* 85**,** 69-82.

GAN, X. Q.;WANG, J. Y.;XI, Y.;WU, Z. L.;LI, Y. P. & LI, L. 2008. Nuclear Dvl, c-Jun, beta-catenin, and TCF form a complex leading to stabilization of beta-catenin-TCF interaction. *J Cell Biol,* 180**,** 1087-100.

GARCIA-GRAS, E.;LOMBARDI, R.;GIOCONDO, M. J.;WILLERSON, J. T.;SCHNEIDER, M. D.;KHOURY, D. S. & MARIAN, A. J. 2006. Suppression of canonical Wnt/beta-

catenin signaling by nuclear plakoglobin recapitulates phenotype of arrhythmogenic right ventricular cardiomyopathy. *J Clin Invest,* 116**,** 2012-21.

GARCIA-PAVIA, P.;SYRRIS, P.;SALAS, C.;EVANS, A.;MIRELIS, J. G.;COBO-MARCOS, M.;VILCHES, C.;BORNSTEIN, B.;SEGOVIA, J.;ALONSO-PULPON, L. & ELLIOTT, P. M. 2011. Desmosomal protein gene mutations in patients with idiopathic dilated cardiomyopathy undergoing cardiac transplantation: a clinicopathological study. *Heart,* 97**,** 1744-52.

GARROD, D.;CHIDGEY, M. & NORTH, A. 1996. Desmosomes: differentiation, development, dynamics and disease. *Curr Opin Cell Biol,* 8**,** 670-8.

GEHMLICH, K.;ASIMAKI, A.;CAHILL, T. J.;EHLER, E.;SYRRIS, P.;ZACHARA, E.;RE, F.;AVELLA, A.;MONSERRAT, L.;SAFFITZ, J. E. & MCKENNA, W. J. 2010. Novel missense mutations in exon 15 of desmoglein-2: role of the intracellular cadherin segment in arrhythmogenic right ventricular cardiomyopathy? *Heart Rhythm,* 7**,** 1446-53.

GEHMLICH, K.;LAMBIASE, P. D.;ASIMAKI, A.;CIACCIO, E. J.;EHLER, E.;SYRRIS, P.;SAFFITZ, J. E. & MCKENNA, W. J. 2011. A novel desmocollin-2 mutation reveals insights into the molecular link between desmosomes and gap junctions. *Heart Rhythm,* 8**,** 711-8.

GEHMLICH, K.;SYRRIS, P.;REIMANN, M.;ASIMAKI, A.;EHLER, E.;EVANS, A.;QUARTA, G.;PANTAZIS, A.;SAFFITZ, J. E. & MCKENNA, W. J. 2012. Molecular changes in the heart of a severe case of arrhythmogenic right ventricular cardiomyopathy caused by a desmoglein-2 null allele. *Cardiovasc Pathol,* 21**,** 275-82.

GERMAIN, S.;HOWELL, M.;ESSLEMONT, G. M. & HILL, C. S. 2000. Homeodomain and winged-helix transcription factors recruit activated Smads to distinct promoter elements via a common Smad interaction motif. *Genes Dev,* 14**,** 435-51.

GERULL, B.;HEUSER, A.;WICHTER, T.;PAUL, M.;BASSON, C. T.;MCDERMOTT, D. A.;LERMAN, B. B.;MARKOWITZ, S. M.;ELLINOR, P. T.;MACRAE, C. A.;PETERS, S.;GROSSMANN, K. S.;DRENCKHAHN, J.;MICHELY, B.;SASSE-KLAASSEN, S.;BIRCHMEIER, W.;DIETZ, R.;BREITHARDT, G.;SCHULZE-BAHR, E. & THIERFELDER, L. 2004. Mutations in the desmosomal protein plakophilin-2 are common in arrhythmogenic right ventricular cardiomyopathy. *Nat Genet,* 36**,** 1162-4.

GODSEL, L. M.;GETSIOS, S.;HUEN, A. C. & GREEN, K. J. 2004. The molecular composition and function of desmosomes. *Handb Exp Pharmacol***,** 137-93.

GOLIASCH, G.;WIESBAUER, F.;KASTL, S. P.;KATSAROS, K. M.;BLESSBERGER, H.;MAURER, G.;SCHILLINGER, M.;HUBER, K.;WOJTA, J. & SPEIDL, W. S. 2012. Premature myocardial infarction is associated with low serum levels of Wnt-1. *Atherosclerosis,* 222**,** 251-6.

GOMES, J.;FINLAY, M.;AHMED, A. K.;CIACCIO, E. J.;ASIMAKI, A.;SAFFITZ, J. E.;QUARTA, G.;NOBLES, M.;SYRRIS, P.;CHAUBEY, S.;MCKENNA, W. J.;TINKER, A. & LAMBIASE, P. D. 2012. Electrophysiological abnormalities precede overt structural changes in arrhythmogenic right ventricular cardiomyopathy due to mutations in desmoplakin-A combined murine and human study. *Eur Heart J,* 33**,** 1942-53.

GRITSMAN, K.;ZHANG, J.;CHENG, S.;HECKSCHER, E.;TALBOT, W. S. & SCHIER, A. F. 1999. The EGF-CFC protein one-eyed pinhead is essential for nodal signaling. *Cell,* 97**,** 121-32.

GROSSMANN, K. S.;GRUND, C.;HUELSKEN, J.;BEHREND, M.;ERDMANN, B.;FRANKE, W. W. & BIRCHMEIER, W. 2004. Requirement of plakophilin 2 for heart morphogenesis and cardiac junction formation. *J Cell Biol,* 167**,** 149-60.

HABAS, R.;KATO, Y. & HE, X. 2001. Wnt/Frizzled activation of Rho regulates vertebrate gastrulation and requires a novel Formin homology protein Daam1. *Cell,* 107**,** 843-54.

HAFFNER, C.;FRAULI, M.;TOPP, S.;IRMLER, M.;HOFMANN, K.;REGULA, J. T.;BALLY-CUIF, L. & HAASS, C. 2004. Nicalin and its binding partner Nomo are novel Nodal signaling antagonists. *EMBO J,* 23**,** 3041-50.

HARMS, P. W. & CHANG, C. 2003. Tomoregulin-1 (TMEFF1) inhibits nodal signaling through direct binding to the nodal coreceptor Cripto. *Genes Dev,* 17**,** 2624-9.

HATZFELD, M. 2005. The p120 family of cell adhesion molecules. *Eur J Cell Biol,* 84**,** 205-14.

HATZFELD, M. 2007. Plakophilins: Multifunctional proteins or just regulators of desmosomal adhesion? *Biochim Biophys Acta,* 1773**,** 69-77.

HEINEKE, J. & MOLKENTIN, J. D. 2006. Regulation of cardiac hypertrophy by intracellular signalling pathways. *Nat Rev Mol Cell Biol,* 7**,** 589-600.

HERREN, T.;GERBER, P. A. & DURU, F. 2009. Arrhythmogenic right ventricular cardiomyopathy/dysplasia: a not so rare "disease of the desmosome" with multiple clinical presentations. *Clin Res Cardiol,* 98**,** 141-58.

HEUSER, A.;PLOVIE, E. R.;ELLINOR, P. T.;GROSSMANN, K. S.;SHIN, J. T.;WICHTER, T.;BASSON, C. T.;LERMAN, B. B.;SASSE-KLAASSEN, S.;THIERFELDER, L.;MACRAE, C. A. & GERULL, B. 2006. Mutant desmocollin-2 causes arrhythmogenic right ventricular cardiomyopathy. *Am J Hum Genet,* 79**,** 1081-8.

HINCK, L.;NELSON, W. J. & PAPKOFF, J. 1994. Wnt-1 modulates cell-cell adhesion in mammalian cells by stabilizing beta-catenin binding to the cell adhesion protein cadherin. *J Cell Biol,* 124**,** 729-41.

HU, N.;SEDMERA, D.;YOST, H. J. & CLARK, E. B. 2000. Structure and function of the developing zebrafish heart. *Anat Rec,* 260**,** 148-57.

HU, P.;BERKOWITZ, P.;MADDEN, V. J. & RUBENSTEIN, D. S. 2006. Stabilization of plakoglobin and enhanced keratinocyte cell-cell adhesion by intracellular O-glycosylation. *J Biol Chem,* 281**,** 12786-91.

HUANG, P.;XIAO, A.;ZHOU, M.;ZHU, Z.;LIN, S. & ZHANG, B. 2011. Heritable gene targeting in zebrafish using customized TALENs. *Nat Biotechnol,* 29**,** 699-700.

HURLSTONE, A. F.;HARAMIS, A. P.;WIENHOLDS, E.;BEGTHEL, H.;KORVING, J.;VAN EEDEN, F.;CUPPEN, E.;ZIVKOVIC, D.;PLASTERK, R. H. & CLEVERS, H. 2003. The Wnt/beta-catenin pathway regulates cardiac valve formation. *Nature,* 425**,** 633-7.

INGERSLEV, H. C.;PETTERSEN, E. F.;JAKOBSEN, R. A.;PETERSEN, C. B. & WERGELAND, H. I. 2006. Expression profiling and validation of reference gene candidates in immune relevant tissues and cells from Atlantic salmon (Salmo salar L.). *Mol Immunol,* 43**,** 1194-201.

JACOB, K. A.;NOORMAN, M.;COX, M. G.;GROENEWEG, J. A.;HAUER, R. N. & VAN DER HEYDEN, M. A. 2012. Geographical distribution of plakophilin-2 mutation prevalence in patients with arrhythmogenic cardiomyopathy. *Neth Heart J,* 20**,** 234-9.

JOSHI-MUKHERJEE, R.;COOMBS, W.;MUSA, H.;OXFORD, E.;TAFFET, S. & DELMAR, M. 2008. Characterization of the molecular phenotype of two arrhythmogenic right ventricular cardiomyopathy (ARVC)-related plakophilin-2 (PKP2) mutations. *Heart Rhythm,* 5**,** 1715-23.

JOUNG, J. K. & SANDER, J. D. 2012. TALENs: a widely applicable technology for targeted genome editing. *Nat Rev Mol Cell Biol*.

KANAZAWA, A.;TSUKADA, S.;KAMIYAMA, M.;YANAGIMOTO, T.;NAKAJIMA, M. & MAEDA, S. 2005. Wnt5b partially inhibits canonical Wnt/beta-catenin signaling pathway and promotes adipogenesis in 3T3-L1 preadipocytes. *Biochem Biophys Res Commun,* 330**,** 505-10.

KAPLAN, S. R.;GARD, J. J.;CARVAJAL-HUERTA, L.;RUIZ-CABEZAS, J. C.;THIENE, G. & SAFFITZ, J. E. 2004a. Structural and molecular pathology of the heart in Carvajal syndrome. *Cardiovasc Pathol,* 13**,** 26-32.

KAPLAN, S. R.;GARD, J. J.;PROTONOTARIOS, N.;TSATSOPOULOU, A.;SPILIOPOULOU, C.;ANASTASAKIS, A.;SQUARCIONI, C. P.;MCKENNA, W. J.;THIENE, G.;BASSO, C.;BROUSSE, N.;FONTAINE, G. & SAFFITZ, J. E. 2004b. Remodeling of myocyte gap junctions in arrhythmogenic right ventricular cardiomyopathy due to a deletion in plakoglobin (Naxos disease). *Heart Rhythm,* 1**,** 3-11.

KEEGAN, B. R.;MEYER, D. & YELON, D. 2004. Organization of cardiac chamber progenitors in the zebrafish blastula. *Development,* 131**,** 3081-91.

KELLY, R. G.;BROWN, N. A. & BUCKINGHAM, M. E. 2001. The arterial pole of the mouse heart forms from Fgf10-expressing cells in pharyngeal mesoderm. *Dev Cell,* 1**,** 435-40.

KIKUCHI, A.;YAMAMOTO, H. & KISHIDA, S. 2007. Multiplicity of the interactions of Wnt proteins and their receptors. *Cell Signal,* 19**,** 659-71.

KIM, E.;SHIN, D. W.;HONG, C. S.;JEONG, D.;KIM, D. H. & PARK, W. J. 2003. Increased Ca2+ storage capacity in the sarcoplasmic reticulum by overexpression of HRC (histidine-rich Ca2+ binding protein). *Biochem Biophys Res Commun,* 300**,** 192-6.

KIRCHHOF, P.;FABRITZ, L.;ZWIENER, M.;WITT, H.;SCHAFERS, M.;ZELLERHOFF, S.;PAUL, M.;ATHAI, T.;HILLER, K. H.;BABA, H. A.;BREITHARDT, G.;RUIZ, P.;WICHTER, T. & LEVKAU, B. 2006. Age- and training-dependent development of arrhythmogenic right ventricular cardiomyopathy in heterozygous plakoglobin-deficient mice. *Circulation,* 114**,** 1799-806.

KNUDSEN, K. A. & WHEELOCK, M. J. 1992. Plakoglobin, or an 83-kD homologue distinct from beta-catenin, interacts with E-cadherin and N-cadherin. *J Cell Biol,* 118**,** 671-9.

KOMIYA, Y. & HABAS, R. 2008. Wnt signal transduction pathways. *Organogenesis,* 4**,** 68-75.

KOTTKE, M. D.;DELVA, E. & KOWALCZYK, A. P. 2006. The desmosome: cell science lessons from human diseases. *J Cell Sci,* 119**,** 797-806.

KOWALCZYK, A. P.;BORNSLAEGER, E. A.;BORGWARDT, J. E.;PALKA, H. L.;DHALIWAL, A. S.;CORCORAN, C. M.;DENNING, M. F. & GREEN, K. J. 1997. The amino-terminal domain of desmoplakin binds to plakoglobin and clusters desmosomal cadherin-plakoglobin complexes. *J Cell Biol,* 139**,** 773-84.

KOYANAGI, M.;IWASAKI, M.;HAENDELER, J.;LEITGES, M.;ZEIHER, A. M. & DIMMELER, S. 2009. Wnt5a increases cardiac gene expressions of cultured human circulating progenitor cells via a PKC delta activation. *PLoS One,* 4**,** e5765.

KREMENEVSKAJA, N.;VON WASIELEWSKI, R.;RAO, A. S.;SCHOFL, C.;ANDERSSON, T. & BRABANT, G. 2005. Wnt-5a has tumor suppressor activity in thyroid carcinoma. *Oncogene,* 24**,** 2144-54.

KUHL, M.;SHELDAHL, L. C.;MALBON, C. C. & MOON, R. T. 2000a. Ca(2+)/calmodulin-dependent protein kinase II is stimulated by Wnt and Frizzled homologs and promotes ventral cell fates in Xenopus. *J Biol Chem,* 275**,** 12701-11.

KUHL, M.;SHELDAHL, L. C.;PARK, M.;MILLER, J. R. & MOON, R. T. 2000b. The Wnt/Ca2+ pathway: a new vertebrate Wnt signaling pathway takes shape. *Trends Genet,* 16**,** 279-83.

LAITINEN, P. J.;BROWN, K. M.;PIIPPO, K.;SWAN, H.;DEVANEY, J. M.;BRAHMBHATT, B.;DONARUM, E. A.;MARINO, M.;TISO, N.;VIITASALO, M.;TOIVONEN, L.;STEPHAN, D. A. & KONTULA, K. 2001. Mutations of the cardiac ryanodine receptor (RyR2) gene in familial polymorphic ventricular tachycardia. *Circulation,* 103**,** 485-90.

LEE, E.;SALIC, A.;KRUGER, R.;HEINRICH, R. & KIRSCHNER, M. W. 2003. The roles of APC and Axin derived from experimental and theoretical analysis of the Wnt pathway. *PLoS Biol,* 1**,** E10.

LEE, R. K.;STAINIER, D. Y.;WEINSTEIN, B. M. & FISHMAN, M. C. 1994. Cardiovascular development in the zebrafish. II. Endocardial progenitors are sequestered within the heart field. *Development,* 120**,** 3361-6.

LENHART, K. F.;LIN, S. Y.;TITUS, T. A.;POSTLETHWAIT, J. H. & BURDINE, R. D. 2011. Two additional midline barriers function with midline lefty1 expression to maintain asymmetric Nodal signaling during left-right axis specification in zebrafish. *Development,* 138**,** 4405-10.

LEVIN, M.;PAGAN, S.;ROBERTS, D. J.;COOKE, J.;KUEHN, M. R. & TABIN, C. J. 1997. Left/right patterning signals and the independent regulation of different aspects of situs in the chick embryo. *Dev Biol,* 189**,** 57-67.

LI, J.;SWOPE, D.;RAESS, N.;CHENG, L.;MULLER, E. J. & RADICE, G. L. 2011a. Cardiac tissue-restricted deletion of plakoglobin results in progressive cardiomyopathy and activation of {beta}-catenin signaling. *Mol Cell Biol,* 31**,** 1134-44.

LI, J. & WANG, C. Y. 2008. TBL1-TBLR1 and beta-catenin recruit each other to Wnt target-gene promoter for transcription activation and oncogenesis. *Nat Cell Biol,* 10**,** 160-9.

LI, T.;HUANG, S.;JIANG, W. Z.;WRIGHT, D.;SPALDING, M. H.;WEEKS, D. P. & YANG, B. 2011b. TAL nucleases (TALNs): hybrid proteins composed of TAL effectors and FokI DNA-cleavage domain. *Nucleic Acids Res,* 39**,** 359-72.

LI, T.;HUANG, S.;ZHAO, X.;WRIGHT, D. A.;CARPENTER, S.;SPALDING, M. H.;WEEKS, D. P. & YANG, B. 2011c. Modularly assembled designer TAL effector

nucleases for targeted gene knockout and gene replacement in eukaryotes. *Nucleic Acids Res,* 39**,** 6315-25.

LI, V. S.;NG, S. S.;BOERSEMA, P. J.;LOW, T. Y.;KARTHAUS, W. R.;GERLACH, J. P.;MOHAMMED, S.;HECK, A. J.;MAURICE, M. M.;MAHMOUDI, T. & CLEVERS, H. 2012. Wnt signaling through inhibition of beta-catenin degradation in an intact Axin1 complex. *Cell,* 149**,** 1245-56.

LIANG, J. O.;ETHERIDGE, A.;HANTSOO, L.;RUBINSTEIN, A. L.;NOWAK, S. J.;IZPISUA BELMONTE, J. C. & HALPERN, M. E. 2000. Asymmetric nodal signaling in the zebrafish diencephalon positions the pineal organ. *Development,* 127**,** 5101-12.

LIU, J.;LI, C.;YU, Z.;HUANG, P.;WU, H.;WEI, C.;ZHU, N.;SHEN, Y.;CHEN, Y.;ZHANG, B.;DENG, W. M. & JIAO, R. 2012. Efficient and specific modifications of the Drosophila genome by means of an easy TALEN strategy. *J Genet Genomics,* 39**,** 209-15.

LIU, W.;SATO, A.;KHADKA, D.;BHARTI, R.;DIAZ, H.;RUNNELS, L. W. & HABAS, R. 2008. Mechanism of activation of the Formin protein Daam1. *Proc Natl Acad Sci U S A,* 105**,** 210-5.

LIU, X.;RUBIN, J. S. & KIMMEL, A. R. 2005. Rapid, Wnt-induced changes in GSK-3beta associations that regulate beta-catenin stabilization are mediated by Galpha proteins. *Curr Biol,* 15**,** 1989-97.

LOGAN, C. Y. & NUSSE, R. 2004. The Wnt signaling pathway in development and disease. *Annu Rev Cell Dev Biol,* 20**,** 781-810.

LOMBARDI, R.;DONG, J.;RODRIGUEZ, G.;BELL, A.;LEUNG, T. K.;SCHWARTZ, R. J.;WILLERSON, J. T.;BRUGADA, R. & MARIAN, A. J. 2009. Genetic fate mapping identifies second heart field progenitor cells as a source of adipocytes in arrhythmogenic right ventricular cardiomyopathy. *Circ Res,* 104**,** 1076-84.

LONG, S.;AHMAD, N. & REBAGLIATI, M. 2003. The zebrafish nodal-related gene southpaw is required for visceral and diencephalic left-right asymmetry. *Development,* 130**,** 2303-16.

LUO, W.;PETERSON, A.;GARCIA, B. A.;COOMBS, G.;KOFAHL, B.;HEINRICH, R.;SHABANOWITZ, J.;HUNT, D. F.;YOST, H. J. & VIRSHUP, D. M. 2007. Protein phosphatase 1 regulates assembly and function of the beta-catenin degradation complex. *EMBO J,* 26**,** 1511-21.

LY, S.;MARCUS, F. I.;XU, T. & TOWBIN, J. A. 2008. A woman with incidental findings of ventricular aneurysms and a desmosomal cardiomyopathy. *Heart Rhythm,* 5**,** 1455-7.

MA, L. & WANG, H. Y. 2006. Suppression of cyclic GMP-dependent protein kinase is essential to the Wnt/cGMP/Ca2+ pathway. *J Biol Chem,* 281**,** 30990-1001.

MACDONALD, B. T.;TAMAI, K. & HE, X. 2009. Wnt/beta-catenin signaling: components, mechanisms, and diseases. *Dev Cell,* 17**,** 9-26.

MAEDA, O.;USAMI, N.;KONDO, M.;TAKAHASHI, M.;GOTO, H.;SHIMOKATA, K.;KUSUGAMI, K. & SEKIDO, Y. 2004. Plakoglobin (gamma-catenin) has TCF/LEF family-dependent transcriptional activity in beta-catenin-deficient cell line. *Oncogene,* 23**,** 964-72.

MAHFOUZ, M. M.;LI, L.;SHAMIMUZZAMAN, M.;WIBOWO, A.;FANG, X. & ZHU, J. K. 2011. De novo-engineered transcription activator-like effector (TALE) hybrid

nuclease with novel DNA binding specificity creates double-strand breaks. *Proc Natl Acad Sci U S A,* 108**,** 2623-8.

MALBON, C. C. & WANG, H. Y. 2006. Dishevelled: a mobile scaffold catalyzing development. *Curr Top Dev Biol,* 72**,** 153-66.

MAO, J.;WANG, J.;LIU, B.;PAN, W.;FARR, G. H., 3RD;FLYNN, C.;YUAN, H.;TAKADA, S.;KIMELMAN, D.;LI, L. & WU, D. 2001. Low-density lipoprotein receptor-related protein-5 binds to Axin and regulates the canonical Wnt signaling pathway. *Mol Cell,* 7**,** 801-9.

MARGUERIE, A.;BAJOLLE, F.;ZAFFRAN, S.;BROWN, N. A.;DICKSON, C.;BUCKINGHAM, M. E. & KELLY, R. G. 2006. Congenital heart defects in Fgfr2-IIIb and Fgf10 mutant mice. *Cardiovasc Res,* 71**,** 50-60.

MARTIN, E. D. 2008. *Signalling by cell adhesion molecules in zebrafish heart development* B. Sc. (Hons), NUI Galway.

MARTIN, E. D. & GREALY, M. 2004. Plakoglobin expression and localization in zebrafish embryo development. *Biochem Soc Trans,* 32**,** 797-8.

MARTIN, E. D.;MORIARTY, M. A.;BYRNES, L. & GREALY, M. 2009. Plakoglobin has both structural and signalling roles in zebrafish development. *Dev Biol,* 327**,** 83-96.

MCCALLUM, C. M.;COMAI, L.;GREENE, E. A. & HENIKOFF, S. 2000. Targeted screening for induced mutations. *Nat Biotechnol,* 18**,** 455-7.

MCCREA, P. D.;TURCK, C. W. & GUMBINER, B. 1991. A homolog of the armadillo protein in Drosophila (plakoglobin) associated with E-cadherin. *Science,* 254**,** 1359-61.

MCGRATH, J. A.;MCMILLAN, J. R.;SHEMANKO, C. S.;RUNSWICK, S. K.;LEIGH, I. M.;LANE, E. B.;GARROD, D. R. & EADY, R. A. 1997. Mutations in the plakophilin 1 gene result in ectodermal dysplasia/skin fragility syndrome. *Nat Genet,* 17**,** 240-4.

MCKENNA, W. J.;THIENE, G.;NAVA, A.;FONTALIRAN, F.;BLOMSTROM-LUNDQVIST, C.;FONTAINE, G. & CAMERINI, F. 1994. Diagnosis of arrhythmogenic right ventricular dysplasia/cardiomyopathy. Task Force of the Working Group Myocardial and Pericardial Disease of the European Society of Cardiology and of the Scientific Council on Cardiomyopathies of the International Society and Federation of Cardiology. *Br Heart J,* 71**,** 215-8.

MCKOY, G.;PROTONOTARIOS, N.;CROSBY, A.;TSATSOPOULOU, A.;ANASTASAKIS, A.;COONAR, A.;NORMAN, M.;BABOONIAN, C.;JEFFERY, S. & MCKENNA, W. J. 2000. Identification of a deletion in plakoglobin in arrhythmogenic right ventricular cardiomyopathy with palmoplantar keratoderma and woolly hair (Naxos disease). *Lancet,* 355**,** 2119-24.

MENG, X.;NOYES, M. B.;ZHU, L. J.;LAWSON, N. D. & WOLFE, S. A. 2008. Targeted gene inactivation in zebrafish using engineered zinc-finger nucleases. *Nat Biotechnol,* 26**,** 695-701.

MENO, C.;GRITSMAN, K.;OHISHI, S.;OHFUJI, Y.;HECKSCHER, E.;MOCHIDA, K.;SHIMONO, A.;KONDOH, H.;TALBOT, W. S.;ROBERTSON, E. J.;SCHIER, A. F. & HAMADA, H. 1999. Mouse Lefty2 and zebrafish antivin are feedback inhibitors of nodal signaling during vertebrate gastrulation. *Mol Cell,* 4**,** 287-98.

MENO, C.;TAKEUCHI, J.;SAKUMA, R.;KOSHIBA-TAKEUCHI, K.;OHISHI, S.;SAIJOH, Y.;MIYAZAKI, J.;TEN DIJKE, P.;OGURA, T. & HAMADA, H. 2001. Diffusion of nodal signaling activity in the absence of the feedback inhibitor Lefty2. *Dev Cell,* 1**,** 127-38.

MERTENS, C.;KUHN, C. & FRANKE, W. W. 1996. Plakophilins 2a and 2b: constitutive proteins of dual location in the karyoplasm and the desmosomal plaque. *J Cell Biol,* 135**,** 1009-25.

MERTENS, C.;KUHN, C.;MOLL, R.;SCHWETLICK, I. & FRANKE, W. W. 1999. Desmosomal plakophilin 2 as a differentiation marker in normal and malignant tissues. *Differentiation,* 64**,** 277-90.

MEURS, K. M.;MAUCELI, E.;LAHMERS, S.;ACLAND, G. M.;WHITE, S. N. & LINDBLAD-TOH, K. 2010. Genome-wide association identifies a deletion in the 3' untranslated region of striatin in a canine model of arrhythmogenic right ventricular cardiomyopathy. *Hum Genet,* 128**,** 315-24.

MILLER, J. C.;TAN, S.;QIAO, G.;BARLOW, K. A.;WANG, J.;XIA, D. F.;MENG, X.;PASCHON, D. E.;LEUNG, E.;HINKLEY, S. J.;DULAY, G. P.;HUA, K. L.;ANKOUDINOVA, I.;COST, G. J.;URNOV, F. D.;ZHANG, H. S.;HOLMES, M. C.;ZHANG, L.;GREGORY, P. D. & REBAR, E. J. 2011. A TALE nuclease architecture for efficient genome editing. *Nat Biotechnol,* 29**,** 143-8.

MILLER, R. K. & MCCREA, P. D. 2010. Wnt to build a tube: contributions of Wnt signaling to epithelial tubulogenesis. *Dev Dyn,* 239**,** 77-93.

MIRAVET, S.;PIEDRA, J.;MIRO, F.;ITARTE, E.;GARCIA DE HERREROS, A. & DUNACH, M. 2002. The transcriptional factor TCF-4 contains different binding sites for beta-catenin and plakoglobin. *J Biol Chem,* 277**,** 1884-91.

MOLDES, M.;ZUO, Y.;MORRISON, R. F.;SILVA, D.;PARK, B. H.;LIU, J. & FARMER, S. R. 2003. Peroxisome-proliferator-activated receptor gamma suppresses Wnt/beta-catenin signalling during adipogenesis. *Biochem J,* 376**,** 607-13.

MOLENAAR, M.;VAN DE WETERING, M.;OOSTERWEGEL, M.;PETERSON-MADURO, J.;GODSAVE, S.;KORINEK, V.;ROOSE, J.;DESTREE, O. & CLEVERS, H. 1996. XTcf-3 transcription factor mediates beta-catenin-induced axis formation in Xenopus embryos. *Cell,* 86**,** 391-9.

MOORE, F. E.;REYON, D.;SANDER, J. D.;MARTINEZ, S. A.;BLACKBURN, J. S.;KHAYTER, C.;RAMIREZ, C. L.;JOUNG, J. K. & LANGENAU, D. M. 2012. Improved somatic mutagenesis in zebrafish using transcription activator-like effector nucleases (TALENs). *PLoS One,* 7**,** e37877.

MORBITZER, R.;ROMER, P.;BOCH, J. & LAHAYE, T. 2010. Regulation of selected genome loci using de novo-engineered transcription activator-like effector (TALE)-type transcription factors. *Proc Natl Acad Sci U S A,* 107**,** 21617-22.

MORIARTY, M. A.;MARTIN, E. D.;BYRNES, L. & GREALY, M. 2008. Molecular cloning and developmental expression of plakophilin 2 in zebrafish. *Biochem Biophys Res Commun,* 367**,** 124-9.

MORIARTY, M. A.;RYAN, R.;LALOR, P.;DOCKERY, P.;BYRNES, L. & GREALY, M. 2012. Loss of plakophilin 2 disrupts heart development in zebrafish. *Int J Dev Biol*.

MOSCOU, M. J. & BOGDANOVE, A. J. 2009. A simple cipher governs DNA recognition by TAL effectors. *Science,* 326**,** 1501.

NAITO, A. T.;SHIOJIMA, I.;AKAZAWA, H.;HIDAKA, K.;MORISAKI, T.;KIKUCHI, A. & KOMURO, I. 2006. Developmental stage-specific biphasic roles of Wnt/beta-

catenin signaling in cardiomyogenesis and hematopoiesis. *Proc Natl Acad Sci U S A,* 103**,** 19812-7.

NAKAMURA, T.;SANO, M.;SONGYANG, Z. & SCHNEIDER, M. D. 2003. A Wnt- and beta -catenin-dependent pathway for mammalian cardiac myogenesis. *Proc Natl Acad Sci U S A,* 100**,** 5834-9.

NASEVICIUS, A. & EKKER, S. C. 2000. Effective targeted gene 'knockdown' in zebrafish. *Nat Genet,* 26**,** 216-20.

NAVARRO-MANCHON, J.;FERNANDEZ, E.;IGUAL, B.;ASIMAKI, A.;SYRRIS, P.;OSCA, J.;SALVADOR, A. & ZORIO, E. 2011. [Left dominant arrhythmogenic cardiomyopathy caused by a novel nonsense mutation in desmoplakin]. *Rev Esp Cardiol,* 64**,** 530-4.

NEAVE, B.;HOLDER, N. & PATIENT, R. 1997. A graded response to BMP-4 spatially coordinates patterning of the mesoderm and ectoderm in the zebrafish. *Mech Dev,* 62**,** 183-95.

NELSON, W. J. 2008. Regulation of cell-cell adhesion by the cadherin-catenin complex. *Biochem Soc Trans,* 36**,** 149-55.

NEUBER, S.;MUHMER, M.;WRATTEN, D.;KOCH, P. J.;MOLL, R. & SCHMIDT, A. 2010. The desmosomal plaque proteins of the plakophilin family. *Dermatol Res Pract,* 2010**,** 1014-52.

NICOT, N.;HAUSMAN, J. F.;HOFFMANN, L. & EVERS, D. 2005. Housekeeping gene selection for real-time RT-PCR normalization in potato during biotic and abiotic stress. *J Exp Bot,* 56**,** 2907-14.

NORGETT, E. E.;HATSELL, S. J.;CARVAJAL-HUERTA, L.;CABEZAS, J. C.;COMMON, J.;PURKIS, P. E.;WHITTOCK, N.;LEIGH, I. M.;STEVENS, H. P. & KELSELL, D. P. 2000. Recessive mutation in desmoplakin disrupts desmoplakin-intermediate filament interactions and causes dilated cardiomyopathy, woolly hair and keratoderma. *Hum Mol Genet,* 9**,** 2761-6.

NORGETT, E. E.;LUCKE, T. W.;BOWERS, B.;MUNRO, C. S.;LEIGH, I. M. & KELSELL, D. P. 2006. Early death from cardiomyopathy in a family with autosomal dominant striate palmoplantar keratoderma and woolly hair associated with a novel insertion mutation in desmoplakin. *J Invest Dermatol,* 126**,** 1651-4.

NORMAN, M.;SIMPSON, M.;MOGENSEN, J.;SHAW, A.;HUGHES, S.;SYRRIS, P.;SEN-CHOWDHRY, S.;ROWLAND, E.;CROSBY, A. & MCKENNA, W. J. 2005. Novel mutation in desmoplakin causes arrhythmogenic left ventricular cardiomyopathy. *Circulation,* 112**,** 636-42.

NUSSE, R. 2012. Wnt signaling. *Cold Spring Harb Perspect Biol,* 2012; 4(5)

OLEYKOWSKI, C. A.;BRONSON MULLINS, C. R.;GODWIN, A. K. & YEUNG, A. T. 1998. Mutation detection using a novel plant endonuclease. *Nucleic Acids Res,* 26**,** 4597-602.

PANDUR, P.;LASCHE, M.;EISENBERG, L. M. & KUHL, M. 2002. Wnt-11 activation of a non-canonical Wnt signalling pathway is required for cardiogenesis. *Nature,* 418**,** 636-41.

PELSTER, B. 1999. Environmental influences on the development of the cardiac system in fish and amphibians. *Comp Biochem Physiol A Mol Integr Physiol,* 124**,** 407-12.

PELSTER, B. & BURGGREN, W. W. 1996. Disruption of hemoglobin oxygen transport does not impact oxygen-dependent physiological processes in developing embryos of zebra fish (Danio rerio). *Circ Res,* 79**,** 358-62.

PICCOLO, S.;AGIUS, E.;LEYNS, L.;BHATTACHARYYA, S.;GRUNZ, H.;BOUWMEESTER, T. & DE ROBERTIS, E. M. 1999. The head inducer Cerberus is a multifunctional antagonist of Nodal, BMP and Wnt signals. *Nature,* 397**,** 707-10.

PILICHOU, K.;NAVA, A.;BASSO, C.;BEFFAGNA, G.;BAUCE, B.;LORENZON, A.;FRIGO, G.;VETTORI, A.;VALENTE, M.;TOWBIN, J.;THIENE, G.;DANIELI, G. A. & RAMPAZZO, A. 2006. Mutations in desmoglein-2 gene are associated with arrhythmogenic right ventricular cardiomyopathy. *Circulation,* 113**,** 1171-9.

PROTONOTARIOS, N.;TSATSOPOULOU, A.;PATSOURAKOS, P.;ALEXOPOULOS, D.;GEZERLIS, P.;SIMITSIS, S. & SCAMPARDONIS, G. 1986. Cardiac abnormalities in familial palmoplantar keratosis. *Br Heart J,* 56**,** 321-6.

RAMPAZZO, A.;NAVA, A.;MALACRIDA, S.;BEFFAGNA, G.;BAUCE, B.;ROSSI, V.;ZIMBELLO, R.;SIMIONATI, B.;BASSO, C.;THIENE, G.;TOWBIN, J. A. & DANIELI, G. A. 2002. Mutation in human desmoplakin domain binding to plakoglobin causes a dominant form of arrhythmogenic right ventricular cardiomyopathy. *Am J Hum Genet,* 71**,** 1200-6.

RANDALL, R. A.;HOWELL, M.;PAGE, C. S.;DALY, A.;BATES, P. A. & HILL, C. S. 2004. Recognition of phosphorylated-Smad2-containing complexes by a novel Smad interaction motif. *Mol Cell Biol,* 24**,** 1106-21.

RAYA, A. & IZPISUA BELMONTE, J. C. 2006. Left-right asymmetry in the vertebrate embryo: from early information to higher-level integration. *Nat Rev Genet,* 7**,** 283-93.

RAYA, A.;KAWAKAMI, Y.;RODRIGUEZ-ESTEBAN, C.;BUSCHER, D.;KOTH, C. M.;ITOH, T.;MORITA, M.;RAYA, R. M.;DUBOVA, I.;BESSA, J. G.;DE LA POMPA, J. L. & IZPISUA BELMONTE, J. C. 2003. Notch activity induces Nodal expression and mediates the establishment of left-right asymmetry in vertebrate embryos. *Genes Dev,* 17**,** 1213-8.

REBAGLIATI, M. R.;TOYAMA, R.;HAFFTER, P. & DAWID, I. B. 1998. cyclops encodes a nodal-related factor involved in midline signaling. *Proc Natl Acad Sci U S A,* 95**,** 9932-7.

REIFERS, F.;WALSH, E. C.;LEGER, S.;STAINIER, D. Y. & BRAND, M. 2000. Induction and differentiation of the zebrafish heart requires fibroblast growth factor 8 (fgf8/acerebellar). *Development,* 127**,** 225-35.

REISSMANN, E.;JORNVALL, H.;BLOKZIJL, A.;ANDERSSON, O.;CHANG, C.;MINCHIOTTI, G.;PERSICO, M. G.;IBANEZ, C. F. & BRIVANLOU, A. H. 2001. The orphan receptor ALK7 and the Activin receptor ALK4 mediate signaling by Nodal proteins during vertebrate development. *Genes Dev,* 15**,** 2010-22.

REITER, J. F.;VERKADE, H. & STAINIER, D. Y. 2001. Bmp2b and Oep promote early myocardial differentiation through their regulation of gata5. *Dev Biol,* 234**,** 330-8.

ROBERTS, J.;HERKERT, J.;RUTBERG, J.;NIKKEL, S.;WIESFELD, A.;DOOIJES, D.;GOW, R.;VAN TINTELEN, J. & GOLLOB, M. 2012. Detection of genomic deletions of PKP2 in arrhythmogenic right ventricular cardiomyopathy. *Clin Genet*.

ROTTBAUER, W.;SAURIN, A. J.;LICKERT, H.;SHEN, X.;BURNS, C. G.;WO, Z. G.;KEMLER, R.;KINGSTON, R.;WU, C. & FISHMAN, M. 2002. Reptin and pontin

antagonistically regulate heart growth in zebrafish embryos. *Cell,* 111**,** 661-72.

RUIZ, P.;BRINKMANN, V.;LEDERMANN, B.;BEHREND, M.;GRUND, C.;THALHAMMER, C.;VOGEL, F.;BIRCHMEIER, C.;GUNTHERT, U.;FRANKE, W. W. & BIRCHMEIER, W. 1996. Targeted mutation of plakoglobin in mice reveals essential functions of desmosomes in the embryonic heart. *J Cell Biol,* 135**,** 215-25.

SACCO, P. A.;MCGRANAHAN, T. M.;WHEELOCK, M. J. & JOHNSON, K. R. 1995. Identification of plakoglobin domains required for association with N-cadherin and alpha-catenin. *J Biol Chem,* 270**,** 20201-6.

SADOT, E.;SIMCHA, I.;IWAI, K.;CIECHANOVER, A.;GEIGER, B. & BEN-ZE'EV, A. 2000. Differential interaction of plakoglobin and beta-catenin with the ubiquitin-proteasome system. *Oncogene,* 19**,** 1992-2001.

SALIC, A.;LEE, E.;MAYER, L. & KIRSCHNER, M. W. 2000. Control of beta-catenin stability: reconstitution of the cytoplasmic steps of the wnt pathway in Xenopus egg extracts. *Mol Cell,* 5**,** 523-32.

SAMPATH, K.;CHENG, A. M.;FRISCH, A. & WRIGHT, C. V. 1997. Functional differences among Xenopus nodal-related genes in left-right axis determination. *Development,* 124**,** 3293-302.

SAMPATH, K.;RUBINSTEIN, A. L.;CHENG, A. M.;LIANG, J. O.;FEKANY, K.;SOLNICA-KREZEL, L.;KORZH, V.;HALPERN, M. E. & WRIGHT, C. V. 1998. Induction of the zebrafish ventral brain and floorplate requires cyclops/nodal signalling. *Nature,* 395**,** 185-9.

SANDER, J. D.;CADE, L.;KHAYTER, C.;REYON, D.;PETERSON, R. T.;JOUNG, J. K. & YEH, J. R. 2011. Targeted gene disruption in somatic zebrafish cells using engineered TALENs. *Nat Biotechnol,* 29**,** 697-8.

SANEYOSHI, T.;KUME, S.;AMASAKI, Y. & MIKOSHIBA, K. 2002. The Wnt/calcium pathway activates NF-AT and promotes ventral cell fate in Xenopus embryos. *Nature,* 417**,** 295-9.

SASAI, Y.;LU, B.;STEINBEISSER, H.;GEISSERT, D.;GONT, L. K. & DE ROBERTIS, E. M. 1994. Xenopus chordin: a novel dorsalizing factor activated by organizer-specific homeobox genes. *Cell,* 79**,** 779-90.

SATO, P. Y.;COOMBS, W.;LIN, X.;NEKRASOVA, O.;GREEN, K. J.;ISOM, L. L.;TAFFET, S. M. & DELMAR, M. 2011. Interactions between ankyrin-G, Plakophilin-2, and Connexin43 at the cardiac intercalated disc. *Circ Res,* 109**,** 193-201.

SATO, P. Y.;MUSA, H.;COOMBS, W.;GUERRERO-SERNA, G.;PATINO, G. A.;TAFFET, S. M.;ISOM, L. L. & DELMAR, M. 2009. Loss of plakophilin-2 expression leads to decreased sodium current and slower conduction velocity in cultured cardiac myocytes. *Circ Res,* 105**,** 523-6.

SCHERZ, P. J.;HUISKEN, J.;SAHAI-HERNANDEZ, P. & STAINIER, D. Y. 2008. High-speed imaging of developing heart valves reveals interplay of morphogenesis and function. *Development,* 135**,** 1179-87.

SCHIER, A. F. & SHEN, M. M. 2000. Nodal signalling in vertebrate development. *Nature,* 403**,** 385-9.

SCHLESSINGER, K.;HALL, A. & TOLWINSKI, N. 2009. Wnt signaling pathways meet Rho GTPases. *Genes Dev,* 23**,** 265-77.

SCHMIDT, A.;LANGBEIN, L.;PRATZEL, S.;RODE, M.;RACKWITZ, H. R. & FRANKE, W. W. 1999. Plakophilin 3--a novel cell-type-specific desmosomal plaque protein. *Differentiation,* 64**,** 291-306.

SCHMIDT, A.;LANGBEIN, L.;RODE, M.;PRATZEL, S.;ZIMBELMANN, R. & FRANKE, W. W. 1997. Plakophilins 1a and 1b: widespread nuclear proteins recruited in specific epithelial cells as desmosomal plaque components. *Cell Tissue Res,* 290**,** 481-99.

SCHOENEBECK, J. J. & YELON, D. 2007. Illuminating cardiac development: Advances in imaging add new dimensions to the utility of zebrafish genetics. *Semin Cell Dev Biol,* 18**,** 27-35.

SEMENOV, M. V.;TAMAI, K.;BROTT, B. K.;KUHL, M.;SOKOL, S. & HE, X. 2001. Head inducer Dickkopf-1 is a ligand for Wnt coreceptor LRP6. *Curr Biol,* 11**,** 951-61.

SHEN, M. M. 2007. Nodal signaling: developmental roles and regulation. *Development,* 134**,** 1023-34.

SHEN, M. M.;WANG, H. & LEDER, P. 1997. A differential display strategy identifies Cryptic, a novel EGF-related gene expressed in the axial and lateral mesoderm during mouse gastrulation. *Development,* 124**,** 429-42.

SHIMIZU, T.;YAMANAKA, Y.;RYU, S. L.;HASHIMOTO, H.;YABE, T.;HIRATA, T.;BAE, Y. K.;HIBI, M. & HIRANO, T. 2000. Cooperative roles of Bozozok/Dharma and Nodal-related proteins in the formation of the dorsal organizer in zebrafish. *Mech Dev,* 91**,** 293-303.

SHIRATORI, H.;SAKUMA, R.;WATANABE, M.;HASHIGUCHI, H.;MOCHIDA, K.;SAKAI, Y.;NISHINO, J.;SAIJOH, Y.;WHITMAN, M. & HAMADA, H. 2001. Two-step regulation of left-right asymmetric expression of Pitx2: initiation by nodal signaling and maintenance by Nkx2. *Mol Cell,* 7**,** 137-49.

SIRNES, S.;BRUUN, J.;KOLBERG, M.;KJENSETH, A.;LIND, G. E.;SVINDLAND, A.;BRECH, A.;NESBAKKEN, A.;LOTHE, R. A.;LEITHE, E. & RIVEDAL, E. 2012. Connexin43 acts as a colorectal cancer tumor suppressor and predicts disease outcome. *Int J Cancer,* 131**,** 570-81.

SOLANAS, G.;MIRAVET, S.;CASAGOLDA, D.;CASTANO, J.;RAURELL, I.;CORRIONERO, A.;DE HERREROS, A. G. & DUNACH, M. 2004. beta-Catenin and plakoglobin N- and C-tails determine ligand specificity. *J Biol Chem,* 279**,** 49849-56.

STAINIER, D. Y. & FISHMAN, M. C. 1992. Patterning the zebrafish heart tube: acquisition of anteroposterior polarity. *Dev Biol,* 153**,** 91-101.

STAINIER, D. Y.;LEE, R. K. & FISHMAN, M. C. 1993. Cardiovascular development in the zebrafish. I. Myocardial fate map and heart tube formation. *Development,* 119**,** 31-40.

STAUDT, D. & STAINIER, D. 2012. Uncovering the Molecular and Cellular Mechanisms of Heart Development Using the Zebrafish. *Annu Rev Genet*.

SUMMERTON, J. 1999. Morpholino antisense oligomers: the case for an RNase H-independent structural type. *Biochim Biophys Acta,* 1489**,** 141-58.

SUMMERTON, J. & WELLER, D. 1997. Morpholino antisense oligomers: design, preparation, and properties. *Antisense Nucleic Acid Drug Dev,* 7**,** 187-95.

SWOPE, D.;CHENG, L.;GAO, E.;LI, J. & RADICE, G. L. 2012a. Loss of cadherin-binding proteins beta-catenin and plakoglobin in the heart leads to gap junction remodeling and arrhythmogenesis. *Mol Cell Biol,* 32**,** 1056-67.

SWOPE, D.;LI, J. & RADICE, G. L. 2012b. Beyond cell adhesion: The role of armadillo proteins in the heart. *Cell Signal,* 25**,** 93-100.

SYRRIS, P.;WARD, D.;ASIMAKI, A.;EVANS, A.;SEN-CHOWDHRY, S.;HUGHES, S. E. & MCKENNA, W. J. 2007. Desmoglein-2 mutations in arrhythmogenic right ventricular cardiomyopathy: a genotype-phenotype characterization of familial disease. *Eur Heart J,* 28**,** 581-8.

SYRRIS, P.;WARD, D.;ASIMAKI, A.;SEN-CHOWDHRY, S.;EBRAHIM, H. Y.;EVANS, A.;HITOMI, N.;NORMAN, M.;PANTAZIS, A.;SHAW, A. L.;ELLIOTT, P. M. & MCKENNA, W. J. 2006. Clinical expression of plakophilin-2 mutations in familial arrhythmogenic right ventricular cardiomyopathy. *Circulation,* 113**,** 356-64.

TADA, M. & KAI, M. 2009. Noncanonical Wnt/PCP signaling during vertebrate gastrulation. *Zebrafish,* 6**,** 29-40.

TAMAI, K.;SEMENOV, M.;KATO, Y.;SPOKONY, R.;LIU, C.;KATSUYAMA, Y.;HESS, F.;SAINT-JEANNET, J. P. & HE, X. 2000. LDL-receptor-related proteins in Wnt signal transduction. *Nature,* 407**,** 530-5.

TAN, B. Y.;JAIN, R.;DEN HAAN, A. D.;CHEN, Y.;DALAL, D.;TANDRI, H.;AMAT-ALARCON, N.;DALY, A.;TICHNELL, C.;JAMES, C.;CALKINS, H. & JUDGE, D. P. 2010. Shared desmosome gene findings in early and late onset arrhythmogenic right ventricular dysplasia/cardiomyopathy. *J Cardiovasc Transl Res,* 3**,** 663-73.

TANG, R.;DODD, A.;LAI, D.;MCNABB, W. C. & LOVE, D. R. 2007. Validation of zebrafish (Danio rerio) reference genes for quantitative real-time RT-PCR normalization. *Acta Biochim Biophys Sin (Shanghai),* 39**,** 384-90.

TANDRI, H.;ASIMAKI, A.;DALAL, D.;SAFFITZ, J. E.;HALUSHKA, M. K. & CALKINS, H. 2008. Gap junction remodeling in a case of arrhythmogenic right ventricular dysplasia due to plakophilin-2 mutation. *J Cardiovasc Electrophysiol,* 19**,** 1212-4.

THISSE, C. & THISSE, B. 1999. Antivin, a novel and divergent member of the TGFbeta superfamily, negatively regulates mesoderm induction. *Development,* 126**,** 229-40.

TISO, N.;STEPHAN, D. A.;NAVA, A.;BAGATTIN, A.;DEVANEY, J. M.;STANCHI, F.;LARDERET, G.;BRAHMBHATT, B.;BROWN, K.;BAUCE, B.;MURIAGO, M.;BASSO, C.;THIENE, G.;DANIELI, G. A. & RAMPAZZO, A. 2001. Identification of mutations in the cardiac ryanodine receptor gene in families affected with arrhythmogenic right ventricular cardiomyopathy type 2 (ARVD2). *Hum Mol Genet,* 10**,** 189-94.

TOLWINSKI, N. S.;WEHRLI, M.;RIVES, A.;ERDENIZ, N.;DINARDO, S. & WIESCHAUS, E. 2003. Wg/Wnt signal can be transmitted through arrow/LRP5,6 and Axin independently of Zw3/GSK-3beta activity. *Dev Cell,* 4**,** 407-18.

TROYANOVSKY, R. B.;CHITAEV, N. A. & TROYANOVSKY, S. M. 1996. Cadherin binding sites of plakoglobin: localization, specificity and role in targeting to adhering junctions. *J Cell Sci,* 109 (Pt 13)**,** 3069-78.

UENO, S.;WEIDINGER, G.;OSUGI, T.;KOHN, A. D.;GOLOB, J. L.;PABON, L.;REINECKE, H.;MOON, R. T. & MURRY, C. E. 2007. Biphasic role for Wnt/beta-catenin signaling in cardiac specification in zebrafish and embryonic stem cells. *Proc Natl Acad Sci U S A,* 104**,** 9685-90.

UZUMCU, A.;NORGETT, E. E.;DINDAR, A.;UYGUNER, O.;NISLI, K.;KAYSERILI, H.;SAHIN, S. E.;DUPONT, E.;SEVERS, N. J.;LEIGH, I. M.;YUKSEL-APAK, M.;KELSELL, D. P. & WOLLNIK, B. 2006. Loss of desmoplakin isoform I causes early onset cardiomyopathy and heart failure in a Naxos-like syndrome. *J Med Genet,* 43**,** e5.

VAN DER HEYDEN, M. A.;ROOK, M. B.;HERMANS, M. M.;RIJKSEN, G.;BOONSTRA, J.;DEFIZE, L. H. & DESTREE, O. H. 1998. Identification of connexin43 as a functional target for Wnt signalling. *J Cell Sci,* 111 (Pt 12)**,** 1741-9.

VAN DER ZWAAG, P. A.;JONGBLOED, J. D.;VAN DEN BERG, M. P.;VAN DER SMAGT, J. J.;JONGBLOED, R.;BIKKER, H.;HOFSTRA, R. M. & VAN TINTELEN, J. P. 2009. A genetic variants database for arrhythmogenic right ventricular dysplasia/cardiomyopathy. *Hum Mutat,* 30**,** 1278-83.

VAN OOYEN, A. & NUSSE, R. 1984. Structure and nucleotide sequence of the putative mammary oncogene int-1; proviral insertions leave the protein-encoding domain intact. *Cell,* 39**,** 233-40.

VERHEULE, S.;VAN KEMPEN, M. J.;TE WELSCHER, P. H.;KWAK, B. R. & JONGSMA, H. J. 1997. Characterization of gap junction channels in adult rabbit atrial and ventricular myocardium. *Circ Res,* 80**,** 673-81.

WANG, Y. 2009. Wnt/Planar cell polarity signaling: a new paradigm for cancer therapy. *Mol Cancer Ther,* 8**,** 2103-9.

WESTERFIELD, M. (1995). *The Zebrafish Book: A Guide for the Laboratory Use of Zebrafish, 4th ed.,* Eugene: University of Oregon Press.

WIENHOLDS, E.;KOUDIJS, M. J.;VAN EEDEN, F. J.;CUPPEN, E. & PLASTERK, R. H. 2003a. The microRNA-producing enzyme Dicer1 is essential for zebrafish development. *Nat Genet,* 35**,** 217-8.

WIENHOLDS, E. & PLASTERK, R. H. 2004. Target-selected gene inactivation in zebrafish. *Methods Cell Biol,* 77**,** 69-90.

WIENHOLDS, E.;VAN EEDEN, F.;KOSTERS, M.;MUDDE, J.;PLASTERK, R. H. & CUPPEN, E. 2003b. Efficient target-selected mutagenesis in zebrafish. *Genome Res,* 13**,** 2700-7.

WILLIAMS, B. O.;BARISH, G. D.;KLYMKOWSKY, M. W. & VARMUS, H. E. 2000. A comparative evaluation of beta-catenin and plakoglobin signaling activity. *Oncogene,* 19**,** 5720-8.

WILLIAMSON, L.;RAESS, N. A.;CALDELARI, R.;ZAKHER, A.;DE BRUIN, A.;POSTHAUS, H.;BOLLI, R.;HUNZIKER, T.;SUTER, M. M. & MULLER, E. J. 2006. Pemphigus vulgaris identifies plakoglobin as key suppressor of c-Myc in the skin. *EMBO J,* 25**,** 3298-309.

WITCHER, L. L.;COLLINS, R.;PUTTAGUNTA, S.;MECHANIC, S. E.;MUNSON, M.;GUMBINER, B. & COWIN, P. 1996. Desmosomal cadherin binding domains of plakoglobin. *J Biol Chem,* 271**,** 10904-9.

WOLF, C. M. & BERUL, C. I. 2008. Molecular mechanisms of inherited arrhythmias. *Curr Genomics,* 9**,** 160-8.

WOLPERT, L., BEDDINGTON, R., BROCKES, J., JESSEL, T., LAWRENCE, P. AND MEYEROWITZ, E. (1998) *Principles of Development*, Oxford: Oxford University Press.

XU, T.;YANG, Z.;VATTA, M.;RAMPAZZO, A.;BEFFAGNA, G.;PILICHOU, K.;SCHERER, S. E.;SAFFITZ, J.;KRAVITZ, J.;ZAREBA, W.;DANIELI, G. A.;LORENZON, A.;NAVA,

A.;BAUCE, B.;THIENE, G.;BASSO, C.;CALKINS, H.;GEAR, K.;MARCUS, F. & TOWBIN, J. A. 2010. Compound and digenic heterozygosity contributes to arrhythmogenic right ventricular cardiomyopathy. *J Am Coll Cardiol,* 55**,** 587-97.

YAN, Y. T.;GRITSMAN, K.;DING, J.;BURDINE, R. D.;CORRALES, J. D.;PRICE, S. M.;TALBOT, W. S.;SCHIER, A. F. & SHEN, M. M. 1999. Conserved requirement for EGF-CFC genes in vertebrate left-right axis formation. *Genes Dev,* 13**,** 2527-37.

YAN, Y. T.;LIU, J. J.;LUO, Y.;E, C.;HALTIWANGER, R. S.;ABATE-SHEN, C. & SHEN, M. M. 2002. Dual roles of Cripto as a ligand and coreceptor in the nodal signaling pathway. *Mol Cell Biol,* 22**,** 4439-49.

YANG, L.;CHEN, Y.;CUI, T.;KNOSEL, T.;ZHANG, Q.;ALBRING, K. F.;HUBER, O. & PETERSEN, I. 2012. Desmoplakin acts as a tumor suppressor by inhibition of the Wnt/beta-catenin signaling pathway in human lung cancer. *Carcinogenesis*.

YELON, D.;HORNE, S. A. & STAINIER, D. Y. 1999. Restricted expression of cardiac myosin genes reveals regulated aspects of heart tube assembly in zebrafish. *Dev Biol,* 214**,** 23-37.

YEO, C. & WHITMAN, M. 2001. Nodal signals to Smads through Cripto-dependent and Cripto-independent mechanisms. *Mol Cell,* 7**,** 949-57.

YU, S. C.;XIAO, H. L.;JIANG, X. F.;WANG, Q. L.;LI, Y.;YANG, X. J.;PING, Y. F.;DUAN, J. J.;JIANG, J. Y.;YE, X. Z.;XU, S. L.;XIN, Y. H.;YAO, X. H.;CHEN, J. H.;CHU, W. H.;SUN, W.;WANG, B.;WANG, J. M.;ZHANG, X. & BIAN, X. W. 2012. Connexin 43 reverses malignant phenotypes of glioma stem cells by modulating E-cadherin. *Stem Cells,* 30**,** 108-20.

ZENG, X.;TAMAI, K.;DOBLE, B.;LI, S.;HUANG, H.;HABAS, R.;OKAMURA, H.;WOODGETT, J. & HE, X. 2005. A dual-kinase mechanism for Wnt co-receptor phosphorylation and activation. *Nature,* 438**,** 873-7.

ZHANG, F.;CONG, L.;LODATO, S.;KOSURI, S.;CHURCH, G. M. & ARLOTTA, P. 2011. Efficient construction of sequence-specific TAL effectors for modulating mammalian transcription. *Nat Biotechnol,* 29**,** 149-53.

ZHANG, J.;TALBOT, W. S. & SCHIER, A. F. 1998. Positional cloning identifies zebrafish one-eyed pinhead as a permissive EGF-related ligand required during gastrulation. *Cell,* 92**,** 241-51.

ZHURINSKY, J.;SHTUTMAN, M. & BEN-ZE'EV, A. 2000. Differential mechanisms of LEF/TCF family-dependent transcriptional activation by beta-catenin and plakoglobin. *Mol Cell Biol,* 20**,** 4238-52.

9 Website References

http://baolab.bme.gatech.edu/Research/BioinformaticTools/assembleTALSequences.html

http://www.arvcdatabase.info/

http://www.blast.ncbi.nlm.nih.gov/

http://www.ebi.ac.uk/Tools/msa/clustalw2/

http://www.ensembl.org/Danio_rerio/index.html

http://www.ncbi.nlm.nih.gov/tools/primer-blast

https://boglab.plp.iastate.edu/node/add/talen

10 Publications

Moriarty, MA, Ryan, R, Lalor, P, Dockery, P, Byrnes, L, Grealy, M. (2012) Loss of plakophilin 2 disrupts heart development in zebrafish. Int. J. Dev. Biol. Sep 14 epub ahead of print doi: 10.1387/ijdb.113390mm